Resource Allocation in Multi-carrier Full-duplex Networks

Nam Changwon

January 27, 2015

Abstract

Recent advances in the physical layer have demonstrated the feasibility of in-band wireless full-duplex for a node to simultaneously transmit and receive on the same frequency band. While the full-duplex operation can ideally double throughput, the network-level gain of full-duplex in large-scale networks remains unclear due to the complicated resource allocation in multi-carrier environments. In this dissertation, we tackle three different resource allocation problems in multi-carrier full-duplex networks.

Firstly, we investigate the power allocation problem in three-node full-duplex OFDM networks where one full-duplex node transmits to a half-duplex node while receiving from another half-duplex node at the same time. We formulate the sum-rate maximization problem with and without joint decoding, and develop a low-complexity solution for each case. Through simulations, we evaluate our proposed solutions and demonstrate the full-duplex gain in various scenarios.

Secondly, we consider the resource allocation problem in full-duplex OFDMA networks where both the base station and mobile nodes are

full-duplex capable. We propose a joint solution to the subcarrier assignment and power allocation problem by establishing a necessary condition for the sum-rate optimality. We show that our algorithm is provably efficient in achieving *local Pareto optimality* under certain conditions that are frequently met in practice. Through extensive simulations, we show that our algorithm empirically achieves near-optimal performance.

Lastly, we investigate the resource allocation problem in full-duplex OFDMA networks where the base station is full-duplex capable while mobile nodes are conventional half-duplex nodes. Specifically, we consider two different cases where i) the BS knows all channel gains and ii) the BS obtains limited channel information through channel feedback from each node. In the former case, we design a sequential resource allocation algorithm which assigns subcarriers to uplink nodes first and downlink nodes or vice versa. In the latter case, we propose a low-overhead channel feedback protocol where downlink nodes can estimate inter-node interference by overheating feedback messages transmitted by uplink nodes. We evaluate our solutions under various scenarios through simulations.

Keywords: full-duplex communications, power allocation, subcarrier assignment, resource allocation, OFDM(A), channel feedback

Student Number: 2008-20870

Contents

List of Tables

List of Figures

Chapter 1

Introduction

1.1 Motivation

One of the fundamental assumptions in wireless system design is that wireless nodes have to operate in half-duplex mode, i.e., they can either transmit or receive in the same frequency band, but not both simultaneously. Through the orthogonalization of wireless resource in temporal or spectral dimensions, transmission and reception are separated into orthogonal resources. The traditional communication paradigms like time division duplex (TDD) and frequency division duplex (FDD) are different embodiments of half-duplex communications.

Recent advances in wireless transceiver design have challenged the half-duplex assumption and demonstrated the feasibility of *full-duplex wireless communications*, in which a node can transmit one signal and

receive another signal at the same time and in the same frequency band. Compared to half-duplex communications, full-duplex communications can boost throughput by simultaneous transmission and reception. Due to the significant potential of improving the spectral efficiency, full-duplex communications have recently received tremendous attention from both academia and industry.

Even though full-duplex communications can ideally double throughput, there are two major bottlenecks to address in physical and network layers: *self-interference* and *inter-node interference*. When a node transmits and receives at the same time, the received signal is interfered by its own transmitted signal, which is called self-interference. Since the self-interference signal travels a short distance from transmission antenna to reception antenna, it is several orders of magnitude (up to 100 dB) stronger than the received signal. To achieve full-duplex communications, the strong self-interference should be suppressed to a sufficiently low level, which is a challenging task. Another problem in network perspective occurs in multi-user environments. When a full-duplex base station transmits to downlink nodes and receives from uplink nodes, the uplink transmissions will interference with the downlink reception at the downlink nodes. This interference between uplink and downlink nodes is called inter-node interference. In full-duplex networks, scheduling and resource allocation algorithms should be carefully designed to mitigate the inter-node interference.

The full-duplex gain can be fully achieved when the two new kinds

of interferences are managed effectively. In the past few years, there has been a significant progress in cancelling the self-interference using various interference cancellation techniques. The sate-of-the art work has demonstrated that the self-interference can be suppressed to the noise power level. Consequently, it is expected that perfect self-interference cancellation can be realized in the near future.

In contrast to the self-interference which is a physical layer issue, the inter-node interference should be addressed from network perspective, i.e., user scheduling and resource allocation. Specifically, when full-duplex communications are deployed in multi-carrier networks such as Orthogonal Division Multiple Access (OFDMA), the subcarrier assignment and power allocation should be performed considering the inter-node interference. There has been few research in resource allocation for multi-carrier full-duplex networks, and the full-duplex gain has not been fully understood from network perspective. This thesis investigates the resource allocation problem in full-duplex networks and proposes solutions for various scenarios.

1.2 Background and Related Work

The main difficulty in implementing a full-duplex system is to suppress the self-interference to a sufficiently low level. In the literature, there are various self-interference cancellation techniques [1, 2, 3, 4, 5, 6], which can be categorized into antenna cancellation, analog cancella-

tion, and digital cancellation. An antenna cancellation technique was first proposed in [1] where a pair of transmission antennas are placed such that the signal from one antenna cancels out that from the other. For a wavelength λ, two transmission antennas are placed at d and $d + \frac{\lambda}{2}$ away from the reception antenna to make their signals add destructively. Analog cancellation uses the known transmission signal to cancel out the self-interference in RF signal domain. The received signal is added with an inverted copy of transmitted analog signal which is generated by a second transmit chain [2] or a special component such as balun transformer [3]. Digital cancellation is used to clean out any remaining self-interference which is generated by non-ideal and non-linear components in an RF chain. The state-of-the-art work has demonstrated that full-duplex can be implemented with a single antenna, covering up to 80 MHz of bandwidth [6]. This can be realized by a hybrid analog-digital cancellation technique that accurately models all linear and non-linear distortions of signals in a TX chain.

Full-duplex communications can be categorized into two types [7]: One is two-node bidirectional transmissions, where two full-duplex nodes transmit and receive simultaneously in a bidirectional manner, and the other is three-node unidirectional transmissions, where one full-duplex node (usually a base station or access point) transmits to a (downlink) node while receiving from another (uplink) node at the same time. While the former type requires both of the two nodes to be full-duplex capable, the latter can be embodied with a single

full-duplex node. Unlike the two-node bidirectional transmissions, the capacity of the three-node full-duplex transmissions will be less than the sum of the two individual (uplink and downlink) transmission rates due to the inter-node interference from the uplink node to the downlink node. Considering the cost and energy consumption of interference cancellation techniques, the three-node unidirectional transmissions will be deployed first in the near future by implementing the full-duplex technology only in base stations (BSs). The two-node bidirectional transmissions will also appear when mobile nodes becomes full-duplex capable with a further advance in interference cancellation techniques.

The power allocation for full-duplex communications has been recently studied in the literature. An power control scheme for two-node bidirectional transmissions with imperfect self-interference cancellation has been proposed in [8]. The authors showed that the sum-rate maximization problem can be converted into a convex optimization problem and a suboptimal solution can be calculated numerically. An optimal power allocation scheme for three-node relay transmission has been developed in [9]. In [10], the authors characterized the achievable rate region in a three-node full-duplex network with a side channel. They also showed how inter-node interference can be mitigated with the help of an orthogonal side-channel between uplink and downlink nodes.

Besides the physical layer research, several MAC layer protocols

were proposed to incorporate full-duplex communications into Wireless Local Area Networks (WLANs) [7, 11, 12, 13]. In addition, network routing and scheduling considering full-duplex is investigated in [14, 15, 16]

1.3 Contributions and Outline

The full-duplex technology can be deployed in OFDMA networks. Dividing the spectrum band into multiple orthogonal subcarriers and distributing them over different nodes, OFDMA benefits from both multiuser and frequency diversities. In full-duplex OFDMA networks, a base station is full-duplex capable while mobile nodes are either full-duplex nodes or conventional half-duplex nodes. In the former case, the BS assigns each subcarrier to a single full-duplex node and communicates with it in a bidirectional manner. In the latter case, each subcarrier is assigned to one uplink node and one downlink node for the three-node unidirectional transmissions.

In full-duplex OFDMA networks, radio resource allocation algorithms handle subcarrier assignment and power allocation. The resource allocation problem becomes challenging due to i) the coexistence of uplink and downlink transmissions in the same subcarrier, and ii) resultant *inter-node interference* from uplink nodes to downlink nodes (when nodes are half-duplex). To fully exploit the full-duplex gain, it is essential to allocate the radio resource considering

the characteristics of the full-duplex transmissions.

In this dissertation, we deal with resource allocation problems in full-duplex OFDM and OFDMA networks. Our objective is to maximize sum-rate performance by jointly optimizing power allocation and subcarrier assignment. We formulate the problems as optimization problems and solve each of them using some optimization frameworks and techniques. The results of extensive simulation demonstrate that our solutions can optimize the performance of the full-duplex networks.

This dissertation is organized as follows. In Chapter 2, we tackle the power allocation problem in the three-node full-duplex OFDM networks to maximize the total sum-rate of the uplink and downlink transmissions. We formulate the sum-rate maximization problem with and without joint decoding capability at the downlink node. We prove that the problem with joint decoding is a convex optimization problem and develop a low-complexity optimal solution using the Lagrangian dual optimization method, which complexity increases linearly with respect to the number of subcarriers. When the joint decoding is not available, we show that the problem is NP-hard and develop an efficient heuristic solution by exploiting the FDMA property for subcarriers with high inter-node interference. Through numerical simulations, we evaluate our solutions in various scenarios and show that they outperform other existing power allocation schemes.

In Chapter 3, we consider the resource allocation problem in the

full-duplex OFDMA networks where both the base station (BS) and mobile nodes are full-duplex capable. We propose a joint solution to the subcarrier assignment and power allocation problem by establishing a necessary condition for the sum-rate optimality. We show that our algorithm is provably efficient in achieving *local Pareto optimality* under certain conditions that are frequently met in practice. Through extensive simulations, we show that our algorithm empirically achieves near-optimal performance and outperforms other resource allocation schemes.

In Chapter 4, we investigate the resource allocation problem in the full-duplex OFDMA networks where the BS is full-duplex capable while mobile nodes are conventional half-duplex nodes. Specifically, we consider two different scenarios where i) the BS knows all channel gains, i.e., full channel state information (CSI) scenario and ii) the BS obtains limited channel information through channel feedback from nodes, i.e., limited CSI. In the full CSI scenario, we design a sequential resource allocation algorithm which assigns subcarriers to uplink nodes first and downlink nodes or vice versa. In the limited CSI scenario, we propose an efficient low-overhead feedback protocol where downlink nodes can estimate interference in a distributed manner. Through simulation, we evaluate our solutions for full and limited CSIs under various

We conclude the dissertation in Chapter 5.

Chapter 2

Power Allocation with Inter-node Interference in Full-duplex OFDM Networks

2.1 Introduction

A long-held assumption in wireless communications is that a radio cannot transmit and receive simultaneously on the same frequency band due to the *self-interference* between its transmit and receive chains [17]. Thus, most of contemporary wireless systems rely on the orthogonalization of wireless resource in temporal or spectral dimen-

sions, e.g., Time Division Duplex (TDD) and Frequency Division Duplex (FDD). Recent advances in the physical layer have challenged this assumption and demonstrated the feasibility of *in-band wireless full-duplex*, in which a radio can countervail against the self-interference and thus perform simultaneous transmission and reception on the same frequency band. Due to its potential to double the spectral efficiency, the full-duplex operation has attracted tremendous attention from both academia and industry as a promising technology for next-generation wireless systems.

The main difficulty in building a full-duplex radio is to suppress self-interference to a sufficiently low level. Existing self-interference cancellation techniques can be categorized into antenna, analog, and digital cancellations [18]. In antenna cancellation techniques, a pair of transmission antennas are placed such that the signal from one antenna destructively adds with that from the other [1, 4, 5]. Analog cancellation methods tap a copy of the transmitted signal from the transmit chain, process it with delay and attenuation, and subtract it on the receive path [1, 3]. Lastly, digital cancellation cleans out any remaining residual self-interference caused by non-ideal and non-linear components in RF chains [1, 3]. The state-of-the-art work has demonstrated that self-interference can be suppressed close to the receiver noise floor level via a combination of various cancellation techniques [6].

In exploiting the full-duplex operation, there are two different ap-

proaches from the network perspective [7, 8]: two bidirectional transmissions between two full-duplex nodes (two-node scenario), and two unidirectional transmissions with one full-duplex node and two half-duplex nodes (three-node scenario). In the two-node scenario, two full-duplex capable nodes transmit and receive simultaneously in a bidirectional manner, and thus ideal doubling of spectral efficiency can be achieved with perfect self-interference cancellation. In the three-node scenario, one full-duplex node (usually a base station or relay) transmits to a (downlink) node while receiving from another (uplink) node at the same time. In this case, the downlink node experiences interference from uplink transmission, which is called *inter-node interference*. Considering the cost and complexity of interference cancellation techniques, the three-node scenario is more likely to be deployed in the near future because only the base station needs to operate in full-duplex while the uplink and downlink user terminals are not necessarily full-duplex capable [18]. Thus, it is of great importance to optimize the performance of three-node full-duplex operation, where the full-duplex gain will decrease due to inter-node interference.

The performance of full-duplex operation has been widely investigated in the literature. There are several works that have focused on the two-node scenario and investigated the achievable sum-rate of bidirectional full-duplex transmissions under imperfect self-interference cancellation. The sum-rate between two full-duplex nodes equipped with one transmit antenna and one receive antenna was studied in

[19]. The case for an arbitary number of antennas was considered in [8], where it has been shown that the sum-rate maximization problem can be approximated as a convex optimization problem and its solution can be obtained in an iterative manner. In [20], the rate region of a bidirectional full-duplex link using orthogonal frequency division multiplexing (OFDM) was studied. The authors proposed two subcarrier-level power allocation algorithms and analyzed the corresponding rate regions.

For the three-node scenario, there are works that focus on a single traffic-flow relayed by a full-duplex node. They have investigated the impact of the full-duplex relay on the capacity of a single-source single-destination relay topology [21, 22, 23, 24], and the network capacity with multi-user pairs [25, 26, 27, 28]. On the other hand, a full-duplex node can work as base station (BS) and support two independent uplink and downlink data flows. In this case, the spectral efficiency of full-duplex operation can be measured by the sum-rate of uplink and downlink transmissions. In [10], the authors have characterized the sum-rate in a three-node network using a side channel. They have shown how the inter-node interference can be mitigated with the help of an orthogonal side-channel between the uplink and downlink nodes. However, the result is limited to a single data channel case without considering multi-carrier environments.

Considering that most of today's cellular systems adopt multi-carrier modulations, a typical deployment scenario will be a three-

node full-duplex OFDM network, where the subcarrier power allocation problem becomes challenging due to inter-node interference. For example, in very weak interference environments, it is expected that an optimal solution is similar to the result obtained by the water-filling algorithm. In contrast, when the inter-node interference is very strong in every subcarrier, the uplink and downlink nodes will use disjoint subcarrier sets to avoid interference, i.e., Frequency Division Multiple Access (FDMA). Then the question is: *what is the optimal power allocation and how can we achieve it with low complexity?*

In this paper, we tackle the subcarrier power allocation problem in a three-node full-duplex OFDM network, where the BS and the uplink node have their own total power constraints. Through the joint power allocation of the uplink and downlink transmissions taking into consideration the inter-node interference, we aim to maximize the sum-rate of the uplink and downlink transmissions. There are two different ways of dealing with inter-node interference: i) the downlink node always treats the interference as noise; ii) the downlink node decodes the interference first, re-encodes and subtracts it from the received signal, and finally decodes the downlink signal without interference, i.e., joint decoding. While we can achieve a better performance by using the joint decoding, its use at user terminals is limited in practice due to high complexity and energy consumption. To this end, we consider both cases with and without joint decoding.

Our contributions are summarized as follows:

- We prove that the problem with joint decoding is a convex optimization problem and find an optimal solution using the Lagrangian dual optimization method, which complexity increases linearly with respect to the number of subcarriers.

- When the joint decoding is not available, we show that the problem is NP-hard, and develop an efficient heuristic solution by exploiting the FDMA property for subcarriers with high inter-node interference.

- Through numerical simulations, we evaluate our solutions in various scenarios and show that they outperform other existing power allocation schemes.

The rest of chapter is organized as follows. In Section 2.2, we present a detailed description of our system model and formulate the sum-rate maximization problem. In Section 2.3, we consider a case where the joint decoding is available and use the Lagrangian dual optimization method to obtain an optimal power allocation. In Section 2.4, we show that the problem without joint decoding is NP-hard and develop a heuristic solution. We evaluate our solutions in Section 2.5 and finally conclude this chapter in Section 2.6.

2.2 System Model and Problem Formulation

We consider a three-node full-duplex network that consists of a single full-duplex node F and two half-duplex nodes U and D, as shown in

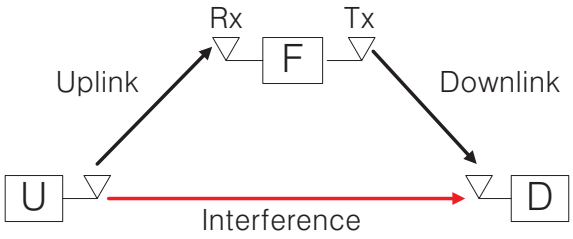

Figure 2.1: A three-node full-duplex network that consists of a single full-duplex node F and two half-duplex nodes U and D. Using its full-duplex capability, node F can transmit (to node D) and receive (from node U) simultaneously. The inter-node interference from node U(uplink transmitter) to node D (downlink receiver) affects the downlink rate.

Fig. 2.1. In practical scenarios, node F is usually a base station while nodes U and F are a user terminal. We denote link $U \to F$ by uplink (or link 1) and link $F \to D$ by downlink (or link 2). Also, we define an index set $\mathcal{K} = \{1, 2\}$ for the uplink and the downlink.

We assume that the self-interference at node F can be successfully suppressed below the noise power level by exploiting multiple cancellation techniques [6, 10]. However, due to the simultaneous uplink and downlink transmissions, there exists inter-node interference from node U to node D [10]. The inter-node interference is a key reason that the sum-rate in full-duplex transmissions is generally smaller than the sum of point-to-point uplink and downlink rates.

We assume that the spectrum band is partitioned into N orthogonal subcarriers. Let $\mathcal{N} = \{1, \cdots, N\}$ denote the set of subcarriers, and in subcarrier n, let h_1^n and h_2^n denote the channel coefficients of the uplink and the downlink, respectively. Similarly, we let h_{12}^n denote

the channel coefficient of the interference link $(U \rightarrow D)$ in subcarrier n. The uplink and downlink transmitted signals in subcarrier n are denoted by x_1^n and x_2^n, respectively, and the corresponding power by $p_k^n := E[|x_k^n|^2], \forall k \in \mathcal{K}$. We assume that the total power budget for the uplink (and the downlink) is constrained by P_1^{max} (and P_2^{max}), i.e., $\sum_{n=1}^{N} p_k^n \leq P_k^{\max}, \ \forall k \in \mathcal{K}$. Also, let us define $\mathbf{P}^n := (p_1^n, p_2^n)$ and $\mathbf{P} := (p_1^1, \cdots, p_1^N, p_2^1, \cdots, p_2^N) \in \mathbb{R}^{2N}$.

Given the channel coefficients and power allocation, the uplink received signal y_1^n and the downlink received signal y_2^n in each subcarrier $n \in \mathcal{N}$ are given by

$$y_1^n = h_1^n x_1^n + z_1^n,$$
$$y_2^n = h_2^n x_2^n + h_{12}^n x_1^n + z_2^n,$$

where $z_k^n \sim CN(0, N_0)$ denotes the complex Gaussian noise with zero mean and variance N_0, and $h_{12}^n x_1^n$ represents the inter-node interference from the uplink to the downlink. Let us define the normalized channel gains $g_1^n := |h_1^n|^2/N_0$, $g_2^n := |h_2^n|^2/N_0$, and $g_{12}^n := |h_{12}^n|^2/N_0$, and let R^n denote the sum of the uplink and downlink rates. From the Shannon capacity formula [17], we obtain

$$R^n(\mathbf{P}^n) = \log(1 + g_1^n p_1^n) + \log\left(1 + \frac{g_2^n p_2^n}{1 + g_{12}^n p_1^n}\right). \tag{2.1}$$

When the joint decoding is applicable [29], node D can decode the uplink signal first, re-encode and subtract it from the received signal,

and finally decode the downlink signal without interference. In this case, we can achieve the following R^n:

$$R^n(\mathbf{P}^n) = \min\left\{\log(1+g_1^n p_1^n) + \log(1+g_2^n p_2^n), \log\left(1+g_{12}^n p_1^n + g_2^n p_2^n\right)\right\}. \tag{2.2}$$

It has been known that when $g_1^n < g_{12}^n$, the joint decoding achieves a greater sum rate satisfying (2.1) $<$ (2.2) [10]. Note that the joint decoding may require high complexity and energy consumption which limit its use at user terminals. To this end, we consider both cases with and without joint decoding.

Our goal is to find an optimal subcarrier power allocation that maximizes the sum-rate $\sum_{n=1}^{N} R^n(\mathbf{P}^n)$ under the total power constraints. We formulate the problem as

$$(\mathsf{P}) \quad \underset{\mathbf{P}}{\text{maximize}} \quad \sum_{n=1}^{N} R^n(\mathbf{P}^n) \tag{2.3a}$$

$$\text{subject to} \quad \sum_{n=1}^{N} p_k^n \leq P_k^{max}, \forall k \in \mathcal{K}. \tag{2.3b}$$

In the following, we first solve the problem with joint decoding and then address the problem without joint decoding.

2.3 Power Allocation with Joint Decoding

In this section, we solve problem P with joint decoding, where we have

$$R^n(\mathbf{P}^n) = \begin{cases} \log(1+g_1^n p_1^n) + \log\left(1+\dfrac{g_2^n p_2^n}{1+g_{12}^n p_1^n}\right), & \text{if } g_1^n \geq g_{12}^n, \\ \min\left\{\log(1+g_1^n p_1^n) + \log(1+g_2^n p_2^n)\right., & \\ \qquad \left.\log\left(1+g_{12}^n p_1^n + g_2^n p_2^n\right)\right\}, & \text{if } g_1^n < g_{12}^n. \end{cases} \tag{2.4a}$$

(2.4b)

We first show that this is a convex optimization problem, and develop a low complexity optimal solution using the Lagrangian dual optimization method.

2.3.1 Convex Problem and Dual Formulation

Since the constraints (2.3b) are linear and the objective function is the sum of R^n's, the problem is a convex optimization problem if each R^n is a concave function of $\mathbf{P}^n$. We first show that R^n is concave, and consider the dual of the original problem to obtain a low-complexity solution.

Proposition 1. $R^n(\mathbf{P}^n)$ is a concave function of $\mathbf{P}^n$.

Proof. For $g_1^n \geq g_{12}^n$, Eq. (2.4a) can be written as

$$R^n(\mathbf{P}^n) = \log\left(\tfrac{1+g_1^n p_1^n}{1+g_{12}^n p_1^n}\right) + \log(1 + g_{12}^n p_1^n + g_2^n p_2^n).$$

The first term is concave of p_1^n, since it is a function of p_1^n and has a non-positive second-order derivative as

$$\tfrac{\partial^2}{\partial\left(p_1^n\right)^2} \log\left(\tfrac{1+g_1^n p_1^n}{1+g_{12}^n p_1^n}\right) = \tfrac{(g_{12}^n - g_1^n)(2g_1^n g_{12}^n p_1^n + g_1^n + g_{12}^n)}{(g_{12}^n p_1^n + 1)^2 (g_1^n p_1^n + 1)^2} \leq 0,$$

where the inequality comes from $g_1^n \geq g_{12}^n$. The second term is a logarithm of a linear function, which is (jointly) concave. Thus $R^n(\mathbf{P}^n)$ is a concave function.

For $g_1^n < g_{12}^n$, $R^n(\mathbf{P}^n)$ is the minimum of two concave functions, and thus it is also concave. □

Since a small non-zero power allocation satisfies the constraints (2.3b) with strict inequality, there is no duality gap by the Slater's condition [30], and an optimal solution to the original problem can be obtained via the dual formulation. In the next subsection, we present a solution to the dual problem.

2.3.2 Optimal Power Allocation via Dual Optimization

The standard dual problem can be written as

$$(\mathsf{D}) \min_{\boldsymbol{\lambda} \geq 0} \mathsf{g}(\boldsymbol{\lambda}), \tag{2.5}$$

where $\boldsymbol{\lambda} := (\lambda_1, \lambda_2)$ is the dual variables, and the dual function $g(\boldsymbol{\lambda})$ and the Lagrangian function $L(\mathbf{P}, \boldsymbol{\lambda})$ are defined as

$$g(\boldsymbol{\lambda}) := \max_{\mathbf{P} \geq 0} L(\mathbf{P}, \boldsymbol{\lambda}), \tag{2.6a}$$

$$L(\mathbf{P}, \boldsymbol{\lambda}) := \sum\nolimits_{k=1}^{2} \lambda_k P_k^{\max} + \sum\nolimits_{n=1}^{N} L^n(\mathbf{P}^n, \boldsymbol{\lambda}), \tag{2.6b}$$

$$L^n(\mathbf{P}^n, \boldsymbol{\lambda}) := R^n(\mathbf{P}^n) - \lambda_1 p_1^n - \lambda_2 p_2^n. \tag{2.6c}$$

We first give a closed-form representation of $g(\boldsymbol{\lambda})$. Let $\hat{\mathbf{P}}^n := \{\hat{p}_1^n(t), \hat{p}_2^n(t)\}$ denote a solution to $\max L^n(\mathbf{P}^n, \boldsymbol{\lambda})$ for given $\boldsymbol{\lambda}$, and let $\partial_k L^n(\mathbf{P}^n) := \frac{\partial}{\partial p_k^n} L^n(\mathbf{P}^n),\ \forall k \in \mathcal{K}$. Given $\boldsymbol{\lambda}$, $L_n(\cdot)$ will satisfy the Karush-Kuhn-Tucker (KKT) conditions at $\hat{\mathbf{P}}^n$. We consider the following two cases according to the channel gains.

1. For $g_1^n \geq g_{12}^n$:

   From $g_1^n \geq g_{12}^n$ and (2.4a), L^n can be written as

   $$L^n(\mathbf{P}^n, \boldsymbol{\lambda}) = \log(1 + g_1^n p_1^n) + \log\left(1 + \frac{g_2^n p_2^n}{1 + g_{12}^n p_1^n}\right) - \lambda_1 p_1^n - \lambda_2 p_2^n.$$

   From the KKT conditions on $\max L^n$, we obtain the following four equations:

   $$\partial_1 L^n(\hat{\mathbf{P}}^n) = 0, \text{ if } \hat{p}_1^n > 0, \quad \partial_1 L^n(\hat{\mathbf{P}}^n) \leq 0, \text{ if } \hat{p}_1^n = 0, \tag{2.7a}$$

   $$\partial_2 L^n(\hat{\mathbf{P}}^n) = 0, \text{ if } \hat{p}_2^n > 0, \quad \partial_2 L^n(\hat{\mathbf{P}}^n) \leq 0, \text{ if } \hat{p}_2^n = 0, \tag{2.7b}$$

where $\partial_1 L^n(\hat{\mathbf{P}}^n)$ and $\partial_2 L^n(\hat{\mathbf{P}}^n)$ are given by

$$\partial_1 L^n(\hat{\mathbf{P}}^n) = \frac{g_1^n}{1+g_1^n\hat{p}_1^n} + \frac{g_{12}^n}{1+g_{12}^n\hat{p}_1^n+g_2^n\hat{p}_2^n} - \frac{g_{12}^n}{1+g_{12}^n\hat{p}_1^n} - \lambda_1, \tag{2.8a}$$

$$\partial_2 L^n(\hat{\mathbf{P}}^n) = \frac{g_2^n}{1+g_{12}^n\hat{p}_1^n+g_2^n\hat{p}_2^n} - \lambda_2. \tag{2.8b}$$

Suppose that $\hat{p}_1^n > 0$ and $\hat{p}_2^n > 0$. From (2.7b) and (2.8b), we have $\frac{1}{1+g_{12}^n\hat{p}_1^n+g_2^n\hat{p}_2^n} = \frac{\lambda_2}{g_2^n}$. Applying this to (2.7a) and (2.8a) yields a quadratic equation of $\hat{p}_1^n$, whose roots are

$$\begin{aligned}
\hat{p}_1^n &= -\tfrac{1}{2}\left(\tfrac{g_1^n+g_{12}^n}{g_1^n g_{12}^n}\right) + \tfrac{1}{2}\sqrt{\left(\tfrac{g_1^n+g_{12}^n}{g_1^n g_{12}^n}\right)^2 - \tfrac{4\left(\lambda_2 g_{12}^n - \lambda_1 g_2^n + g_2^n g_1^n - g_2^n g_{12}^n\right)}{\left(\lambda_2 g_{12}^n - \lambda_1 g_2^n\right) g_{12}^n g_1^n}}, \\
\hat{p}_2^n &= \tfrac{1}{\lambda_2} - \tfrac{g_{12}^n\hat{p}_1^n}{g_2^n} - \tfrac{1}{g_2^n}.
\end{aligned} \tag{2.9}$$

If $\hat{p}_1^n$ and $\hat{p}_2^n$ in (2.9) are positive, they are the solution. Otherwise, i.e., if one of them is either negative or zero, the solution is given by

$$\begin{aligned}
&(\hat{p}_1^n, \hat{p}_2^n) \\
&= \begin{cases}
\left([\tfrac{1}{\lambda_1} - \tfrac{1}{g_1^n}]^+, 0\right), \text{ if } \log\left(1 + g_1^n[\tfrac{1}{\lambda_1} - \tfrac{1}{g_1^n}]^+\right) - \lambda_1\left[\tfrac{1}{\lambda_1} - \tfrac{1}{g_1^n}\right]^+ \\
\qquad\qquad > \log\left(1 + g_2^n[\tfrac{1}{\lambda_2} - \tfrac{1}{g_2^n}]^+\right) - \lambda_2\left[\tfrac{1}{\lambda_2} - \tfrac{1}{g_2^n}\right]^+, \\
\left(0, [\tfrac{1}{\lambda_2} - \tfrac{1}{g_2^n}]^+\right), \text{ otherwise,}
\end{cases}
\end{aligned} \tag{2.10}$$

where $[x]^+ := \max\{x, 0\}$.

2. For $g_1^n < g_{12}^n$:

   From $g_1^n < g_{12}^n$ and (2.4b), we have

$$L^n(\mathbf{P}^n, \boldsymbol{\lambda}) = \min\{\log(1 + g_1^n p_1^n) + \log(1 + g_2^n p_2^n), \\ \log(1 + g_{12}^n p_1^n + g_2^n p_2^n)\} - \lambda_1 p_1^n - \lambda_2 p_2^n.$$

   We introduce the following two definitions:

$$L_a^n(\mathbf{P}^n, \boldsymbol{\lambda}) := \log(1 + g_{12}^n p_1^n + g_2^n p_2^n) - \lambda_1 p_1^n - \lambda_2 p_2^n,$$
$$L_b^n(\mathbf{P}^n, \boldsymbol{\lambda}) := \log(1 + g_1^n p_1^n) + \log(1 + g_2^n p_2^n) - \lambda_1 p_1^n - \lambda_2 p_2^n.$$

   Then we have $L^n = \min\{L_a^n, L_b^n\}$, where both L_a^n and L_b^n are concave. Thus the solution $\hat{\mathbf{P}}^n$ is either a maximum point of L_a^n (as shown in Fig. 2.2(a)), a maximum point of L_b^n, or a cross point of L_a^n and L_b^n (as shown in Fig. 2.2(b)). We consider each case as follows:

   (i) If $\hat{\mathbf{P}}^n$ maximizes L_a^n, the KKT conditions on $\max L_a^n$ imply

that

$$\begin{aligned}
\frac{g_{12}^n}{1+g_{12}^n\hat{p}_1^n+g_2^n\hat{p}_2^n}-\lambda_1 &= 0, \text{ if } \hat{p}_1^n>0,\\
\frac{g_{12}^n}{1+g_{12}^n\hat{p}_1^n+g_2^n\hat{p}_2^n}-\lambda_1 &\le 0, \text{ if } \hat{p}_1^n=0,\\
\frac{g_2^n}{1+g_{12}^n\hat{p}_1^n+g_2^n\hat{p}_2^n}-\lambda_2 &= 0, \text{ if } \hat{p}_2^n>0,\\
\frac{g_2^n}{1+g_{12}^n\hat{p}_1^n+g_2^n\hat{p}_2^n}-\lambda_2 &\le 0, \text{ if } \hat{p}_2^n=0.
\end{aligned}$$

We obtain the solution to $\max L_a^n$ as

$$(\hat{p}_1^n,\hat{p}_2^n)=\begin{cases}
\left(\left[\frac{1}{\lambda_1}-\frac{1}{g_{12}^n}\right]^+,0\right), \text{ if } \frac{\lambda_1}{g_{12}^n}<\frac{\lambda_2}{g_2^n}, & \text{(2.12a)}\\
\left(0,\left[\frac{1}{\lambda_2}-\frac{1}{g_2^n}\right]^+\right), \text{ if } \frac{\lambda_1}{g_{12}^n}>\frac{\lambda_2}{g_2^n}, & \text{(2.12b)}\\
(x^*,y^*), \text{ if } \frac{\lambda_1}{g_{12}^n}=\frac{\lambda_2}{g_2^n}<1, & \text{(2.12c)}\\
(0,0), \text{ if } \frac{\lambda_1}{g_{12}^n}=\frac{\lambda_2}{g_2^n}\ge 1. & \text{(2.12d)}
\end{cases}$$

where (x^*,y^*) is a non-negative solution to $1+g_{12}^n x+g_2^n y=\frac{g_{12}^n}{\lambda_1}=\frac{g_2^n}{\lambda_2}$.

Since the solution $\hat{\mathbf{P}}^n$ satisfies $L_a^n(\hat{\mathbf{P}}^n,\boldsymbol{\lambda})\le L_b^n(\hat{\mathbf{P}}^n,\boldsymbol{\lambda})$, the following additional condition holds:

$$\log(1+g_{12}^n\hat{p}_1^n+g_2^n\hat{p}_2^n)\le\log(1+g_1^n\hat{p}_1^n)+\log(1+g_2^n\hat{p}_2^n).$$

As Eq. (2.12a) does not satisfy the above condition, it cannot be

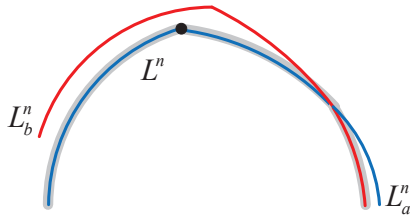

(a) The solution $\hat{\mathbf{P}}^n$ is the point where L_a^n is maximized.

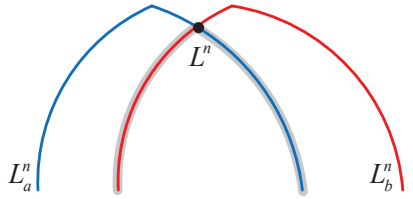

(b) The solution $\hat{\mathbf{P}}^n$ is a point where $L_a^n = L_b^n$.

Figure 2.2: The Lagrangian function L^n (shaded) is the minimum of two concave functions L_a^n (blue) and L_b^n (red). The solution $\hat{\mathbf{P}}^n$ that maximizes L^n is marked by a bullet.

a solution. Also, the probability of $\frac{\lambda_1}{g_{12}^n} = \frac{\lambda_2}{g_2^n}$ is zero considering that channel gains and dual variables are real numbers. As a result, the solution is likely to be (2.12b) in practice.

(ii) If $\hat{\mathbf{P}}^n$ maximizes L_b^n, the partial differentiation on L_b^n implies that the well-known water-filling power allocation is optimal, i.e.,

$$(\hat{p}_1^n, \hat{p}_2^n) = \left([\tfrac{1}{\lambda_1} - \tfrac{1}{g_1^n}]^+, [\tfrac{1}{\lambda_2} - \tfrac{1}{g_2^n}]^+ \right). \tag{2.13}$$

Again since $L_b^n(\hat{\mathbf{P}}^n, \boldsymbol{\lambda})$ is not greater than $L_a^n(\hat{\mathbf{P}}^n, \boldsymbol{\lambda})$, the fol-

lowing additional condition holds:

$$\log(1+g_1^n\hat{p}_1^n)+\log(1+g_2^n\hat{p}_2^n)\leq\log(1+g_{12}^n\hat{p}_1^n+g_2^n\hat{p}_2^n).$$

This condition is satisfied when $g_{12}^n \geq g_1^n(1+g_2^n\hat{p}_2^n)$. Hence, when the inter-node interference is strong and the downlink signal is weak, we can cancel the interference and use the water-filling to achieve the sum of (point-to-point) uplink and downlink rates [32].

(iii) If $\hat{\mathbf{P}}^n$ is a cross point of L_a^n and L_b^n, we obtain

$$(\hat{p}_1^n,\hat{p}_2^n)=\left([\tfrac{1}{\lambda_1}-\tfrac{1}{g_{12}^n}]^+,\tfrac{g_{12}^n-g_1^n}{g_1^n g_2^n}\right). \tag{2.14}$$

The equations of (2.9) – (2.14) provide a closed-form solution $\hat{\mathbf{P}}^n$, and allow us to solve the dual problem (2.5) by optimizing the dual variables $\boldsymbol{\lambda}$. Note that $g(\boldsymbol{\lambda})$ is a point-wise maximum of linear functions and may not be differentiable at some points [33]. Thus, we use the subgradient method to update $\boldsymbol{\lambda}$ iteratively. Specifically, in iteration t, the subgradient method updates $\boldsymbol{\lambda}$ by

$$\lambda_k^{(t+1)}=\left[\lambda_k^{(t)}-s_t\left(P_k^{max}-\sum\nolimits_{n=1}^{N}\hat{p}_k^n(t)\right)\right]^+,\forall k\in\mathcal{K}, \tag{2.15}$$

where s_t is the t-th step size and $\{\hat{p}_1^n(t),\hat{p}_2^n(t)\}_{n=1}^N$ are the solution from (2.9) – (2.14) for given $(\lambda_1^{(t)},\lambda_2^{(t)})$. It is known that the subgradient method converges to the optimal value as $t\to\infty$ if the step size

s_t satisfies $\lim_{t\to\infty} s_t = 0$ and $\sum_{t=1}^{\infty} s_t = \infty$ [34]. We summarize the proposed dual optimization method in Algorithm 1.

To the best of our knowledge, it is a first solution to the power allocation problem in the full-duplex transmissions with joint decoding. Also, for given $\boldsymbol{\lambda}$, we can obtain $\hat{\mathbf{P}}^n$ for each subcarrier n from (2.9) - (2.14). Thus our algorithm has a linear complexity with respect to the number of subcarriers.

Algorithm 1: Optimal Power Allocation for Problem P with Joint Decoding

Data: channel gains $\{g_1^n, g_2^n, g_{12}^n\}_{n=1}^N$ and maximum power budgets (P_1^{max}, P_2^{max}).

1 Initialize the dual variables $(\lambda_1^{(1)}, \lambda_2^{(1)})$ and $t \leftarrow 1$.

2 Compute $\{\hat{p}_1^n(t), \hat{p}_2^n(t)\}_{n=1}^N$ from (2.9) – (2.14).

3 Update $(\lambda_1^{(t+1)}, \lambda_2^{(t+1)})$ according to (2.15).

4 If $\|(\lambda_1^{(t+1)}, \lambda_2^{(t+1)}) - (\lambda_1^{(t)}, \lambda_2^{(t)})\| \leq \varepsilon$, terminate; otherwise, set $t \leftarrow t+1$ and go to Step 2.

Result: Optimal power allocation $\mathbf{P}^*$.

2.4 Power Allocation without Joint Decoding

In this section, we solve the problem where the joint decoding is not available. In this case, we have $R^n(\mathbf{P}^n) = \log(1 + g_1^n p_1^n) + \log\left(1 + \frac{g_2^n p_2^n}{1+g_{12}^n p_1^n}\right)$. We first derive necessary conditions for local optimality, and then establish a sufficient condition under which any local optimal solution has a certain property. We show that finding an optimal power allocation with such property is NP-hard. Based

on the results, we develop an iterative heuristic algorithm to achieve high performance.

2.4.1 Necessary Conditions for Local Optimality

Recall that the problem can be formulated as (2.3) with $R^n(\mathbf{P}^n) = \log(1+g_1^n p_1^n) + \log\left(1+\frac{g_2^n p_2^n}{1+g_{12}^n p_1^n}\right)$. Since R^n is not concave in general, the problem is not a convex optimization problem. We first introduce local optimality and derive several necessary conditions for local optimality, which will help us understand an optimal solution. Let us define local optimality as follows:

Definition 1 (Local Optimality)**.** A power allocation vector is said to be feasible if it satisfies the maximum power constraints (2.3b). A feasible power allocation vector $\widetilde{\mathbf{P}}$ is a *local optimum* (maximum) of problem P without joint decoding if there exists an $\epsilon > 0$ such that

$$\sum_{n=1}^{N} R^n(\widetilde{\mathbf{P}}^n) \geq \sum_{n=1}^{N} R^n(\mathbf{P}^n), \quad \forall \mathbf{P} \in \mathcal{P} \text{ with } ||\mathbf{P} - \widetilde{\mathbf{P}}|| < \epsilon,$$

where $\mathcal{P}$ is the set of all feasible power allocation vectors.

We now prove that in any local optimum, the downlink consumes all of its power budget while the uplink power allocation is binary, i.e., allocating either the maximum uplink power or no power. We now find some properties of R^n.

Definition 2 (Quasi-Convexity [31])**.** Let $f : \Omega \subseteq \mathbb{R}^n \to \mathbb{R}$ be a twice

differentiable function. Then f is quasi-convex on Ω if

$$v^T \nabla^2 f(x) v > 0 \tag{2.16}$$

for any $x \in \Omega$ and $v \in \mathbb{R}^n$ such that $\nabla f(x)v = 0$ and $v \neq 0$.

Lemma 1. If $g_1^n \geq g_{12}^n$, then $R^n(p_1^n, p_2^n)$ is a strictly increasing and concave function of (p_1^n, p_2^n). On the other hand, if $g_1^n < g_{12}^n$, $R^n(p_1^n, p_2^n)$ is a quasi-convex function of $(p_1^n, p_2^n) \in [0, \infty) \times [0, \infty)$ and for a fixed p_2^n, it is either (i) strictly increasing, (ii) strictly decreasing, or (iii) unimodal[1] on $p_1^n \in [0, P_1^{max}]$.

Proof. We first prove the case of $g_1^n \geq g_{12}^n$. Since the proof for $g_1^n = g_{12}^n$ is trivial, we assume that $g_1^n > g_{12}^n$. Let us write R^n as

$$R^n(p_1^n, p_2^n) = \log(\frac{1 + g_1^n p_1^n}{1 + g_{12}^n p_1^n}) + \log(1 + g_2^n p_2^n + g_{12}^n p_1^n).$$

The first term is a strictly increasing function of p_1^n because its first-order derivative satisfies

$$\frac{\partial}{\partial(p_1^n)} \log(\tfrac{1+g_1^n p_1^n}{1+g_{12}^n p_1^n}) = \tfrac{g_1^n - g_{12}^n}{(g_1^n p_1^n + 1)(g_{12}^n p_1^n + 1)} > 0,$$

where the inequality holds because $g_1^n > g_{12}^n$. It is clear that the second term is a strictly increasing function of $\mathbf{P}^n$ (i.e., logarithmic function), and thus R^n is a strictly increasing function of $\mathbf{P}^n$. Moreover, as

[1] $f(x)$ is a unimodal function if for some value m, it is strictly increasing for $x \leq m$ and strictly decreasing for $x \geq m$. In this case, the maximum value of $f(x)$ is $f(m)$ and there is no other local maximum.

shown in Proposition 1, R^n is concave when $g_1^n \geq g_{12}^n$.

Let us prove the case of $g_1^n < g_{12}^n$. Referring to Theorem 3.2 in [31] for the proof of quasi-convexity, we now prove the remaining part. Given $p_2^n = \tilde{p}_2^n$, $R^n(p_1^n|\tilde{p}_2^n) := R^n(p_1^n, \tilde{p}_2^n)$ can be written as

$$R^n(p_1^n|\tilde{p}_2^n) = \log\left(1 + g_1^n p_1^n\right) + \log\left(1 + \frac{g_2^n \tilde{p}_2^n}{1 + g_{12}^n p_1^n}\right).$$

Then the first-order derivative $\partial_1 R^n(p_1^n|\tilde{p}_2^n)$ is given by

$$\partial_1 R^n(p_1^n|\tilde{p}_2^n) := \frac{\partial R^n(p_1^n|\tilde{p}_2^n)}{\partial p_1^n} = \frac{A\left(p_1^n\right)^2 + 2Bp_1^n + C}{D},$$

where A, B, C, and D are defined as

$$\begin{aligned}
A &:= g_1^n (g_{12}^n)^2, \\
B &:= g_1^n g_{12}^n, \\
C &:= g_1^n + \left(g_1^n - g_{12}^n\right) g_2^n \tilde{p}_2^n, \\
D &:= \left(1 + g_1^n p_1^n\right)\left(1 + g_{12}^n p_1^n\right)\left(1 + g_{12}^n p_1^n + g_2^n \tilde{p}_2^n\right).
\end{aligned}$$

Since D is always strictly positive, the quadratic equation of $A\left(p_1^n\right)^2 + 2Bp_1^n + C = 0$ determines the sign of $\partial R^n(p_1^n|\tilde{p}_2^n)$. Now, let us consider the existence of a solution $p^* \in [0, P_1^{max}]$ to the quadratic equation. Since $A > 0$ and $B > 0$, there exists either a solution $p^* \in [0, P_1^{max}]$ or no solution in $[0, P_1^{max}]$. If there exists a solution p^*, then we have $\partial_1 R^n(p_1^n|\tilde{p}_2^n) < 0$ for $0 \leq p_1^n < p^*$ and $\partial_1 R^n(p_1^n|\tilde{p}_2^n) > 0$ for $p^* < p_1^n \leq P_1^{max}$. In this case, R^n is a unimodal function. When

there is no solution in $[0, P_1^{max}]$, we have either $\partial_1 R^n(p_1^n|\tilde{p}_2^n) > 0$ or $\partial_1 R^n < 0(p_1^n|\tilde{p}_2^n)$ for $p_1^n \in [0, P_1^{max}]$, which means that $R^n(p_1^n|\tilde{p}_2^n)$ is either a strictly increasing or a strictly decreasing function of $p_1^n \in [0, P_1^{max}]$. □

Based on Lemma 1, we can derive the following result.

Proposition 2. If $\widetilde{\mathbf{P}}$ is a local optimum, then we have

$$\sum_{n=1}^{N} \tilde{p}_1^n = 0 \text{ or } P_1^{max}, \tag{2.17a}$$

$$\sum_{n=1}^{N} \tilde{p}_2^n = P_2^{max}. \tag{2.17b}$$

Proof. We prove this by contradiction. Since $\widetilde{\mathbf{P}}$ is a local optimum, there exists an $\epsilon > 0$ such that $\sum_{n=1}^{N} R^n(\widetilde{\mathbf{P}}^n) \geq \sum_{n=1}^{N} R^n(\mathbf{P}^n),\ \forall \mathbf{P} \in \mathcal{P}$ with $||\mathbf{P} - \widetilde{\mathbf{P}}|| < \epsilon$. Assume to the contrary of (2.17b) that $\sum_{n=1}^{N} \tilde{p}_2^n = P < P_2^{max}$. Let us construct a new power allocation vector $\mathbf{S}$ by slightly increasing $\tilde{p}_2^1$ such that $s_2^1 = \tilde{p}_2^1 + \min(P_2^{max} - P, \epsilon/2)$ and $s_k^n = \tilde{p}_k^n$ for all the other $k \in \mathcal{K}$ and $n \in \mathcal{N}$. Clearly, $\mathbf{S}$ is feasible and satisfies $||\mathbf{S} - \widetilde{\mathbf{P}}|| < \epsilon$. Since R^n is a strictly increasing function of p_2^n, we have $R^1(s_1^1, s_2^1) > R^1(\tilde{p}_1^1, \tilde{p}_2^1)$ from $s_2^1 > \tilde{p}_2^1$ and thus $\sum_{n=1}^{N} R^n(\mathbf{S}^n) > \sum_{n=1}^{N} R^n(\widetilde{\mathbf{P}}^n)$, which is a contradiction.

Next, assume to the contrary of (2.17a) that $0 < \sum_{n=1}^{N} \tilde{p}_1^n = P < P_1^{max}$. If there exists a subcarrier n such that $g_1^n \geq g_{12}^n$, then R^n is a strictly increasing function of p_1^n by Lemma 1, and we can reach a contradiction by slightly increasing $\tilde{p}_1^n$ as in the above. Now, suppose

that $g_1^n < g_{12}^n,\ \forall n \in \mathcal{N}$ and choose a subcarrier n with $\tilde{p}_1^n > 0$. By Lemma 1, $R^n(p_1^n|\tilde{p}_2^n) := R^n(p_1^n, \tilde{p}_2^n)$ is either strictly increasing, strictly decreasing, or unimodal on p_1^n. If $R^n(p_1^n|\tilde{p}_2^n)$ is a strictly increasing function, we can reach a contradiction by slightly increasing p_1^n. If $R^n(p_1^n|\tilde{p}_2^n)$ is a strictly decreasing function, we can find a new power allocation vector $\mathbf{S}$ such that $s_1^n = \max(\tilde{p}_1^n - \epsilon/2, 0)$ and $s_k^n = \tilde{p}_k^n$ for all the other $k \in \mathcal{K}$ and $n \in \mathcal{N}$. It is clear that $\mathbf{S}$ is feasible and $||\mathbf{S} - \widetilde{\mathbf{P}}|| < \epsilon$. Since $s_1^n < \tilde{p}_1^n$, we have $R^n(s_1^n, s_2^n) > R^n(\tilde{p}_1^n, \tilde{p}_2^n)$ and thus $\sum_{n=1}^N R^n(\mathbf{S}^n) > \sum_{n=1}^N R^n(\widetilde{\mathbf{P}}^n)$, which is a contradiction. Lastly, if $R^n(p_1^n|\tilde{p}_2^n)$ is a unimodal function, we have either $\partial_1 R^n(p_1^n|\tilde{p}_2^n) \geq 0$ or $\partial_1 R^n(p_1^n|\tilde{p}_2^n) < 0$ at $p_1^n = \tilde{p}_1^n$. Then we reach a contradiction again by slightly increasing or decreasing $\tilde{p}_1^n$. □

We next show some well-known necessary conditions for local optimality. For given $\mathbf{P}$, let $\mathcal{N}_k(\mathbf{P})$ denote the set of subcarriers used by link k, i.e., $\mathcal{N}_k(\mathbf{P}) := \{n \in \mathcal{N} | p_k^n > 0\}$, and let $\mathcal{K}^n(\mathbf{P})$ denote the set of links using subcarrier n, i.e., $\mathcal{K}^n(\mathbf{P}) := \{k \in \mathcal{K} | p_k^n > 0\}$. Also, let us denote $\partial_k R^n(\mathbf{P}^n) := \frac{\partial}{\partial p_k^n} R^n(\mathbf{P}^n)$ and $\partial_{kl} R^n(\mathbf{P}^n) := \frac{\partial}{\partial p_k^n p_l^n} R^n(\mathbf{P}^n)$. Proposition 3 and Proposition 4 represent the KKT conditions and second-order necessary conditions for local optimality, respectively. Since those conditions can be easily obtained from the standard optimization theory [33], we omit the proof.

Proposition 3 (KKT Conditions)**.** Let $\widetilde{\mathbf{P}}$ be a local optimum. Then

there exist constants $\boldsymbol{\lambda}$ such that for all $k \in \mathcal{K}$ and $n \in \mathcal{N}$

$$\lambda_k \geq 0, \tilde{p}_k^n \geq 0, P_k^{max} - \sum_{n=1}^{N} \tilde{p}_k^n \geq 0, \tag{2.18a}$$

$$\lambda_k \left(P_k^{max} - \sum_{n=1}^{N} \tilde{p}_k^n \right) = 0, \tag{2.18b}$$

$$\lambda_k - \partial_k R^n(\widetilde{\mathbf{P}}^n) \geq 0, \tag{2.18c}$$

$$\tilde{p}_k^n \left(\lambda_k - \partial_k R^n(\widetilde{\mathbf{P}}) \right) = 0. \tag{2.18d}$$

Proposition 4 (Second-order Necessary Conditions)**.** Let $\widetilde{\mathbf{P}}$ be a feasible power allocation vector satisfying the KKT conditions (2.18) and $\sum_{n=1}^{N} \tilde{p}_k^n = P_k^{max},\ \forall k \in \mathcal{K}$. If $\widetilde{\mathbf{P}}$ is a local optimum, then for any vector $v = \left(v_1^1, \ldots, v_2^N\right) \in \mathbb{R}^{2N}$ such that

$$v_k^n = 0, \forall n \notin \mathcal{N}_k \text{ and } \sum_{n \in \mathcal{N}_k} v_k^n = 0, \forall k \in \mathcal{K}, \tag{2.19}$$

we should have

$$\sum_{n=1}^{N} (v^n)^T \nabla^2 R^n(\widetilde{\mathbf{P}}^n) v^n \leq 0, \tag{2.20}$$

where $v^n := (v_1^n, v_2^n)^T \in \mathbb{R}^2$.

Proposition 4 implies that for a certain power allocation $\mathbf{P}$ with $\sum_{n=1}^{N} p_k^n = P_k^{max},\ \forall k \in \mathcal{K}$, if we can find a vector v that satisfies (2.19) but does not (2.20), then $\mathbf{P}$ is not a local optimum.

In the following subsection, we use the necessary conditions to prove the optimality of FDMA power allocation in very strong inter-

ference environments.

2.4.2 Optimality of FDMA Power Allocation

In this subsection, we show that when the interference channel gain g_{12}^n for subcarier n is very large, either the uplink or the downlink allocates non-zero power to subcarrier n. If such a property holds for all subcarriers, we call it an FDMA power allocation.

Definition 3. For a feasible power allocation vector $\mathbf{P}$, we define the set $\mathcal{N}_S(\mathbf{P})$ of subcarriers shared by the uplink and the downlink as $\mathcal{N}_S(\mathbf{P}) := \{n \in \mathcal{N} || \mathcal{K}^n(\mathbf{P})| = 2\}$. Then $\mathbf{P}$ is said to have the *FDMA property* if there is no subcarrier shared by the uplink and the downlink, i.e., $\mathcal{N}_S(\mathbf{P}) = \emptyset$.

We assume the following non-strict conditions.

Assumption 1. An optimal solution $\mathbf{P}$ to problem P without joint decoding satisfies

(a) $M := \min_{k \in \mathcal{K}} |\mathcal{N}_k(\mathbf{P})| \geq 2$,

(b) $\sum_{n=1}^{N} p_k^n = P_k^{max}, \forall k \in \mathcal{K}$.

In the above, condition (a) indicates that each link uses at least two subcarriers. In most cellular systems and WLANs, there are a number of subcarriers, which is constantly increasing due to the growing bandwidth demand. For instance, the IEEE 802.11ac standard specifies 468 subcarriers over 160 MHz bandwidth [35]. Hence, it is highly likely that condition (a) holds in practice. Condition (b) means that both

the links consume all of their power budgets. From Proposition 2, this may not hold for the uplink ($k = 1$). However, we have $\sum_{n=1}^{N} p_1^n = 0$ for a local optimum $\mathbf{P}$ in limited cases, e.g., $g_{12}^n \gg g_2^n \gg g_1^n$, and we can also assume that condition (b) generally holds in practice.

Now, we find a sufficient condition under which any optimal solution has FDMA property. From Definition 3, it suffices to show that any feasible $\mathbf{P}$ with $|\mathcal{N}_S(\mathbf{P})| \geq 1$ cannot be a local optimum. Specifically, we will show that for any $\mathbf{P}$ with $|\mathcal{N}_S(\mathbf{P})| \geq 1$, there exists a vector v such that the second-order necessary condition (2.20) does not hold. We first consider the case $|\mathcal{N}_S(\mathbf{P})| \geq 2$. Let us define $\mathcal{N}_F := \{n \in \mathcal{N} | g_{12}^n > g_1^n\}$. The following proposition shows that if the uplink and the downlink share two or more subcarriers $n \in \mathcal{N}_F$, then $\mathbf{P}$ cannot be a local optimum.

Proposition 5. Let $\mathbf{P}$ be a feasible power allocation vector such that $|\mathcal{N}_S(\mathbf{P})| \geq 2$. If Assumption 1 holds and

$$|\mathcal{N}_S(\mathbf{P}) \cap \mathcal{N}_F| \geq 2, \tag{2.21}$$

then $\mathbf{P}$ cannot be a local optimum.

Proof. We prove this by contradiction following the technique in [31]. Assume to the contrary that a feasible power allocation vector $\mathbf{P}$ with $|\mathcal{N}_S(\mathbf{P}) \cap \mathcal{N}_F| \geq 2$ is a local optimum. Choose two subcarriers $n_1, n_2 \in \mathcal{N}_S(\mathbf{P}) \cap \mathcal{N}_F$. Then, from the KKT conditions (2.18d), we

have

$$0 < \lambda_1 = \partial_1 R^{n_1}(\mathbf{P}^{n_1}) = \partial_1 R^{n_2}(\mathbf{P}^{n_2}),$$
$$0 < \lambda_2 = \partial_2 R^{n_1}(\mathbf{P}^{n_1}) = \partial_2 R^{n_2}(\mathbf{P}^{n_2}).$$

Now, let us define $v \in \mathbb{R}^{2N}$ as

$$v_1^{n_1} = \partial_2 R^{n_1}(\mathbf{P}^{n_1}), v_2^{n_1} = -\partial_1 R^{n_1}(\mathbf{P}^{n_1}),$$
$$v_1^{n_2} = -\partial_2 R^{n_2}(\mathbf{P}^{n_2}), v_2^{n_2} = \partial_1 R^{n_2}(\mathbf{P}^{n_2}),$$
$$v_1^n = v_2^n = 0, \forall n \in \mathcal{N} \backslash \{n_1, n_2\}.$$

Note that v satisfies (2.19) and $\nabla R^n(\mathbf{P}^n)v^n = 0$ where $v^n := (v_1^n, v_2^n)^T$. From the fact that subcarriers $n_1, n_2 \in \mathcal{N}_F$, R^{n_1} and R^{n_2} are quasi-convex by Proposition 1. Then we have

$$\begin{aligned}
&\sum_{n=1}^{N} (v^n)^T \nabla^2 R^n(\mathbf{P}^n) v^n \\
&= \begin{pmatrix} v_1^{n_1} \\ v_2^{n_1} \end{pmatrix}^T \nabla^2 R^{n_1}(\mathbf{P}^{n_1}) \begin{pmatrix} v_1^{n_1} \\ v_2^{n_1} \end{pmatrix} + \begin{pmatrix} v_1^{n_2} \\ v_2^{n_2} \end{pmatrix}^T \nabla^2 R^{n_2}(\mathbf{P}^{n_2}) \begin{pmatrix} v_1^{n_2} \\ v_2^{n_2} \end{pmatrix} \\
&= \begin{pmatrix} \partial_2 R^{n_1}(\mathbf{P}^{n_1}) \\ -\partial_1 R^{n_1}(\mathbf{P}^{n_1}) \end{pmatrix}^T \nabla^2 R^{n_1}(\mathbf{P}^{n_1}) \begin{pmatrix} \partial_2 R^{n_1}(\mathbf{P}^{n_1}) \\ -\partial_1 R^{n_1}(\mathbf{P}^{n_1}) \end{pmatrix} \\
&\quad + \begin{pmatrix} -\partial_2 R^{n_2}(\mathbf{P}^{n_2}) \\ \partial_1 R^{n_2}(\mathbf{P}^{n_2}) \end{pmatrix}^T \nabla^2 R^{n_2}(\mathbf{P}^{n_2}) \begin{pmatrix} -\partial_2 R^{n_2}(\mathbf{P}^{n_2}) \\ \partial_1 R^{n_2}(\mathbf{P}^{n_2}) \end{pmatrix} > 0,
\end{aligned}$$

where the last inequality comes from the quasi-convexity (2.16) of R^{n_1}

and R^{n_2}. Since the second-order necessary condition (2.20) does not hold, $\mathbf{P}$ cannot be a local optimum.

□

For the case of $|\mathcal{N}_S(\mathbf{P})|= 1$, suppose without loss of generality that $\mathcal{N}_S(\mathbf{P}) = \{n\}$, i.e., only subcarrier n is shared by the uplink and the downlink. The following proposition proves that if the interference channel gain g_{12}^n is large enough (in the sense of being larger than a certain threshold), then $\mathbf{P}$ cannot be a local optimum.

Proposition 6. Let us define

$$g_M := \max_{n\in\mathcal{N},k\in\mathcal{K}} g_k^n \quad \text{and} \quad g_m := \min_{n\in\mathcal{N},k\in\mathcal{K}} g_k^n.$$

Let $\mathbf{P}$ be a feasible power allocation vector such that $\mathcal{N}_S(\mathbf{P}) = \{n\}$, i.e., $|\mathcal{N}_S(\mathbf{P})|= 1$. If Assumption 1 holds and

$$g_{12}^n \geq 2\frac{g_M^3}{g_m^2}\left(1 + 2g_m P_2^{max}\right)^2, \tag{2.22}$$

then $\mathbf{P}$ cannot be a local optimum.

Proof. We first calculate the first- and second-order derivatives of R^n. To simplify the notations of the derivatives, let us write R^n as

$$R^n(\mathbf{P}^n) = \log\left(1 + \frac{p_1^n}{\sigma_1^n}\right) + \log\left(1 + \frac{p_2^n}{\sigma_2^n + \alpha_{12}^n p_1^n}\right),$$

where $\sigma_k^n := 1/g_k^n$ and $\alpha_{12}^n := g_{12}^n/g_2^n$. Also, given $\mathbf{P}$, let us define that

for all $n \in \mathcal{N}$ and $k \in \mathcal{K}$,

$$\begin{aligned} X_1^n(\mathbf{P}^n) &:= \sigma_1^n, \\ X_2^n(\mathbf{P}^n) &:= \sigma_2^n + \alpha_{12}^n p_1^n, \\ A_k^n(\mathbf{P}^n) &:= \frac{1}{X_k^n}, \\ B_k^n(\mathbf{P}^n) &:= \frac{1}{X_k^n + p_k^n}. \end{aligned} \tag{2.23}$$

Note that $A_k^n \geq B_k^n$ where the equality holds when $p_k^n = 0$. Using (2.23), we obtain the partial derivatives as

$$\partial_1 R^n(\mathbf{P}^n) = B_1^n + \alpha_{12}^n \left(B_2^n - A_2^n\right), \tag{2.24a}$$

$$\partial_2 R^n(\mathbf{P}^n) = B_2^n, \tag{2.24b}$$

$$\partial_{11} R^n(\mathbf{P}^n) = -(B_1^n)^2 + (\alpha_{12}^n)^2 \left\{(A_2^n)^2 - (B_2^n)^2\right\}, \tag{2.24c}$$

$$\partial_{12} R^n(\mathbf{P}^n) = \partial_{21} R^n(\mathbf{P}^n) = -\alpha_{12}^n (B_2^n)^2, \tag{2.24d}$$

$$\partial_{22} R^n(\mathbf{P}^n) = -(B_2^n)^2. \tag{2.24e}$$

Since this is a simple calculation, we omit the proof due to the lack of space.

We now prove Proposition 6 by contradiction. Assume to the contrary that $\mathbf{P}$ is a local optimum. Also, suppose without loss of generality that subcarrier 1 is shared by the uplink and the downlink, i.e., $\mathcal{N}_S(\mathbf{P}) = \{1\}$. Let us define $\mathcal{N}_E(\mathbf{P}) := \{n \in \mathcal{N} || \mathcal{K}^n(\mathbf{P})| = 1\}$, i.e., the set of subcarriers used by either the uplink or the downlink. From Assumption 1 ($M := \min_k |\mathcal{N}_k(\mathbf{P})| \geq 2$), there exist subcarriers

$n_1, \cdots, n_{M-1}$ and $m_1, \cdots, m_{M-1}$ such that

$$n_1, \cdots, n_{M-1} \in \mathcal{N}_1(\mathbf{P}) \cap \mathcal{N}_E(\mathbf{P}),$$
$$m_1, \cdots, m_{M-1} \in \mathcal{N}_2(\mathbf{P}) \cap \mathcal{N}_E(\mathbf{P}).$$

Then from the KKT conditions (2.18d), we have

$$0 \leq \lambda_1 = \partial_1 R^1(\mathbf{P}^1) = \cdots = \partial_1 R^{n_{M-1}}(\mathbf{P}^{n_{M-1}}). \tag{2.25}$$

Also, from $n_j \in \mathcal{N}_1(\mathbf{P}) \cap \mathcal{N}_E(\mathbf{P})$, we have $p_2^{n_j} = 0$ and thus $A_2^{n_j} = B_2^{n_j}$. This simplifies (2.24a) and (2.24c) as

$$\begin{aligned} \partial_1 R^{n_j}(\mathbf{P}^{n_j}) &= B_1^{n_j}, \\ \partial_{11} R^{n_j}(\mathbf{P}^{n_j}) &= -\left(B_1^{n_j}\right)^2. \end{aligned} \tag{2.26}$$

Then we have for all $j = 1, \cdots, M-1$,

$$\partial_{11} R^{n_j}(\mathbf{P}^{n_j}) \overset{\text{(a)}}{=} -(\partial_1 R^{n_j}(\mathbf{P}^{n_j}))^2 \overset{\text{(b)}}{=} -\left(\partial_1 R^1(\mathbf{P}^1)\right)^2 = -\left(B_1^1\right)^2, \tag{2.27}$$

where the equalities (a) and (b) come from (2.26) and (2.25), respectively. Similarly, we obtain

$$\partial_{22} R^{m_j}(\mathbf{P}^{m_j}) = -(\partial_2 R^{m_j}(\mathbf{P}^{m_j}))^2 = -\left(\partial_2 R^1(\mathbf{P}^1)\right)^2 = -\left(B_2^1\right)^2, \tag{2.28}$$

for all $j = 1, \cdots, M-1$.

Next, let us define $v \in \mathbb{R}^{2N}$ as

$$
\begin{aligned}
& v_1^1 = \alpha_{12}^1, \\
& v_2^1 = -\alpha_{12}^1, \\
& v_1^{n_j} = -\alpha_{12}^1 (M-1)^{-1}, \ \ (j = 1, \cdots, M-1), \\
& v_2^{m_j} = \alpha_{12}^1 (M-1)^{-1}, \quad (j = 1, \cdots, M-1), \\
& v_1^n = v_2^n = 0, \qquad\qquad \text{others.}
\end{aligned}
$$

By inserting v into $\sum_n (v^n)^T \nabla^2 R^n (\mathbf{P}^n) v^n$, we have (2.29), where the equality (a) comes from (2.27) and (b) from $A_2^1 \geq B_2^1$.

To show that $\sum_{n=1}^N (v^n)^T \nabla^2 R^n (\mathbf{P}^n) v^n > 0$, we find a lower bound of B_2^1 and an upper bound of B_1^1 and B_2^1. Let us define $\sigma_M := \frac{1}{g_m}$ and $\sigma_m := \frac{1}{g_M}$. Since $\mathbf{P}$ is a local optimum, given the uplink power allocation $\{p_1^n\}_{n \in \mathcal{N}}$, the downlink power $\{p_2^n\}_{n \in \mathcal{N}}$ is allocated according to the water-filling algorithm as

$$
p_2^n = \begin{cases} \gamma_2 - \left(\sigma_2^1 + \alpha_{12}^1 p_1^1\right), \text{ if } n = 1, \\ \gamma_2 - \sigma_2^n, \qquad\qquad \text{if } n \in \mathcal{N}_2(\mathbf{P}) \backslash \{1\}, \\ 0, \qquad\qquad\qquad \text{otherwise,} \end{cases}
$$

where γ_2 is the downlink water-level such that $\sum_{n=1}^N p_2^n = P_2^{\max}$. Since $|\mathcal{N}_2(\mathbf{P})| \geq M \geq 2$ by Assumption 1, we have $\gamma_2 < \sigma_M + P_2^{\max}$, where $\sigma_M + P_2^{\max}$ is the water-level when the total power P_2^{max} is allocated to only one subcarrier with the minimum channel gain $g_m = \frac{1}{\sigma_M}$.

$$
\begin{aligned}
&\sum_{n=1}^{N} (v^n)^T \nabla^2 R^n\left(\mathbf{P}^n\right) v^n \\
&= \begin{pmatrix} v_1^1 \\ v_2^1 \end{pmatrix}^T \begin{pmatrix} \partial_{11} R^1(\mathbf{P}^1)\ \partial_{12} R^1(\mathbf{P}^1) \\ \partial_{21} R^1(\mathbf{P}^1)\ \partial_{22} R^1(\mathbf{P}^1) \end{pmatrix} \begin{pmatrix} v_1^1 \\ v_2^1 \end{pmatrix} \\
&\quad + \sum_{j=1}^{M-1} \begin{pmatrix} v_1^{n_j} \\ 0 \end{pmatrix}^T \begin{pmatrix} \partial_{11} R^{n_j}(\mathbf{P}^{n_j})\ \partial_{12} R^{n_j}(\mathbf{P}^{n_j}) \\ \partial_{21} R^{n_j}(\mathbf{P}^{n_j})\ \partial_{22} R^{n_j}(\mathbf{P}^{n_j}) \end{pmatrix} \begin{pmatrix} v_1^{n_j} \\ 0 \end{pmatrix} \\
&\quad + \sum_{j=1}^{M-1} \begin{pmatrix} 0 \\ v_2^{m_j} \end{pmatrix}^T \begin{pmatrix} \partial_{11} R^{m_j}(\mathbf{P}^{m_j})\ \partial_{12} R^{m_j}(\mathbf{P}^{m_j}) \\ \partial_{21} R^{m_j}(\mathbf{P}^{m_j})\ \partial_{22} R^{m_j}(\mathbf{P}^{m_j}) \end{pmatrix} \begin{pmatrix} 0 \\ v_2^{m_j} \end{pmatrix} \\
&= -\left(v_1^1\right)^2 \left(B_1^1\right)^2 + \left(v_1^1\right)^2 \left(\alpha_{12}^1\right)^2 \left\{ \left(A_2^1\right)^2 - \left(B_2^1\right)^2 \right\} \\
&\quad + \left\{ -2 v_1^1 v_2^1 \alpha_{12}^1 - \left(v_2^1\right)^2 \right\} \left(B_2^1\right)^2 \\
&\quad + \sum_{j=1}^{M-1} \{ - \left(v_1^{n_j}\right)^2 \left(B_1^{n_j}\right)^2 \} + \sum_{j=1}^{M-1} \{ - \left(v_2^{m_j}\right)^2 \left(B_2^{m_j}\right)^2 \} \\
&\overset{\text{(a)}}{=} -\left(\alpha_{12}^1\right)^2 \left(B_1^1\right)^2 + \left(\alpha_{12}^1\right)^4 \left\{ \left(A_2^1\right)^2 - \left(B_2^1\right)^2 \right\} \\
&\quad + \left\{ 2\left(\alpha_{12}^1\right)^3 - \left(\alpha_{12}^1\right)^2 \right\} \left(B_2^1\right)^2 \\
&\quad + \{ - \left(\alpha_{12}^1\right)^2 (M-1)^{-1} \} \left(B_1^1\right)^2 + \{ - \left(\alpha_{12}^1\right)^2 (M-1)^{-1} \} \left(B_2^1\right)^2 \\
&\overset{\text{(b)}}{\geq} \left(\alpha_{12}^1\right)^2 \left[2 \left(\alpha_{12}^1\right) \left(B_2^1\right)^2 - \left(1 + (M-1)^{-1}\right) \left\{ \left(B_2^1\right)^2 + \left(B_1^1\right)^2 \right\} \right],
\end{aligned}
\tag{2.29}
$$

Furthermore, from $p_2^1 > 0$, we also have

$$\sigma_2^1 + \alpha_{12}^1 p_1^1 < \gamma_2 < \sigma_M + P_2^{\max}. \tag{2.30}$$

Then we obtain a lower bound of B_2^1 as

$$B_2^1 = \frac{1}{\sigma_2^1 + \alpha_{12}^1 p_1^1 + p_2^1} \overset{(a)}{>} \frac{1}{\sigma_M + P_2^{\max} + p_2^1} \overset{(b)}{>} \frac{1}{\sigma_M + 2P_2^{\max}}, \tag{2.31}$$

where the equality (a) comes from (2.30) and (b) holds because $p_2^1 < P_2^{max}$. In addition, we find an upper bound of B_1^1 and B_2^1 as

$$\begin{aligned} B_1^1 \le A_1^1 &= \frac{1}{\sigma_1^1} \le \frac{1}{\sigma_m}, \\ B_2^1 \le A_2^1 &= \frac{1}{\sigma_2^1 + \alpha_{12}^1 p_1^1} < \frac{1}{\sigma_2^1} \le \frac{1}{\sigma_m}. \end{aligned} \tag{2.32}$$

By inserting (2.31) and (2.32) into the last equation of (2.29), we have

$$\begin{aligned} &\sum_{n=1}^{N} (v^n)^T \nabla^2 R^n (\mathbf{P}^n) v^n \\ &\ge \left(\alpha_{12}^1\right)^2 \left[2\left(\alpha_{12}^1\right)\left(B_2^1\right)^2 - \left(1 + (M-1)^{-1}\right)\left\{\left(B_2^1\right)^2 + \left(B_1^1\right)^2\right\}\right] \\ &> \left(\alpha_{12}^1\right)^2 \left[2\left(\alpha_{12}^1\right)\left(\frac{1}{\sigma_M + 2P_2^{\max}}\right)^2 - \left(1 + (M-1)^{-1}\right)\left\{2\left(\frac{1}{\sigma_m}\right)^2\right\}\right] \\ &\ge 0, \end{aligned}$$

where the last inequality comes from

$$\left(\alpha_{12}^1\right) = \frac{g_{12}^1}{g_2^1} \geq \frac{g_{12}^1}{g_M} \overset{\text{(a)}}{\geq} 2\frac{g_M^2}{g_m^2}\left(1+2g_m P_2^{max}\right)^2 \overset{\text{(b)}}{\geq} \frac{\left(1+(M-1)^{-1}\right)\left(\sigma_M + 2P_2^{\max}\right)^2}{\left(\sigma_m\right)^2},$$

where the inequality (a) is from (2.22) and (b) holds because $M \geq 2$. Since the second-order necessary condition (2.20) does not hold, $\mathbf{P}$ cannot be a local optimum. □

Combining Propositions 5 and Proposition 6, we establish a sufficient condition, under which any global optimal solution has the FDMA property.

Theorem 1. If Assumption 1 holds and

$$g_{12}^n \geq 2\frac{g_M^3}{g_m^2}\left(1+2g_m P_2^{max}\right)^2, \forall n \in \mathcal{N}, \tag{2.33}$$

then any global optimal power allocation should have the FDMA property.

Proof. If Eq. (2.33) holds, Eq. (2.21) holds in any $\mathbf{P}$ with $|\mathcal{N}_S| \geq 2$, and Eq. (2.22) holds in any $\mathbf{P}$ with $|\mathcal{N}_S| = 1$ Thus, the proof is straightforward from Proposition 5 ($|\mathcal{N}_S| \geq 2$) and Proposition 6 ($|\mathcal{N}_S| = 1$). □

Notice that condition (2.33) is satisfied if for every subcarrier $n \in \mathcal{N}$, the interference channel gain g_{12}^n is sufficiently larger than the channel

gains g_1^n and g_2^n. This happens when node U and node D are close to each other and both are distant from node F. In cellular networks, this is the case when two uplink and downlink terminals are in proximity and located at cell edge.

2.4.3 NP-hardness of Finding Optimal Power Allocation

We show that finding an optimal FDMA power allocation is NP-hard, which in turn implies that problem P without joint decoding is also NP-hard.

Let us define $\mathcal{P}_{FDMA} := \{\mathbf{P} \geq 0 | p_1^n p_2^n = 0, \forall n \in \mathcal{N}\}$, i.e., the set of all FDMA power allocation vectors. Under the constraint of $\mathbf{P} \in \mathcal{P}_{FDMA}$, the problem becomes a subcarrier allocation problem where each subcarrier is exclusively assigned to either the uplink or the downlink. We formulate the FDMA subcarrier assignment problem $\mathsf{P}_{\mathsf{FDMA}}$ as follows:

$$\begin{aligned} (\mathsf{P}_{\mathsf{FDMA}}) \quad \underset{\mathbf{P}}{\text{maximize}} \quad & \sum_{n=1}^{N} \log\left(1 + g_1^n p_1^n\right) + \log\left(1 + g_2^n p_2^n\right) \\ \text{subject to} \quad & \mathbf{P} \in \mathcal{P}_{FDMA}, \\ & \sum_{n=1}^{N} p_k^n \leq P_k^{max}, \forall k \in \mathcal{K}. \end{aligned} \tag{2.34}$$

Note that the inter-node interference $g_{12}^n p_1^n$ disappears. Also, given a subcarrier assignment pattern, the uplink and downlink powers are

allocated by the water-filling over the assigned subcarriers.

Theorem 2. Finding an optimal solution subcarrier assignment to problem $\mathsf{P}_{\mathsf{FDMA}}$ is NP-hard. Thus, problem P without the joint decoding is also NP-hard.

Proof. Without loss of generality, assume that N is an even integer. As in [31], we set the uplink and downlink channel gains to be the same for each subcarrier $n \in \mathcal{N},$, i.e., $g_1^n = g_2^n = g^n$, and $g_{12}^n = L$ where L is sufficiently large to satisfy the condition (2.33). Also, we set $P_1^{max} = P_2^{max} = P_M := (N+1)^3\sigma_M$ where $\sigma_M := \max_n \frac{1}{g^n}$. In the below, we prove that Assumption 1 holds under our channel setting.

Let us first show that in any optimal solution $\mathbf{P}$ to problem P, the number of subcarriers used by the uplink (and the downlink) is at least greater than or equal to 2, i.e., $M := \min\{\mathcal{N}_1(\mathbf{P}), \mathcal{N}_2(\mathbf{P})\} \geq 2$. We prove this by contradiction. Assume to the contrary that in an optimal power allocation $\mathbf{P}$, the uplink uses only subcarrier 1, i.e.,

$\mathcal{N}_1(\mathbf{P}) = \{1\}$. Then we find an upper bound of $\sum_{n=1}^{N} R^n(\mathbf{P}^n)$ as

$$\begin{aligned}
&\sum_{n=1}^{N} R^n(\mathbf{P}^n) \\
&= \log\left(1+g^1p_1^1\right) + \log\left(1+\frac{g^1p_2^1}{1+g_{12}^1p_1^1}\right) + \sum_{n=2}^{N}\log\left(1+g^np_2^n\right) \\
&\le \log\left(1+g^1p_1^1\right) + \sum_{n=1}^{N}\log\left(1+g^np_2^n\right) \\
&\le \log\left(1+g^1P_M\right) + \sum_{n=1}^{N}\log\left(p_2^n+\frac{1}{g^n}\right) + \sum_{n=1}^{N}\log g^n \\
&\le \log\left(1+g^1P_M\right) + \sum_{n=1}^{N}\log\left(\check{p}_2^n+\frac{1}{g^n}\right) + \sum_{n=1}^{N}\log g^n \qquad (2.35)\\
&= \log\left(1+g^1P_M\right) + \sum_{n=1}^{N}\log\left(\frac{P_M+\sum_{n=1}^{N}\frac{1}{g^n}}{N}\right) + \sum_{n=1}^{N}\log g^n \\
&< \log\left(P_M+N\sigma_M\right) - \log g^1 + N\log\left(P_M+N\sigma_M\right) \\
&\quad - N\log N + \sum_{n=1}^{N}\log g^n \\
&< (N+1)\log P_M - N\log N + \sum_{n=2}^{N}\log g^n + O(1/N),
\end{aligned}$$

where $\check{p}_2^n$ is the water-filling power allocation over subcarriers 1 to N as

$$\frac{1}{g^n} + \check{p}_2^n = \gamma_2 = \frac{P_M+\sum_{n=1}^{N}\frac{1}{g^n}}{N}, \forall n \in \mathcal{N},$$

where γ_2 is the corresponding water-level.

Now, consider a power allocation vector $\mathbf{S}$ where the uplink uses subcarriers 1 to $\frac{N}{2}$ and the downlink uses subcarriers $\frac{N}{2}+1$ to N with

the water-filling power allocation over the assigned subcarriers. In this case, we obtain a lower bound of the sum-rate $\sum_{n=1}^{N} R^n(\mathbf{S}^n)$ as

$$\begin{aligned}
&\sum_{n=1}^{N} R^n\left(\mathbf{S}^n\right) \\
&= \sum_{n=1}^{N/2} \log\left(1+g^n s_1^n\right) + \sum_{n=1+N/2}^{N} \log\left(1+g^n s_2^n\right) \\
&= \frac{N}{2}\log\left(\frac{P_M + \sum_{n=1}^{N/2}\frac{1}{g^n}}{N/2}\right) + \frac{N}{2}\log\left(\frac{P_M + \sum_{n=N/2+1}^{N}\frac{1}{g^n}}{N/2}\right) \\
&\quad + \sum_{n=1}^{N} \log g^n \\
&= \frac{N}{2}\log\left(P_M + \sum\nolimits_{n=1}^{N/2}\frac{1}{g^n}\right) + \frac{N}{2}\log\left(P_M + \sum\nolimits_{n=1+N/2}^{N}\frac{1}{g^n}\right) \\
&\quad - N\log\frac{N}{2} + \sum_{n=1}^{N}\log g^n \\
&> N\log P_M - N\log\frac{N}{2} + \sum_{n=1}^{N}\log g^n.
\end{aligned} \tag{2.36}$$

By comparing (2.35) and (2.36), it is clear that $\sum_{n=1}^{N} R^n(\mathbf{S}^n) > \sum_{n=1}^{N} R^n\left(\mathbf{P}^n\right)$ for a large N, which contradicts $\mathbf{P}$ is optimal. In a similar way, we can also cover the case that the downlink uses only one subcarrier, i.e., $\mathcal{N}_2(\mathbf{P}) = \{1\}$. Therefore, we have $M \geq 2$ in any optimal solution

We next show that $\sum_{n=1}^{N} p_1^n = P_1^{max}$ in any optimal solution. Since any local optimum $\widetilde{\mathbf{P}}$ should satisfy $\sum_{n=1}^{N} \tilde{p}_1^n = P_1^{max}$ or $\sum_{n=1}^{N} \tilde{p}_1^n =$

0 by Proposition 2, it suffices to prove that any $\mathbf{P}$ with $\sum_{n=1}^{N} p_1^n = 0$ cannot be optimal. When $\sum_{n=1}^{N} p_1^n = 0$, the downlink uses all the subcarriers without interference, and the corresponding optimal solution is the water-filling power allocation. It is clear that we have a larger sum-rate with the power allocation $\mathbf{S}$, i.e., subcarriers 1 to $\frac{N}{2}$ for the uplink and subcarriers $\frac{N}{2}+1$ to N for the downlink. Therefore, any optimal solution $\mathbf{P}$ with $\sum_{n=1}^{N} \tilde{p}_1^n = 0$ cannot be optimal.

Since condition (2.33) and Assumption 1 hold, any optimal solution has the FDMA property by Theorem 1, which means that the power allocation problem P is equivalent to the subcarrier allocation problem $\mathsf{P}_{\mathsf{FDMA}}$. We can show that problem $\mathsf{P}_{\mathsf{FDMA}}$ is NP-hard by reducing the equipartition problem to problem $\mathsf{P}_{\mathsf{FDMA}}$. Specifically, the equipartition problem is the task of deciding whether a given set $G = \{g^1, \cdots, g^N\}$ can be partitioned into two equal-sized subsets G_1 and G_2 such that the sum of the element values in G_1 equals that in G_2. It can be shown that for any optimal solution $\mathbf{P}$ to problem $\mathsf{P}_{\mathsf{FDMA}}$, the following condition holds

$$\sum_{n=1}^{N} R^n\left(\mathbf{P}^n\right) = N\log\left(\frac{2P_M + \sum_{n=1}^{N} \frac{1}{g^n}}{N}\right) + \sum_{n=1}^{N} \log g^n,$$

if and only if the equipartition problem has a "yes" answer (refer to Theorem 5.1 of [31] for details). This indicates that problem $\mathsf{P}_{\mathsf{FDMA}}$ is NP-hard and thus problem P is also NP-hard. □

Since problem P without joint decoding is in general NP-Hard, we

develop a heuristic solution in the next section. Recall that problem P with joint decoding is a convex optimization problem, since the downlink node can successfully cancel strong inter-node interference.

2.4.4 Partial FDMA Power Allocation

From Proposition 5, any power allocation vector $\mathbf{P}$ with $|\mathcal{N}_S(\mathbf{P}) \cap \mathcal{N}_F| \geq 2$ cannot be a (local) optimum. Motivated by this fact[2], we develop a power allocation algorithm where every subcarrier $n \in \mathcal{N}_F$ is exclusively used by either the uplink or the downlink. We start with some definitions.

Definition 4. A feasible power allocation vector $\mathbf{P}$ is said to have *Partial FDMA* property if every subcarrier $n \in \mathcal{N}_F$ is exclusively used by either the uplink or the downlink., i.e., $p_1^n p_2^n = 0, \forall n \in \mathcal{N}_F$.

Also, let us define $\mathcal{P}_{PF} = \{\mathbf{P} \geq 0 | p_1^n p_2^n = 0, \forall n \in \mathcal{N}_F\}$, i.e., the set of all partial FDMA power allocation vectors. It is clear that $\mathcal{P}_{PF}$ is not a convex set because a convex combination of two partial FDMA power allocation vectors does not have the partial FDMA property [30].

Now, we confine the solution space to $\mathcal{P}_{PF}$ and convert the problem P without the joint decoding to the following partial FDMA power

[2]Unfortunately, we have no proof for the non-optimality of a power allocation vector $\mathbf{P}$ with $|\mathcal{N}_S(\mathbf{P}) \cap \mathcal{N}_F| = 1$.

allocation problem.

$$
\begin{aligned}
(\mathsf{P_{PF}}) \quad \underset{\mathbf{P}}{\text{maximize}} \quad & \sum_{n \notin \mathcal{N}_F} \left(\log\left(1 + g_1^n p_1^n\right) + \log\left(1 + \frac{g_2^n p_2^n}{1 + g_{12}^n p_1^n}\right)\right) \\
& + \sum_{n \in \mathcal{N}_F} \left(\log\left(1 + g_1^n p_1^n\right) + \log\left(1 + g_2^n p_2^n\right)\right) \\
\text{subject to} \quad & \mathbf{P} \in \mathcal{P}_{PF}, \\
& \sum_{n=1}^{N} p_k^n \leq P_k^{max}, \forall k \in \mathcal{K}.
\end{aligned}
\tag{2.37}
$$

Notice that due to the partial FDMA constraint, the interference term $g_{12}^n p_1^n$ only appears in subcarriers $n \notin \mathcal{N}_F$. Although the objective function is concave, problem $\mathsf{P_{PF}}$ is not a convex optimization problem because the constraint set $\mathcal{P}_{PF}$ is not a convex set.

To solve problem $\mathsf{P_{PF}}$, we apply the standard Lagrangian dual

optimization method. The dual function $g(\boldsymbol{\lambda})$ is given by

$$
\begin{aligned}
& g(\boldsymbol{\lambda}) \\
& := \max_{\mathbf{P}\in\mathcal{P}_{PF}} \left\{ \sum_{n\notin\mathcal{N}_F} \log\left(1+g_1^n p_1^n\right) + \log\left(1+\frac{g_2^n p_2^n}{1+g_{12}^n p_1^n}\right) \right. \\
& \qquad + \sum_{n\in\mathcal{N}_F} \log\left(1+g_1^n p_1^n\right) + \log\left(1+g_2^n p_2^n\right) \\
& \qquad \left. + \sum_{k=1}^{2} \lambda_k \left(P_k^{max} - \sum_{n=1}^{N} p_k^n \right) \right\} \\
& = \sum_{k=1}^{2} \lambda_k P_k^{\max} \\
& \quad + \sum_{n\notin\mathcal{N}_F} \max_{p_1^n\geq 0, p_2^n\geq 0} \left\{ \log\left(1+g_1^n p_1^n\right) + \log\left(1+\frac{g_2^n p_2^n}{1+g_{12}^n p_1^n}\right) - \lambda_1 p_1^n - \lambda_2 p_2^n \right\} \qquad \text{(2.38a)} \\
& \quad + \sum_{n\in\mathcal{N}_F} \max_{\substack{p_1^n\geq 0, p_2^n\geq 0, \\ p_1^n p_2^n = 0}} \left\{ \log\left(1+g_1^n p_1^n\right) + \log\left(1+g_2^n p_2^n\right) - \lambda_1 p_1^n - \lambda_2 p_2^n \right\}, \qquad \text{(2.38b)}
\end{aligned}
$$

where $\boldsymbol{\lambda} = (\lambda_1, \lambda_2)$ are dual variables. The additional constraints $p_1^n p_2^n = 0$ in (2.38b) come from the partial FDMA constraint $\mathbf{P} \in \mathcal{P}_{PF}$. The closed-form solution $\{\hat{p}_1^n, \hat{p}_2^n\}_{\forall n\notin\mathcal{N}_F}$ to the inner maximization problem (2.38a) can be obtained as (2.9) and (2.10), and the solution

$\{\hat{p}_1^n, \hat{p}_2^n\}_{\forall n \in \mathcal{N}_F}$ to problem (2.38b) as (2.10). They are

$$(\hat{p}_1^n, \hat{p}_2^n) = \begin{cases} \left([\frac{1}{\lambda_1} - \frac{1}{g_1^n}]^+, 0\right), \text{ if } \log\left(1 + g_1^n[\frac{1}{\lambda_1} - \frac{1}{g_1^n}]^+\right) - \lambda_1\left[\frac{1}{\lambda_1} - \frac{1}{g_1^n}\right]^+ \\ \qquad\qquad > \log\left(1 + g_2^n[\frac{1}{\lambda_2} - \frac{1}{g_2^n}]^+\right) - \lambda_2\left[\frac{1}{\lambda_2} - \frac{1}{g_2^n}\right]^+, \\ \left(0, [\frac{1}{\lambda_2} - \frac{1}{g_2^n}]^+\right), \text{ otherwise.} \end{cases}$$

This means that subcarrier $n \in \mathcal{N}_F$ is given to link k satisfying with a larger $\max\left(\log(1 + g_k^n p_k^n) - \lambda_k p_k^n\right)$, and λ_k along with g_k^n decides which link will use subcarrier n.

The dual problem $\min_{\boldsymbol{\lambda} \geq 0}\left(g(\boldsymbol{\lambda})\right)$ can be solved by the subgradient method. In iteration t, the subgradient method updates $\boldsymbol{\lambda}$ by

$$\lambda_k^{(t+1)} = \left[\lambda_k^{(t)} - s_t\left(P_k^{max} - \sum\nolimits_{n \notin \mathcal{N}_F} \hat{p}_k^n(t) - \sum\nolimits_{n \in \mathcal{N}_F} \hat{p}_k^n(t)\right)\right]^+, \forall k \in \mathcal{K}, \tag{2.39}$$

where s_t is the t-th step size, $\{\hat{p}_k^n(t)\}_{n \notin \mathcal{N}_F}$ are the solution from (2.9) and (2.10), and $\{\hat{p}_k^n(t)\}_{n \in \mathcal{N}_F}$ are from (2.10) for given $(\lambda_1^{(t)}, \lambda_2^{(t)})$. As $\boldsymbol{\lambda}$ is updated, the link using subcarrier $n \in \mathcal{N}_F$ changes accordingly in each iteration. The update process is terminated when $\|\boldsymbol{\lambda}(t+1) - \boldsymbol{\lambda}(t)\| \leq \varepsilon$. It is clear that the final output $\hat{\mathbf{P}}$ will have the partial FDMA property, but it may not be feasible, i.e., $\sum_{n=1}^N \hat{p}_k^n > P_k^{max}$. To this end, we take the last step of normalization by $\frac{P_k^{\max}}{\sum_{n=1}^N \hat{p}_k^n}$ if $\hat{\mathbf{P}}$ is not feasible.

Table 2.1: Simulation Parameters

Parameter	Value
Center frequency	2.1 GHz
Subcarrier bandwidth	15 kHz
Noise power	-130 dBm
Antenna gain	0.0
h_{BS}	30 m
h_N	1.5 m

2.5 Performance Evaluation

In this section, we evaluate our solutions through numerical simulations. We configure simulation parameters by adopting typical values of LTE system [36]. We assume that each subcarrier has 15 kHz bandwidth, and set the noise power to -130 dBm. The Hata urban propagation model for urban environments has been used for the path loss P_{loss} (in dB) [36]:

$$\begin{aligned} P_{loss}(d) = 69.55 + 26.16 \cdot \log f - 13.83 \cdot \log h_B - C_H(f) \\ + (44.9 - 6.55 \cdot \log h_{BS}) \log d, \end{aligned} \tag{2.40}$$

where d (km) denotes the distance between the transmitter and the receiver, f (MHz) is the center frequency, h_{BS} (m) denotes the height of BS antenna, and $C_H(f)$ denotes the antenna height correlation factor defined as,

$$C_H(f) = 0.8 + (1.1 \cdot \log f - 0.7)\, h_N - 1.56 \cdot \log f, \tag{2.41}$$

where h_N (m) is the height of terminal node. Along with the path loss, we assume *i.i.d.* Rayleigh fading for each subcarrier. It is assumed that node U and node D are placed at an equal distance d from node F. Let $\bar{g}_2$ ($\bar{g}_1$) and $\bar{g}_{12}$ denote the average downlink (uplink) and inter-node channel gains, respectively, i.e., $\bar{g}_2 = E[g_2^n], \forall n$. Since the average channel gain only depends on the distance d, we have $\bar{g}_2 = \bar{g}_1$. We denote the ratio of $\bar{g}_{12}$ over $\bar{g}_2$ as $r_{I/S} := \frac{\bar{g}_{12}}{\bar{g}_2}$. Given the distance d and the corresponding $\bar{g}_2 = \bar{g}_1$, we change $\bar{g}_{12}$ to see how the performance varies with the inter-node interference. Also, for a power allocation vector $\mathbf{P}$, we define share ratio as the number of shared subcarriers over the number of subcarriers, i.e., $r_s = \frac{|\mathcal{N}_S(\mathbf{P})|}{N}$. The total transmission power for the uplink and the downlink is set to $P_1^{max} = P_2^{max} = 20$ dBm (100 mW) unless otherwise mentioned. Table 2.1 summarizes our simulation settings. Each point in the following figures is an average of 100 different channel realizations.

We denote the optimal power allocation scheme (Section 2.3) by OPT, and the partial FDMA scheme (Section 2.4.4) by P-FDMA. For performance comparison, we consider the following heuristic algorithms:

- Successive Convex Approximations (SCA) [37]: The problem without joint decoding is solved by a technique called successive convex approximations (SCA). The key idea is to transform $R^n = \log(1 + g_1^n p_1^n) + \log\left(1 + \frac{g_2^n p_2^n}{1+g_{12}^n p_1^n}\right)$ into a concave function and then solve a series of convex problems iteratively.

- Water-Filling (WF): The uplink (downlink) power is allocated by the water-filling algorithm without considering the inter-node interference.

We first examine the subcarrier-level power allocation under OPT and P-FDMA for given channel gains. We consider 12 subcarriers and set $P_1^{max} = P_2^{max} = 30$ dBm. We generate an instance of channel gains as in Figs. 2.3(a), 2.3(b), and 2.3(c), where a log scale is used for the y-axis. We intentionally set large interference channel gains for subcarriers 5 – 8 to observe how OPT and P-FDMA allocate power differently across those subcarriers. The power allocations under OPT and P-FDMA are shown in Fig. 2.3(d) and Fig. 2.3(e), respectively. In the case of OPT, the uplink and the downlink use subcarriers 1 – 8 and 5 – 12, respectively, with the water-filling power allocation. Even though the interference channel gains for subcarriers 5 – 8 are sufficiently large, those subcarriers are shared by the uplink and the downlink. This is because node D successfully remove the inter-node interference using the joint decoding when it is much stronger than the downlink signal. In contrast, P-FDMA allocates power in an FDMA manner such that the uplink and downlink use disjoint subcarrier sets, i.e., subcarriers 1 – 6 for uplink and subcarriers 7 – 12 for downlink. As expected, subcarriers 5 – 8 are not shared due to the excessive inter-node interference, which is treated as noise.

Next, we investigate how the inter-node interference impacts on overall performance. We consider 20 subcarriers and generate the

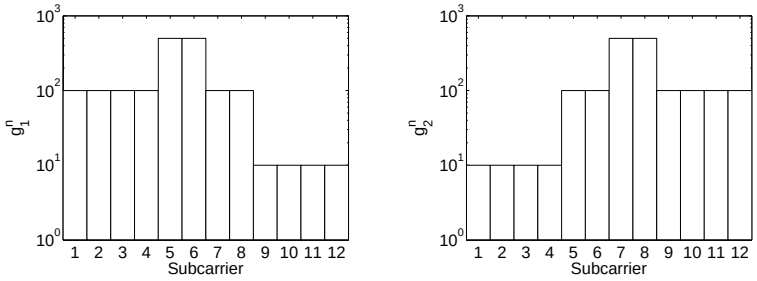

(a) Uplink channel gain

(b) Downlink channel gain

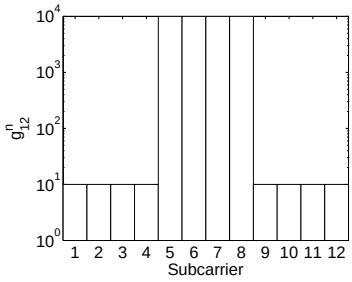

(c) Inter-node channel gain

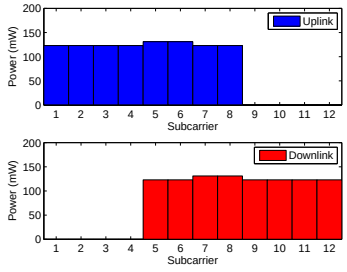

(d) OPT

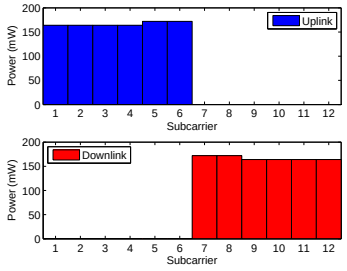

(e) P-FDMA

Figure 2.3: Channel gains and the corresponding power allocations under OPT and P-FDMA. The inter-node channel gains for subcarriers 5 – 8 are intentionally set as large to see how OPT and P-FDMA allocate power differently in those subcarriers. Subcarriers 5 – 8 are shared by the uplink and the downlink in OPT while they are not shared in P-FDMA due to the excessive inter-node interference, which is treated as noise.

channel gains according to the Hata propagation model and the Rayleigh fading. The performance of OPT is depicted in Fig. 2.4 where a log scale is used for the x-axis. The sum-rate decreases as $r_{I/S}$ increases from 10^{-3} to 1, and bounds up afterwards. This means that the sum-rate is maximized when the downlink signal dominates the interference (or vice versa), and is minimized when they have a similar strength.

Fig. 2.5 shows the performance of P-FDMA, which is different from that of OPT in strong interference region. As $r_{I/S}$ increases, the sum-rate of P-FDMA constantly decreases and converges to a point as shown in Fig. 2.5(a). This is a straightforward result since achievable rate shrinks as the interference (treated as noise) grows. Fig. 2.5(b) illustrates that r_s decreases with $r_{I/S}$ and eventually becomes zero, i.e., FDMA power allocation, as proved in Theorem 1. This also explains why the sum-rate converges to a point (rather than keep decreasing) when $r_{I/S}$ increases beyond a certain value.

We vary the downlink power budget P_2^{max} to see the impact of asymmetric uplink and downlink power budgets. We fix $P_1^{max} =$ 20 dBm and change P_2^{max} from 20 dBm to 40 dBm. Fig. 2.6(a) shows the uplink rate for various P_2^{max} values. When $r_{I/S}$ is small ($r_{I/S} < 10^{-2}$), the uplink rate remains similar regardless of P_2^{max}. As $r_{I/S}$ grows beyond 10^{-2}, the uplink rate decreases with P_2^{max}. For example, when $P_2^{max} = 40$ dBm, the uprate rate at $r_{I/S} = 10^3$ is almost zero. In contrast, the downlink rate increases with P_2^{max}

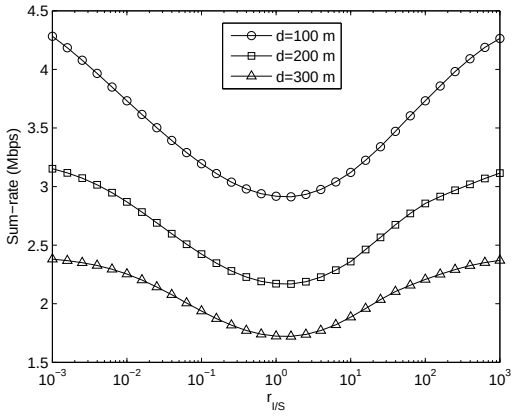

Figure 2.4: Performance of OPT under various interference levels.

as shown in Fig. 2.6(b). This result indicates that under strong interference environments, P-FDMA gives priority to the downlink since it can achieve a larger rate than the uplink due to the large downlink power budget.

Fig. 2.7 shows the number of subcarriers used by uplink and downlink for various P_2^{max} values. In strong interference environments, i.e., $r_{I/S} > 1$, the uplink uses less subcarriers as P_2^{max} increases. In contrast, the downlink are assigned more subcarriers with P_2^{max}. When $P_2^{max} = 40$ dBm, the downlink uses almost all subcarrieres for each value of $r_{I/S}$. In case of strong interference, each subcarrier should be assigned to either the uplink or the downlink. When P_2^{max} is sufficiently larger than P_1^{max}, the downlink can achieve a larger rate than the uplink, and consequently, almost all subcarriers are assigned to the downlink.

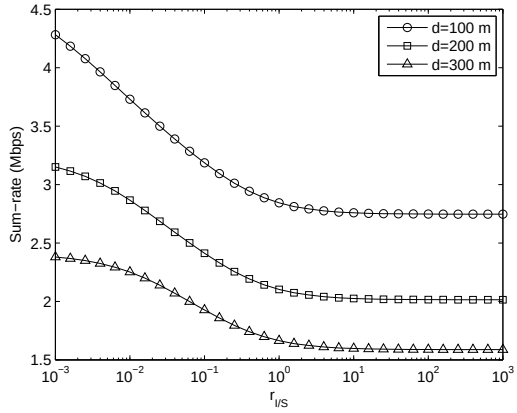

(a) Sum-rate

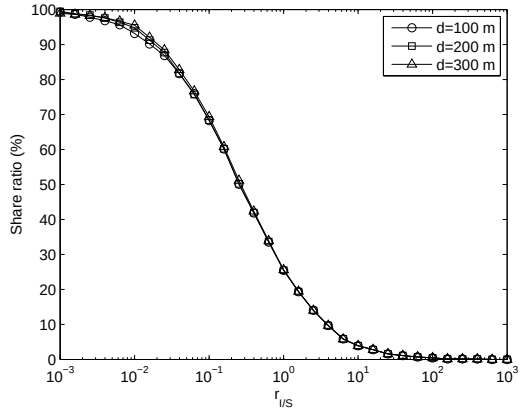

(b) Share ratio

Figure 2.5: Performance of P-FDMA under various interference levels. Fig. 2.5(a) shows that the sum-rate of P-FDMA constantly decreases and converges to a point as $r_{I/S}$ increases. Fig. 2.5(b) illustrates that the share ratio decreases with $r_{I/S}$ and eventually becomes zero, i.e., FDMA power allocation.

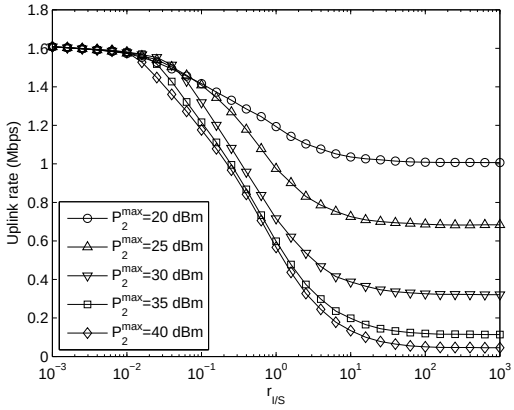

(a) Uplink rate

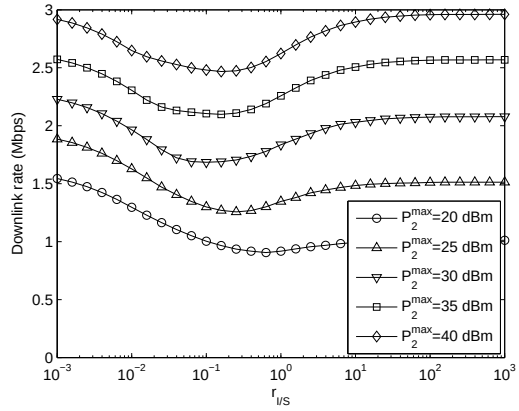

(b) Downlink rate

Figure 2.6: Impact of downlink power budget P_2^{max} on uplink and downlink rates.

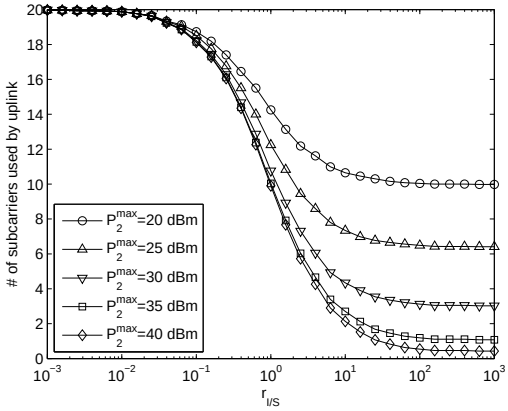

(a) Uplink

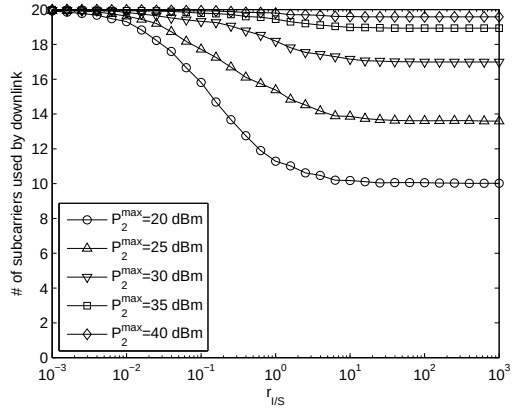

(b) Downlink

Figure 2.7: Impact of downlink power budget P_2^{max} on the number of subcarriers used by uplink (downlink).

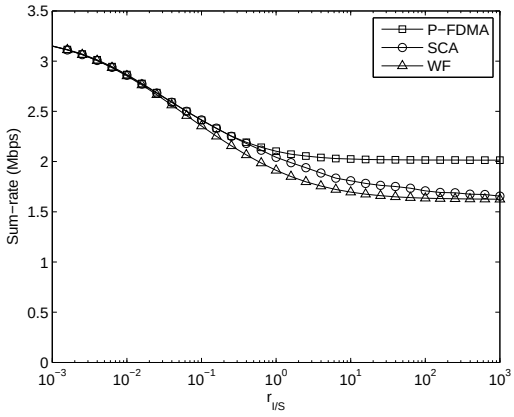

(a) Uplink

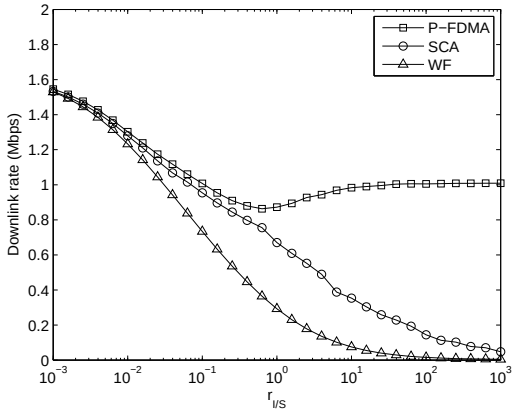

(b) Downlink

Figure 2.8: Performance comparison between P-FDMA and existing schemes.

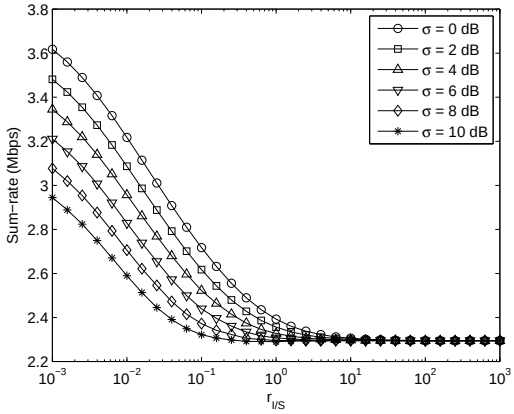

Figure 2.9: Impact of residual self-interference σ on performance.

The performance comparison between P-FDMA, SCA, and WF is shown in Fig. 2.8 when $d = 200$ m. When $r_{I/S}$ is small, all three schemes achieve a similar performance. This is because the optimal power allocation in weak interference region is similar to the water-filling algorithm. However, as the interference grows, P-FDMA outperforms SCA and WF with a substantial gain. In WF, the uplink power is allocated without considering the inter-node interference, and all the subcarriers are shared. As a result, as $r_{I/S}$ increases, the downlink rate becomes almost zero due to the excessive interference, as shown in Fig. 2.8(b) Similarly, the downlink rate of SCA converges to zero in very strong interference region because all subcarriers are shared. In contrast, P-FDMA converges to an FDMA power allocation where the uplink and the downlink use disjoint subcarrier subsets with an almost equal size. Hence, it avoids the excessive interference

without causing the starvation of the downlink transmission.

Lastly, we investigate the impact of residual self-interference on the performance. We assume that under imperfect interference cancellation, the noise power increases by σ dB due to the residual self-interference. Fig. 2.9 shows the sum-rate of P-FDMA for various σ values when $d = 200$ m. As expected, the sum-rate decreases with σ due to the growing noise power. However, as $r_{I/S}$ increases beyond a value, the sum-rate remains the same regardless of σ. This is because all subcarriers are used in half-duplex mode in high interference region.

2.6 Summary

In this chapter, we have considered the OFDM subcarrier power allocation problem for the case of three-node full-duplex transmissions under the inter-node interference. We have formulated the sum-rate maximization problem with and without joint decoding. We have proved that when the joint decoding is used, the problem is a convex optimization problem, which can be efficiently solved through our low-complexity Lagrangian dual method. When the inter-node interference is always treated as noise, finding an optimal (FDMA) power allocation is proven to be NP-hard. Thus, we have proposed a heuristic power allocation algorithm where only subcarriers with lower interference channel gains (compared to uplink channel gains) are shared

by the uplink and downlink. Through extensive simulations, we have evaluated the performance of our solution in various scenarios, and demonstrated that they outperform other existing schemes.

Chapter 3

Resource Allocation in Full-duplex OFDMA Networks

3.1 Introduction

Half-duplex has been a most common assumption in wireless communications and restricts a node to either transmit or receive at a time on the same frequency [17]. Recent advances in signal processing have challenged this assumption and demonstrated the feasibility of *in-band wireless full-duplex*, which enables a node to transmit and receive simultaneously on the same frequency band by countervailing against the self-interference caused by its own transmission. Due to its potential to boost throughput, the full-duplex capability has re-

ceived tremendous attention from both the academic and industrial world.

The main difficulty in building a full-duplex system is suppressing self-interference to a sufficiently low level. Extensive researches have been conducted for self-interference cancellation techniques, which can be categorized into antenna cancellation, analog cancellation, and digital cancellation. In antenna cancellation, a pair of transmission antennas are placed such that the signal from one antenna adds destructively with the signal from the other [1, 4, 5]. Analog cancellation taps a copy of the transmitted signal from the transmit chain, processes it with delay and attenuation, and subtracts it on the receive path [1, 3]. Lastly, digital cancellation is used to clean out any residual self-interference caused by non-ideal and non-linear components in RF chains [1, 3]. The state-of-the-art work has demonstrated that self-interference can be suppressed to the noise floor level by the combination of multiple cancellation techniques [6].

The full-duplex operation was first applied to a relay, which receives a signal from a source and re-transmits it to a destination in the same frequency. The full-duplex relay has been extensively studied in the context of information-theoretic analysis, assuming perfect or imperfect self-interference cancellations [21, 22, 23, 25, 26, 27, 28]. The impact of the full-duplex relay on the capacity of a single-source single-destination relay topology has been studied [21, 22, 23], and the capacity of a network with multi-user pairs has been also investi-

gated in [25, 26, 27, 28]. While these works provide the capacity or achievable rate of the full-duplex relay, their results are limited to a simple three-node relay topology or single-carrier environments.

Beyond the physical layer, full-duplex has the potential to significantly improve the throughput of a network by allowing more concurrent transmissions. Network-level mechanisms should be carefully addressed to fully exploit the benefits of full-duplex from network perspective. An important issue is how to apply full-duplex to wireless local area networks (WLANs), where the existing MAC protocols were designed for half-duplex links. New MAC protocols proposed in [7, 11, 12, 13] capture additional transmission opportunities created by full-duplex and activate as many transmissions as possible by modifying contention and backoff mechanisms. In addition, several MAC techniques were proposed to mitigate hidden node problem by sending a busy tone signal while receiving a packet [3, 7].

In contrast to full-duplex MAC protocols, there have been a few efforts to redesign the scheduling and resource allocation algorithms for full-duplex cellular networks. Most cellular systems adopt Orthogonal Frequency Division Multiple Access (OFDMA) as a key technology for multiple access [38, 39, 40]. Resource management in (half-duplex) downlink or uplink OFDMA systems has been extensively studied in the literature to maximize the sum-rate by assigning subcarriers and allocating transmission power. An optimal solution to the downlink problem is to assign each subcarrier to the user with the largest chan-

nel gain and allocate power according to the water-filling policy [41]. On the other hand, the uplink problem is more challenging due to distributive per-node power constraints, i.e., each node has its own power budget. Most previous results achieve suboptimal performance [42, 43, 44]. In full-duplex OFDMA networks, the base station (BS) is allowed to transmit downlink traffic to nodes while receiving uplink traffic from them simultaneously. Since the uplink and the downlink transmissions coexist, previous solutions considering either the downlink or the uplink are unlikely to optimize the performance, thus necessitating new solutions that account for the characteristics of the full-duplex transmissions.

In this chapter, we consider a single-cell full-duplex OFDMA networks which consists of one full-duplex BS and multiple full-duplex nodes. Our goal is to maximize the sum-rate by jointly optimizing subcarrier assignment and power allocation in the presence of the full-duplex transmissions. The contributions of this paper can be summarized as follows:

- We propose a joint solution to the subcarrier assignment and power allocation problem by establishing a necessary condition for optimality.

- We show that our algorithm is provably efficient in achieving *local Pareto optimality* under certain conditions that are frequently met in practice.

- By decoupling uplink and downlink transmissions and ignoring inter-node interference, we characterize the optimal performance in polynomial time complexity.

- Through extensive simulations, we show that our algorithm empirically achieves near-optimal performance and outperforms other resource allocation schemes. Also, our simulation results reveal the impact of various factors such as the channel correlation, the residual self-interference, and the distance between BS and nodes on the full-duplex gain. .

The rest of this chapter is organized as follows. The full-duplex sum-rate maximization problem is formally formulated in Section 3.2, and a necessary condition for optimality is derived in Section 3.3. Our proposed subcarrier assignment and power allocation algorithm is described in Section 3.4, and its performance is analytically evaluated in Section 3.5. We further characterize the full-duplex sum-rate and obtain a performance bound in Section 3.6, and empirically evaluate our solution in comparison with the bound and other resource allocation schemes in Section 3.7. Finally, we conclude this paper in Section 3.8.

3.2 System Model

We consider a single-cell full-duplex OFDMA network, as shown in Fig. 3.1. There are one full-duplex base station (BS) and N full-

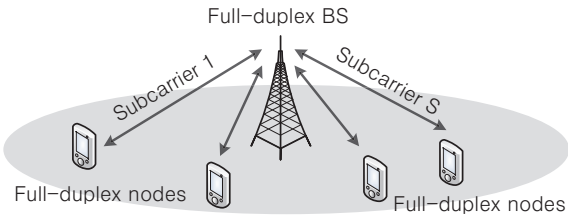

Figure 3.1: A single-cell full-duplex OFDMA network which consists of one full-duplex base station (BS) and multiple full-duplex mobile nodes. Using the full-duplex capability, the BS transmits downlink traffic to nodes while receiving uplink traffic from them simultaneously.

duplex mobile nodes, and let $\mathcal{N} = \{1, 2, \ldots, N\}$ denote the set of nodes. The entire frequency band is partitioned into S subcarriers[1], and let $\mathcal{S} = \{1, 2, \ldots, S\}$ denote the set of subcarriers. All subcarriers are perfectly orthogonal to each other without inter-subcarrier interference. Using the full-duplex capability, the BS transmits downlink traffic to nodes while receiving uplink traffic from them simultaneously. Due to imperfect interference cancellation, there exists residual self-interference in each subcarrier. Experimental results show that the increase in the noise floor due to the residual self-interference is similar regardless of the transmission power [6]. This is because the amount of interference cancellation increases with the transmission power (refer to Fig. 7 in [6] for details). Based on this fact, we assume that the residual self-interference increases the noise power by

[1]A *subcarrier* refers to the scheduling unit of the system rather than a physical subcarrier. In practical wireless systems, the basic scheduling unit can be a single physical subcarrier or a cluster of subcarriers. For example, the basic scheduling unit of LTE system is a resource block that consists of 12 physical subcarriers [38].

σ regardless of the transmission power.

We denote a subcarrier assignment pattern by a binary vector $\mathbf{X} := \{x_{n,s}\}_{n\in\mathcal{N},s\in\mathcal{S}}$, where element $x_{n,s}$'s are defined as

$$x_{n,s} = \begin{cases} 1, \text{ if subcarrier } s \text{ is assigned to node } n, \\ 0, \text{ otherwise.} \end{cases} \tag{3.1}$$

We assume that a subcarrier is exclusively assigned to a node for both uplink and downlink transmissions together. If we do not restrict the exclusive subcarrier assignment assumption, then we can achieve a better performance. However, in the full-duplex scenarios, it is highly unlikely for an optimal solution to assign a subcarrier to two different nodes due to *inter-node interference* from uplink node to downlink node [10]. An exclusive subcarrier assignment will be more common, in particular, when the uplink and the downlink channels have a strong positive correlation (due to the symmetry). Furthermore, to assign a subcarrier to two different nodes, the BS needs to know the inter-node channel information, which is hard to obtain in practice. Thus, we focus only on node-exclusive subcarrier assignment for both uplink and downlink transmissions.

The BS is assumed to know the perfect channel information[2] for

[2]In practice, the BS can obtain the channel state information through the channel feedback (downlink channel) or pilot signals from nodes (uplink channel) [44]. For example, in LTE systems [38], the BS can obtain the uplink channel information by listening to the sounding reference signal transmitted by nodes. In addition, the downlink channel information can be obtained through the channel quality indicator (CQI) feedback from each node.

each node and subcarrier [42, 43, 44]. For each subcarrier s, let $h^u_{n,s}$ denote the uplink channel coefficient between the BS and node n and $h^d_{n,s}$ denote the downlink channel coefficient. Note that $h^u_{n,s}$ and $h^d_{n,s}$ include the location-dependent path loss and the fast fading effect. Also, $p^u_{n,s}$ denotes the uplink power allocated by node n in subcarrier s, and $p^d_{n,s}$ denotes the downlink power allocated by the BS to subcarrier s for node n. Let $\mathbf{P}^u := \left\{p^u_{n,s}\right\}_{n\in\mathcal{N},s\in\mathcal{S}}$ denote the uplink power allocation vector, and $\mathbf{P}^d := \left\{p^d_{n,s}\right\}_{n\in\mathcal{N},s\in\mathcal{S}}$ denote the downlink power allocation vector. Also, let us define $\mathbf{P} := (\mathbf{P}^u, \mathbf{P}^d)$. The total transmission powers at the BS and node n are limited to P_{BS} and P_n, respectively. From now on, we omit the subscript $n \in \mathcal{N}, s \in \mathcal{S}$ for brevity unless confusion arises.

Assuming that self-interference is treated as noise, the rate $R_{n,s}$ of node n in subcarrier s is given by

$$R_{n,s}\left(\mathbf{X},\mathbf{P}\right) = x_{n,s}\left\{\log\left(1+\frac{p^u_{n,s}|h^u_{n,s}|^2}{\sigma N_0}\right)+\log\left(1+\frac{p^d_{n,s}|h^d_{n,s}|^2}{\sigma N_0}\right)\right\},$$

where N_0 denotes the receiver noise floor and σ represents the increase in the noise power due to the residual self-interference. For notational simplicity, we rewrite the above equation as

$$R_{n,s}\left(\mathbf{X},\mathbf{P}\right) = x_{n,s}\left\{\log\left(1+p^u_{n,s}g^u_{n,s}\right)+\log\left(1+p^d_{n,s}g^d_{n,s}\right)\right\}, \quad (3.2)$$

where $g^u_{n,s} = \frac{|h^u_{n,s}|^2}{\sigma N_0}$ and $g^d_{n,s} = \frac{|h^d_{n,s}|^2}{\sigma N_0}$ represent the normalized (with

respect to σN_0) uplink and downlink channel gains, respectively. Let $\mathbf{G} := \left\{g_{n,s}^u, g_{n,s}^d\right\}$ denote the (normalized) channel gain vector. Given $R_{n,s}$, let $R_n(\mathbf{X}, \mathbf{P})$ denote the rate of node n over all subcarriers, i.e., $R_n(\mathbf{X}, \mathbf{P}) = \sum_{s=1}^{S} R_{n,s}$ and let $R(\mathbf{X}, \mathbf{P})$ denote the total sum-rate, i.e., $R(\mathbf{X}, \mathbf{P}) = \sum_{n=1}^{N} R_n$.

In this chapter, our goal is to maximize the total sum-rate $R(\mathbf{X}, \mathbf{P})$ by jointly optimizing the subcarrier assignment X and the power allocation (P, Q) under the power constraints of the BS and each node. Then we formally formulate the full-duplex sum-rate maximization problem P as follows:

$$(\mathsf{P}) \text{ maximize } R(\mathbf{X}, \mathbf{P}) \tag{3.3}$$

$$\text{subject to } \sum_{n=1}^{N} x_{n,s} \leq 1, \forall s \in \mathcal{S} \tag{3.4}$$

$$\sum_{s=1}^{S} p_{n,s}^u \leq P_n, \forall n \in \mathcal{N} \tag{3.5}$$

$$\sum_{n=1}^{N} \sum_{s=1}^{S} p_{n,s}^d \leq P_{BS}, \tag{3.6}$$

$$p_{n,s}^u, p_{n,s}^d \geq 0, \forall n \in \mathcal{N}, \forall s \in \mathcal{S} \tag{3.7}$$

$$x_{n,s} \in \{0, 1\}, \forall n \in \mathcal{N}, \forall s \in \mathcal{S}. \tag{3.8}$$

Note that each subcarrier is exclusively assigned to a single node according to (3.4) and (3.8).

3.3 Necessary Condition for Optimality

Due to the exclusive nature of subcarrier assignment, the original problem P is an integer optimization problem, which generally requires exponential complexity to be solved. Therefore, we relax the constraints and allow multiple nodes to share a subcarrier together. The binary constraints (3.8) are replaced with

$$x_{n,s} \geq 0, \forall n \in \mathcal{N}, \forall s \in \mathcal{S}. \tag{3.9}$$

From (3.4) and (3.9), we have $x_{n,s} \in [0, 1]$.

The relaxed problem P' obtained by replacing (3.8) with (3.9) is still not a convex problem because $R(\mathbf{X}, \mathbf{P})$ is not (jointly) concave in $(\mathbf{X}, \mathbf{P})$. However, the optimal solution still satisfies the Karush-Kuhn-Tucker (KKT) condition [33], so we can obtain the following proposition.

Proposition 7. Let $\mathbf{X}^* = \left\{x_{n,s}^*\right\}$ and $\mathbf{P}^* = \left\{p_{n,s}^{u*}, p_{n,s}^{d*}\right\}$ denote the optimal solution to problem P'. Then $\mathbf{X}^*$ and $\mathbf{P}^*$ satisfy the following conditions:

1. For $x_{n,s}^* > 0$,

$$n = \arg\max_{m \in \mathcal{N}} \left\{ \log\left(1 + p_{m,s}^u g_{m,s}^u\right) + \log\left(1 + p_{m,s}^d g_{m,s}^d\right) \right\}. \tag{3.10}$$

2. For $p_{n,s}^{u*} > 0$,

$$s = \arg\max_{l \in \mathcal{S}} \left(\frac{x_{n,l} g_{n,l}^{u}}{1 + p_{n,l}^{u} g_{n,l}^{u}} \right). \tag{3.11}$$

3. For $p_{n,s}^{d*} > 0$,

$$(n, s) = \arg\max_{(m \in \mathcal{N}, l \in \mathcal{S})} \left(\frac{x_{m,l} g_{m,l}^{d}}{1 + p_{m,l}^{d} g_{m,l}^{d}} \right). \tag{3.12}$$

Proof. We can define the Lagrangian function L as

$$\begin{aligned} & L(\mathbf{X}, \mathbf{P}, \boldsymbol{\lambda}, \boldsymbol{\mu}, \nu) \\ & := \sum_{n=1}^{N} \sum_{s=1}^{S} x_{n,s} \left\{ \log\left(1 + p_{n,s}^{u} g_{n,s}^{u}\right) + \log\left(1 + p_{n,s}^{d} g_{n,s}^{d}\right) \right\} \\ & + \sum_{s=1}^{S} \lambda_s \left(1 - \sum_{n=1}^{N} x_{n,s} \right) + \sum_{n=1}^{N} \mu_n \left(P_n - \sum_{s=1}^{S} p_{n,s}^{u} \right) \\ & + \nu \left(P_{BS} - \sum_{n=1}^{N} \sum_{s=1}^{S} p_{n,s}^{d} \right), \end{aligned} \tag{3.13}$$

where $\boldsymbol{\lambda} = \{\lambda_s\}$, $\boldsymbol{\mu} = \{\mu_n\}$, and ν are the dual variables (or the Lagrangian multipliers). Since the constraints (3.4), (3.5), and (3.6) are affine functions, $\mathbf{X}^*$ and $\mathbf{P}^*$ satisfy the regularity condition [45]. Then from Proposition 3.3.1 of [33], there exist unique dual variables $\boldsymbol{\lambda}^* = \{\lambda_s^*\}$, $\boldsymbol{\mu}^* = \{\mu_n^*\}$, and ν^* such that

$$\begin{aligned} \left. \frac{\partial L}{\partial x_{n,s}} \right|_{\mathbf{X}^*, \mathbf{P}^*} &= \log\left(1 + p_{n,s}^{u*} g_{n,s}^{u}\right) + \log\left(1 + p_{n,s}^{d*} d_{n,s}\right) \\ & \quad - \lambda_s \begin{cases} = 0, \text{if } x_{n,s}^* > 0 \\ \leq 0, \text{if } x_{n,s}^* = 0, \end{cases} \end{aligned} \tag{3.14}$$

$$\left.\frac{\partial L}{\partial p^u_{n,s}}\right|_{\mathbf{X}^*,\mathbf{P}^*} = \frac{x^*_{n,s} g^u_{n,s}}{1 + p^{u*}_{n,s} g^u_{n,s}} - \mu_n \begin{cases} = 0, \text{if } p^{u*}_{n,s} > 0 \\ \leq 0, \text{if } p^{u*}_{n,s} = 0, \end{cases} \tag{3.15}$$

$$\left.\frac{\partial L}{\partial p^d_{n,s}}\right|_{\mathbf{X}^*,\mathbf{P}^*} = \frac{x^*_{n,s} g^d_{n,s}}{1 + p^{d*}_{n,s} g^d_{n,s}} - \nu \begin{cases} = 0, \text{if } p^{d*}_{n,s} > 0 \\ \leq 0, \text{if } p^{d*}_{n,s} = 0. \end{cases} \tag{3.16}$$

From (3.14), if subcarrier s is assigned to node n (i.e., $x^*_{n,s} > 0$), node n has the largest subcarrier sum-rate $R_{n,s} = \lambda_s$, which implies (3.10). Similarly, we can obtain (3.11) from (3.15) and (3.12) from (3.16). □

Although Proposition 7 gives a necessary condition for optimality, we cannot directly obtain an optimal solution because the conditions for $\mathbf{X}^*$ and $\mathbf{P}^*$ are interdependent. Instead, we can have an intuition from (3.10) that each subcarrier s should be allocated to node n with the largest subcarrier sum-rate. Motivated by this intuition, we propose a resource allocation algorithm next.

3.4 Proposed Resource Allocation Algorithm

In this section, we develop a solution that blends greedy subcarrier assignment and water-falling power allocation under per-node power constraints. We start with describing power allocation, and then consider subcarrier assignment.

3.4.1 Power Allocation

Given an optimal subcarrier assignment $\mathbf{X}^*$, problem P is reduced to a power allocation problem that can be easily solved by the well-known *water-filling* power allocation at the BS and each node. Specifically, each node n allocates its uplink power $p_{n,s}^u$ to the assigned subcarrier s as

$$p_{n,s}^u = \begin{cases} \left[\alpha_n - 1/g_{n,s}^u\right]^+, \text{if } x_{n,s}^* = 1 \\ 0, \qquad\qquad\quad \text{if } x_{n,s}^* = 0, \end{cases} \tag{3.17}$$

where $[\cdot]^+ := \max\{\cdot, 0\}$ and α_n is a constant (called water level) satisfying $\sum_{s=1}^{S} p_{n,s}^u = P_n$. Similarly, the BS can optimally allocate the downlink power $p_{n,s}^d$ to subcarrier s for node n with $x_{n,s}^* = 1$ as

$$p_{n,s}^d = \begin{cases} \left[\alpha - 1/g_{n,s}^d\right]^+, \text{if } x_{n,s}^* = 1 \\ 0, \qquad\qquad\quad \text{if } x_{n,s}^* = 0, \end{cases} \tag{3.18}$$

where α is a constant satisfying $\sum_{n=1}^{N} \sum_{s=1}^{S} p_{n,s}^d = P_{BS}$.

3.4.2 Subcarrier Assignment

Next, we present a subcarrier assignment algorithm that sequentially assigns each subcarrier to the node with the largest rate. We take into account the dependency on the transmission power by re-allocating the power in each iteration. The detailed algorithm is provided in Algorithm 2.

Let $\mathcal{S}_n^{(k)}$ denote the set of subcarriers assigned to node n up to

iteration k. If subcarrier s is assigned to a node, we denote the node by n_s. Let $\mathcal{A}^{(k)}$ denote the set of assigned subcarriers up to iteration k, i.e., $\mathcal{A}^{(k)} = \cup_n \mathcal{S}_n^{(k)}$, and let $\mathcal{U}^{(k)} = \mathcal{S} \backslash \mathcal{A}^{(k)}$. We also use the superscript (k) to denote new power allocations, rates, and downlink channel gains, calculated in iteration k. We use the superscript (0) to denote the initial value, e.g., $\mathcal{A}^{(0)} = \emptyset$.

In iteration k $(1 \leq k \leq S)$, we compute the rate for each pair of node and unassigned subcarrier given the subcarrier assignment of up to iteration $(k-1)$, and select the pair that offers the largest rate. To further elaborate, we first allocate the uplink power $p_{n,s}^{u(k)}$ and the downlink power $p_{n,s}^{d(k)}$ for each n as follows:

1. For each node n, re-allocate the uplink power $p_{n,s}^{u(k)}$ using the water-filling algorithm (3.17) to the subcarriers that are assigned to node n or unassigned, i.e., $\mathcal{S}_n^{(k-1)} \cup \mathcal{A}^{(k-1)}$.

2. For each node n, reset its downlink channel gain $g_{n,s}^{d(k)} = g_{n_s,s}^{d}$ for already assigned subcarrier $s \in \mathcal{A}^{(k-1)}$, and $g_{n,s}^{d(k)} = g_{n,s}^{d}$ for unassigned subcarrier $s \in \mathcal{U}^{(k-1)}$. Note that we use the downlink channel gain of node n_s for already assigned subcarrier s to reflect the downlink rate dependency on other nodes' downlink channel gains. Then, allocate the downlink power $p_{n,s}^{d(k)}$ with channel gain $d_{n,s}^{(k)}$, using the water-filling algorithm (3.18).

Given $p_{n,s}^{u(k)}$ and $p_{n,s}^{d(k)}$, we compute the rate $R_{n,s}^{(k)}$ of each pair of node

and unassigned subcarrier as

$$R_{n,s}^{(k)} = \log\left(1 + p_{n,s}^{u(k)} g_{n,s}^{u}\right) + \log\left(1 + p_{n,s}^{d(k)} g_{n,s}^{d(k)}\right), s \in \mathcal{U}^{(k-1)} \quad (3.19)$$

Lastly, we find a pair (n^*, s^*) of node and unassigned subcarrier that achieves the largest rate as follows:

1. $(n^*, s^*) = \underset{n \in \mathcal{N}, s \in \mathcal{U}^{(k-1)}}{\arg\max} R_{n,s}^{(k)}$.
2. $\tilde{x}_{n^*,s^*} \leftarrow 1$.
3. $\mathcal{U}^{(k)} \leftarrow \mathcal{U}^{(k-1)} \backslash \{s^*\}$, $\mathcal{A}^{(k)} \leftarrow \mathcal{A}^{(k-1)} \cup \{s^*\}$, and $\mathcal{S}_{n^*}^{(k)} \leftarrow \mathcal{S}_{n^*}^{(k-1)} \cup \{s^*\}$.

We repeat the above procedures S times and obtain the subcarrier assignment vector $\widetilde{\mathbf{X}}$. Given $\widetilde{\mathbf{X}}$, we obtain the final power allocation vector $\widetilde{\mathbf{P}}$ by solving (3.17) and (3.18).

In each iteration, we perform the water-filling for (uplink and downlink) power allocation for each node, which has the complexity of $O(S)$ [42]. Considering N nodes and S iterations, our solution has the complexity of $O(NS^2)$. Also, our solution runs at the BS, and given the channel gains $\mathbf{G}$, it returns $\widetilde{\mathbf{X}}$ and $\widetilde{\mathbf{P}}$ as the final outcomes.

3.5 Local Pareto Optimality

In this section, we show that our subcarrier assignment algorithm is provably efficient in achieving a certain optimal property. We start with several definitions related to local Pareto optimality [43].

Algorithm 2: Full-Duplex Resource Allocation Algorithm

Data: channel gains $\mathbf{G} = \{g^u_{n,s}, g^d_{n,s}\}$.
maximum power constraints $\{P_n\}$ and P_{BS}.

Initialization
  $\mathcal{A}^{(0)} \leftarrow \emptyset$;
  $\mathcal{U}^{(0)} \leftarrow \mathcal{S}$;
  $\mathcal{S}_n^{(0)} \leftarrow \emptyset$ for $\forall n \in \mathcal{N}$;
for *iteration* $k = 1 \rightarrow S$ **do**
  for *node* $n = 1 \rightarrow N$ **do**
    [**Temporal uplink power in iteration** k]
      Allocate uplink power $p^{u(k)}_{n,s}$ by (3.17) to the subcarriers that are assigned to node n or unassigned;
    [**Temporal downlink power in iteration** k]
      Reset $g^{d(k)}_{n,s} = g^d_{n(s),s}$ for assigned subcarrier $s \in \mathcal{A}^{(k-1)}$, and $g^{d(k)}_{n,s} = g^d_{n,s}$ for unassigned subcarrier $s \in \mathcal{U}^{(k-1)}$;
      Allocate downlink power $g^{d(k)}_{n,s}$ by (3.18) to node n with channel gain $g^{d(k)}_{n,s}$;
    [**Rate in iteration** k]
      Compute the rate
      $R^{(k)}_{n,s} = \log\left(1 + p^{d(k)}_{n,s} g^u_{n,s}\right) + \log\left(1 + p^{d(k)}_{n,s} g^{d(k)}_{n,s}\right)$;
  [**Subcarrier assignment in iteration** k]
    Find (n^*, s^*) such that $(n^*, s^*) = \underset{n \in \mathcal{N}, s \in \mathcal{U}^{(k-1)}}{\arg\max} R^{(k)}_{n,s}$;
    $\tilde{x}_{n^*,s^*} \leftarrow 1$;
    $n_{s^*} \leftarrow n^*$;
    $\mathcal{S}^{(k)}_{n^*} \leftarrow \mathcal{S}^{(k-1)}_{n^*} \cup \{s^*\}$;
    $\mathcal{A}^{(k)} \leftarrow \mathcal{A}^{(k-1)} \cup \{s^*\}$;
    $\mathcal{U}^{(k)} \leftarrow \mathcal{U}^{(k-1)} \backslash \{s^*\}$;
[**Power allocation**]
  Given $\tilde{x}_{n,s}$, allocate uplink power $\tilde{p}^u_{n,s}$ by (3.17) and downlink power $\tilde{p}^d_{n,s}$ by (3.18);

Result: subcarrier assignment $\hat{\mathbf{X}}$ and power allocation $\hat{\mathbf{P}}$.

Let $\mathcal{X}$ denote the set of all feasible subcarrier assignments satisfying the constraints (3.4) and (3.8). Given a feasible subcarrier assignment $\mathbf{X} \in \mathcal{X}$, let $\mathcal{S}_n^{\mathbf{X}}$ denote the set of subcarriers assigned to node n.

Definition 5. We define the distance $D(\mathbf{X}, \mathbf{Y})$ between two feasible subcarrier assignments $\mathbf{X}, \mathbf{Y} \in \mathcal{X}$ as

$$D(\mathbf{X}, \mathbf{Y}) := \max_{n \in \mathcal{N}} \{d_n(\mathbf{X}, \mathbf{Y})\}, \tag{3.20}$$

where

$$d_n(\mathbf{X}, \mathbf{Y}) := \max \left\{ |\mathcal{S}_n^{\mathbf{X}} \backslash \mathcal{S}_n^{\mathbf{Y}}|, |\mathcal{S}_n^{\mathbf{Y}} \backslash \mathcal{S}_n^{\mathbf{X}}| \right\}. \tag{3.21}$$

By definition, if subcarrier assignment is changed from $\mathbf{X}$ to $\mathbf{Y}$, each node can win or lose at most $D(\mathbf{X}, \mathbf{Y})$ subcarriers. It can be shown that $< \mathcal{X}, D >$ is a metric space, in which ϵ-*ball* is defined as follows: [43]

Definition 6. The ϵ-*ball* $B(\mathbf{X}, \epsilon)$ of a feasible subcarrier assignment $\mathbf{X}$ is defined as

$$B(\mathbf{X}, \epsilon) := \{\mathbf{Y} \in \mathcal{X} | D(\mathbf{X}, \mathbf{Y}) \leq \epsilon\}. \tag{3.22}$$

Clearly, $B(\mathbf{X}, \epsilon)$ is the set of subcarrier assignments whose distance to $\mathbf{X}$ is no greater than ϵ.

Given a feasible subcarrier assignment $\mathbf{X}$, let $\mathbf{P}^{\mathbf{X}}$ denote the power allocation vector by the water-filling and $R_n^{\mathbf{X}}$ denote the rate of node

n, i.e., $R_n^{\mathbf{X}} = R_n(\mathbf{X}, \mathbf{P}^X)$.

We now introduce the following definitions of *Pareto domination* and *local Pareto optimality* [43].

Definition 7. A subcarrier assignment $\mathbf{X}$ *Pareto dominates* another subcarrier assignment $\mathbf{Y}$ if $R_1^{\mathbf{X}} \geq R_1^{\mathbf{Y}}, \cdots, R_N^{\mathbf{X}} \geq R_N^{\mathbf{Y}}$ for every node and $R_m^{\mathbf{X}} > R_m^{\mathbf{Y}}$ for at least one node $m \in \mathcal{N}$.

Definition 8. A subcarrier assignment $\mathbf{X}$ is *local Pareto optimal* in $B(\mathbf{X}, \epsilon)$ if there is no subcarrier assignment $\mathbf{Y} \in B(\mathbf{X}, \epsilon)$ that Pareto dominates $\mathbf{X}$.

Thus, if $\mathbf{X}$ is local Pareto optimal in $B(\mathbf{X}, \epsilon)$, we cannot (strictly) increase the rate of every node n by adding/removing at most ϵ subcarriers to/from $\mathcal{S}_n^{\mathbf{X}}$.

To obtain some properties of our solution, we need the following three conditions.

Condition 1 (All-positive power allocation)**.** Either positive uplink power or positive downlink power is allocated to each subcarrier, i.e.,

$$\sum_{n=1}^{N} \left(p_{n,s}^u + p_{n,s}^d \right) > 0, \forall s \in \mathcal{S}. \tag{3.23}$$

Condition 2 (Elementwise-unique channel gain)**.** For each node n, each subcarrier has a distinctive channel gain both in uplink and downlink, i.e.,

$$g^u_{n,s} \neq g^u_{n,l}, \forall s, l \in \mathcal{S}, \tag{3.24}$$

$$g^d_{n,s} \neq g^d_{n,l}, \forall s, l \in \mathcal{S}. \tag{3.25}$$

Since $g^u_{n,s}$'s (and also $g^d_{n,s}$'s) are continuous real random variables, the probability that any two of them have an equal value is zero. Therefore, we can assume that a channel gain vector is elementwise-unique in practice.

Condition 3 (reciprocity-in-order)**.** For each node n, for any two subcarriers s and l, $g^u_{n,s} > g^u_{n,l}$ implies $g^d_{n,s} > g^d_{n,l}$ and vice versa, i.e., $g^u_{n,s} > g^u_{n,l} \leftrightarrow g^d_{n,s} > g^d_{n,l}$. This means that the order of subcarriers in terms of uplink channel gain is equal to their order in terms of downlink channel gain.

Note that two channels are said to be reciprocal (channel reciprocity) when the uplink channel gain and the downlink channel gain for each subcarrier are the same, i.e., $g^u_{n,s} = g^d_{n,s}, \forall n, s$. The reciprocal channels are reciprocal-in-order (but the reverse does not hold in general).

Finally, we show the local Pareto optimality of our solution. From now on, we assume a channel gain vector $\mathbf{G} = \left\{g^u_{n,s}, g^d_{n,s}\right\}$ satisfying conditions 2 and 3. Let us choose a subcarrier assignment $\mathbf{Y}$ in $B(\mathbf{X}, 1)$. That is, $\mathbf{Y}$ can be obtained from $\mathbf{X}$ by reassigning subcarriers such that each node wins and/or loses at most 1 subcarrier. Assume that $\mathbf{P}^{\mathbf{X}}$ satisfies condition 1. Let $R^u_n(\mathbf{X})$ and $R^d_n(\mathbf{X})$ denote the uplink rate and the downlink rate of node n, respectively, defined

as

$$R_n^u(\mathbf{X}) = \sum_{s \in S_n(\mathbf{X})} \log\left(1 + p_{n,s}^u(\mathbf{X}) g_{n,s}^u\right), \tag{3.26}$$

$$R_n^d(\mathbf{X}) = \sum_{s \in S_n(\mathbf{X})} \log\left(1 + p_{n,s}^d(\mathbf{X}) g_{n,s}^d\right). \tag{3.27}$$

Then we have $R_n(\mathbf{X}) = R_n^u(\mathbf{X}) + R_n^d(\mathbf{X})$. The following lemma shows a necessary condition under which $\mathbf{Y}$ Pareto dominates $\mathbf{X}$.

Lemma 2. Suppose that subcarrier assignment is changed from $\mathbf{X}$ to $\mathbf{Y} \in B(\mathbf{X}, 1)$. If there exists a node which only loses a subcarrier and wins no subcarrier, then $\mathbf{Y}$ does not Pareto dominate $\mathbf{X}$.

Proof. We prove this by contradiction. Suppose $\mathbf{Y}$ Pareto dominates $\mathbf{X}$. Without loss of generality, assume that there exists only one node which loses a subcarrier. Suppose that node n loses subcarrier s, i.e., $\mathcal{S}_n(\mathbf{Y}) = \mathcal{S}_n(\mathbf{X}) \backslash \{s\}$. Since $\mathbf{Y}$ Pareto dominates $\mathbf{X}$, we have $R_n(\mathbf{Y}) \geq R_n(\mathbf{X})$. From the assumption that $\mathbf{P}(\mathbf{X})$ is an all-positive power allocation vector, we have $p_{n,s}^u(\mathbf{X}) + p_{n,s}^d(\mathbf{X}) > 0$. Now, we can consider the following two cases.

1. For $p_{n,s}^u(\mathbf{X}) > 0$:

   Since node n loses subcarrier s with positive uplink power, $R_n^u(\mathbf{Y}) < R_n^u(\mathbf{X})$ must be true considering the characteristic of the water-filling algorithm. The reduced uplink rate should be compensated by the increase in the downlink rate, i.e., $R_n^d(\mathbf{Y}) > R_n^d(\mathbf{X})$, which implies $P_n^d(\mathbf{Y}) > P_n^d(\mathbf{X})$.

2. For $p_{n,s}^d(\mathbf{X}) > 0$:

   Since node n loses subcarrier s with positive downlink power, more downlink power should be allocated in $\mathbf{Y}$ than in $\mathbf{X}$, i.e., $P_n^d(\mathbf{Y}) > P_n^d(\mathbf{X})$.

In both cases, we should have $P_n^d(\mathbf{Y}) > P_n^d(\mathbf{X})$, which means that (i) the downlink water level $\alpha(\mathbf{Y})$ in $\mathbf{Y}$ is greater than the downlink water level $\alpha(\mathbf{X})$ in $\mathbf{X}$, and (ii) there exists at least one node which loses some of its downlink power, part of which is reallocated to node n. Now consider a node m which obtains subcarrier l, i.e., $\mathcal{S}_m(\mathbf{Y}) = \mathcal{S}_m(\mathbf{X}) \cup \{l\}$. Since $\alpha(\mathbf{Y}) > \alpha(\mathbf{X})$, we can prove that $P_m^d(\mathbf{Y}) \geq P_m^d(\mathbf{X})$ as follows:

$$\begin{aligned} P_m^d(\mathbf{Y}) &= \sum_{s \in \mathcal{S}_m(\mathbf{Y})} \left[\alpha(\mathbf{Y}) - \frac{1}{g_{m,s}^d}\right]^+ \\ &= \sum_{s \in \mathcal{S}_m(\mathbf{X})} \left[\alpha(\mathbf{Y}) - \frac{1}{g_{m,s}^d}\right]^+ + \left[\alpha(\mathbf{Y}) - \frac{1}{g_{m,l}^d}\right]^+ \\ &\geq \sum_{s \in \mathcal{S}_m(\mathbf{X})} \left[\alpha(\mathbf{Y}) - \frac{1}{g_{m,s}^d}\right]^+ \\ &\geq \sum_{s \in \mathcal{S}_m(\mathbf{X})} \left[\alpha(\mathbf{X}) - \frac{1}{g_{m,s}^d}\right]^+ = P_m^d(\mathbf{X}). \end{aligned} \tag{3.28}$$

Next, consider node m which swaps subcarrier i for subcarrier j, i.e., $\mathcal{S}_m(\mathbf{X}) \backslash \{i\} = \mathcal{S}_m(\mathbf{Y}) \backslash \{j\}$. If $g_{m,i}^d < g_{m,j}^d$ and also $g_{m,i}^u < g_{m,j}^u$ by the reciprocity-in-order, $P_m^d(\mathbf{Y})$ should be larger than $P_m^d(\mathbf{X})$ to have $R_m(\mathbf{Y}) \geq R_m(\mathbf{X})$. If $g_{m,i}^d > g_{m,j}^d$, we have $P_m^d(\mathbf{Y}) \geq P_m^d(\mathbf{X})$, which can be proven as

$$
\begin{aligned}
P_m^d(\mathbf{Y}) &= \sum_{s\in S_m(\mathbf{Y})} \left[\alpha(\mathbf{Y}) - \frac{1}{g_{m,s}^d}\right]^+ \\
&= \sum_{s\in S_m(\mathbf{Y})\setminus\{j\}} \left[\alpha(\mathbf{Y}) - \frac{1}{g_{m,s}^d}\right]^+ + \left[\alpha(\mathbf{Y}) - \frac{1}{g_{m,j}^d}\right]^+ \\
&= \sum_{s\in S_m(\mathbf{X})\setminus\{i\}} \left[\alpha(\mathbf{Y}) - \frac{1}{g_{m,s}^d}\right]^+ + \left[\alpha(\mathbf{Y}) - \frac{1}{g_{m,j}^d}\right]^+ \\
&\geq \sum_{s\in S_m(\mathbf{X})\setminus\{i\}} \left[\alpha(\mathbf{X}) - \frac{1}{g_{m,s}^d}\right]^+ + \left[\alpha(\mathbf{X}) - \frac{1}{g_{m,j}^d}\right]^+ \\
&\geq \sum_{s\in S_m(\mathbf{X})\setminus\{i\}} \left[\alpha(\mathbf{X}) - \frac{1}{g_{m,s}^d}\right]^+ + \left[\alpha(\mathbf{X}) - \frac{1}{g_{m,i}^d}\right]^+ \\
&\geq \sum_{s\in S_m(\mathbf{X})} \left[\alpha(\mathbf{X}) - \frac{1}{g_{m,s}^d}\right]^+ = P_m^d(\mathbf{X}).
\end{aligned}
\tag{3.29}
$$

Considering the above cases, there exists no node which is allocated less downlink power in $\mathbf{Y}$ than in $\mathbf{X}$. As a result, $R_n^d(\mathbf{Y}) > R_n^d(\mathbf{X})$ does not hold. This means that we have $R_n(\mathbf{Y}) < R_n(\mathbf{X})$, which contradicts that $\mathbf{Y}$ Pareto dominates $\mathbf{X}$. □

Lemma 3. Assume that each node swaps a subcarrier for another one or maintains its subcarrier assignment. If there exists a node which swaps a subcarrier for another one with a smaller (uplink and downlink) channel gain, then $\mathbf{Y}$ does not Pareto dominate $\mathbf{X}$.

Proof. Again, we prove this by contradiction. Without loss of generality, assume that node n swaps subcarrier s for subcarrier l with

$g^d_{n,s} < g^d_{n,l}$ and $g^u_{n,s} < g^u_{n,l}$, while each of the other nodes swaps one of its subcarriers for another one with a larger channel gain. Since $g^d_{n,l} > g^d_{n,s}$ and $p^u_{n,s}(\mathbf{X}) + p^d_{n,s}(\mathbf{X}) > 0$, $P^d_m(\mathbf{X}) = P^d_m(\mathbf{Y})$ leads to $R_n(\mathbf{Y}) < R_n(\mathbf{Y})$. Thus we should have $P^d_m(\mathbf{Y}) > P^d_m(\mathbf{X})$, which means that there exists a node which is allocated less downlink power in $\mathbf{Y}$ than in $\mathbf{X}$. However, we can prove by (3.29) that there exists no such node, which is a contradiction. Thus, $\mathbf{Y}$ does not Pareto dominate $\mathbf{X}$. □

Lemma 4. Assume that $\mathbf{Y} \in B(\mathbf{X}, 1)$ Pareto dominates $\mathbf{X}$. When subcarrier assignment is changed from $\mathbf{X}$ to $\mathbf{Y}$, every node either retains its subcarrier assignment unchanged or swaps one subcarrier for another one with a larger channel gain.

Proof. When subcarrier assignment is changed from $\mathbf{X}$ to $\mathbf{Y} \in B(\mathbf{X}, 1)$, if there exists either a node that loses a subcarrier (Lemma 2) or swaps a subcarrier for another one with a smaller channel gain (Lemma 3), $\mathbf{Y}$ does not Pareto dominate $\mathbf{X}$. The proof of Lemma 4 is straightforward using Lemma 2 and Lemma 3. □

In addition, the following lemma shows a useful property of our algorithm.

Lemma 5. By our algorithm, when node n is assigned subcarrier s, it has the largest (uplink and downlink) channel gain in subcarrier s among all unassigned subcarriers.

Proof. We prove this by contradiction. Suppose that subcarrier s is assigned to node n in iteration k. This means that $R_{n,s}^{(k)} > R_{n,l}^{(k)}, \forall l \in \mathcal{U}^{(k-1)} \backslash \{s\}$. Now, assume that in the beginning of iteration k, there is subcarrier $l \in \mathcal{U}^{(k-1)}$ with $g_{n,l}^u > g_{n,s}^u$ and also $g_{n,l}^d > g_{n,s}^d$. Now, let $\alpha_n^{(k)}$ denote the uplink water-level of node n, and $\alpha^{(k)}$ denote the downlink water level. Then the rates $R_{n,s}^{(k)}$ and $R_{n,l}^{(k)}$ are given as

$$R_{n,s}^{(k)} = \left[\alpha_n^{(k)} - \frac{1}{g_{n,s}^u}\right]^+ + \left[\alpha^{(k)} - \frac{1}{g_{n,s}^d}\right]^+, \tag{3.30}$$

$$R_{n,l}^{(k)} = \left[\alpha_n^{(k)} - \frac{1}{g_{n,l}^u}\right]^+ + \left[\alpha^{(k)} - \frac{1}{g_{n,l}^d}\right]^+. \tag{3.31}$$

Since $g_{n,l}^u > g_{n,s}^u$ and $g_{n,l}^d > g_{n,s}^d$, we have $R_{n,l}^{(k)} \geq R_{n,s}^{(k)}$, which contradicts $R_{n,s}^{(k)} > R_{n,l}^{(k)}$. □

Based on the above lemmas, we can prove that $\widetilde{\mathbf{X}}$ is local Pareto optimal in its 1-ball if $\widetilde{\mathbf{P}}$ is an all-positive power allocation vector.

Theorem 3. Given a channel gain vector $\mathbf{G}$ satisfying Conditions 2 and 3, if $\widetilde{\mathbf{P}}$ satisfies Condition 1, $\widetilde{\mathbf{X}}$ is local Pareto optimal in its 1-ball.

Proof. We prove this by contradiction. Assume that a subcarrier assignment $\mathbf{Y} \in B(\widetilde{\mathbf{X}}, 1)$ Pareto dominates $\widetilde{\mathbf{X}}$. Then from Lemma 4, when subcarrier assignment is changed from $\widetilde{\mathbf{X}}$ to $\mathbf{Y}$, each node swaps a subcarrier for another one with a larger channel gain. Without loss of generality, assume that subcarrier s_n is reallocated from node n to

node $n+1$ for $1 \leq n \leq M-1$, and subcarrier s_M from node M to node 1. In this case, we have $g^u_{n,s_{n-1}} > g^u_{n,s_n}$ and $g^d_{n,s_{n-1}} > g^d_{n,s_n}$ for $2 \leq n \leq M$, and $g^u_{1,s_M} > g^u_{1,s_1}$ and $g^d_{1,s_M} > g^d_{1,s_1}$.

Let k_n $(1 \leq n \leq M)$ denote the iteration index when subcarrier s_n is assigned to node n in our algorithm. By Lemma 5, node 1 has the largest channel gain in subcarrier s_1 among all unassigned subcarriers in iteration k_1. This implies that subcarrier s_M is assigned to node M before iteration k_1, i.e.,

$$k_1 > k_M. \tag{3.32}$$

Similarly, from node n's point of view $(2 \leq n \leq M)$, we have

$$k_2 > k_1, \tag{3.33}$$

$$k_3 > k_2, \tag{3.34}$$

$$\vdots$$

$$k_M > k_{M-1}. \tag{3.35}$$

Then we have a contradiction in the relation between $k_1, \cdots, k_M$. □

Remark 1. When Conditions 1 – 3 do not hold, we can find a counter example where our solution $\widetilde{\mathbf{X}}$ is not local Pareto optimal in $B(\widetilde{\mathbf{X}}, 1)$. We show later by simulations that Condition 1 is frequently met in practice (Fig. 3.5). Although the techniques we used above are similar

to those in [43], there is an important difference: when subcarrier assignment is changed from $\widetilde{\mathbf{X}}$ to $\mathbf{Y}$, the downlink rate of each node n should be carefully considered because it depends on the channel gains of other nodes, e.g., Eqs. (3.28) and (3.29) in Lemma 2.

3.6 Performance Bound

In this section, we provide a performance upper bound (UB) by considering uplink and downlink transmissions separately.

For the original problem P, we assume that a subcarrier is used by only one node for a full-duplex link. We now relax this constraint and allow two different nodes to share a single subcarrier: one for uplink and the other for downlink. Also, we introduce two assignment variables $x^u_{n,s}$ and $x^d_{n,s}$ defined as follows:

$$x^u_{n,s} = \begin{cases} 1, \text{ if subcarrier } s \text{ is assigned to node } n \text{ in uplink,} \\ 0, \text{ otherwise.} \end{cases} \tag{3.36a}$$

$$x^d_{n,s} = \begin{cases} 1, \text{ if subcarrier } s \text{ is assigned to node } n \text{ in downlink,} \\ 0, \text{ otherwise.} \end{cases} \tag{3.36b}$$

Also, $x^u_{n,s}$ and $x^d_{n,s}$ should satisfy $\sum_{n=1}^{N} x^u_{n,s} \leq 1$ and $\sum_{n=1}^{N} x^d_{n,s} \leq 1, \forall s \in \mathcal{S}$, respectively. By replacing (3.8) with (3.36a) and (3.36b), we have another problem $\mathsf{P_R}$. Note that the optimal solution to P is still feasible in $\mathsf{P_R}$, i.e., $x^*_{n,s} = 1$ in P can be mapped to $x^u_{n,s} = x^d_{n,s} = 1$

in $\mathsf{P_R}$. Thus, the optimal solution to $\mathsf{P_R}$ achieves an upper bound of P.

When two different nodes use a subcarrier, the maximum achievable rate is less than the sum of (point-to-point) uplink rate and downlink rate because the uplink transmission can cause inter-node interference at the downlink node. By assuming that there is no inter-node interference, we can separate problem $\mathsf{P_R}$ into two individual problems $\mathsf{P_D}$ and $\mathsf{P_U}$, which maximizes the downlink sum-rate and the uplink sum-rate, respectively, defined as follows:

$$(\mathsf{P_D}) \text{ maximize } \sum_{n=1}^{N}\sum_{s=1}^{S} x_{n,s}^{d} \log\left(1 + p_{n,s}^{d} g_{n,s}^{d}\right) \tag{3.37}$$

$$\text{subject to } \sum_{n=1}^{N} x_{n,s} \leq 1, \forall s \in \mathcal{S} \tag{3.38}$$

$$\sum_{n=1}^{N}\sum_{s=1}^{S} p_{n,s}^{d} \leq \mathrm{P}_{BS}, \tag{3.39}$$

$$p_{n,s}^{d} \geq 0, \forall n \in \mathcal{N}, \forall s \in \mathcal{S} \tag{3.40}$$

$$x_{n,s}^{d} \in \{0,1\}, \forall n \in \mathcal{N}, \forall s \in \mathcal{S}. \tag{3.41}$$

$$(\mathsf{P_U}) \text{ maximize } \sum_{n=1}^{N}\sum_{s=1}^{S} x_{n,s}^{u} \log\left(1 + p_{n,s}^{u} g_{n,s}^{u}\right) \tag{3.42}$$

$$\text{subject to } \sum_{n=1}^{N} x_{n,s}^{u} \leq 1, \forall s \in \mathcal{S} \tag{3.43}$$

$$\sum_{s=1}^{S} p_{n,s}^{u} \leq P_n, \forall n \in \mathcal{N} \tag{3.44}$$

$$p_{n,s}^{u} \geq 0, \forall n \in \mathcal{N}, \forall s \in \mathcal{S} \tag{3.45}$$

$$x_{n,s}^{u} \in \{0,1\}, \forall n \in \mathcal{N}, \forall s \in \mathcal{S}. \tag{3.46}$$

The optimal solution of $\mathsf{P_D}$ is to assign a subcarrier to a node with the largest (downlink) channel gain and to allocate power according to the water-filling algorithm [41]. For $\mathsf{P_U}$, although no low-complexity optimal solution has been known, its upper bound can be characterized in polynomial time [43]. To find an upper bound, we relax $\mathsf{P_U}$ to problem $\mathsf{P_U'}$ by replacing S constraints in (3.43) with a single constraint

$$\sum_{n=1}^{N}\sum_{s=1}^{S} x_{n,s}^{u} \leq S. \tag{3.47}$$

Eq. (3.47) means that a subcarrier can be assigned to more than one node (e.g., $x_{n,s}^{u} = 1$ and $x_{m,s}^{u} = 1$) as long as the number of assigned subcarriers is no greater than S. Since $\{x_{n,s}^{u}\}$ satisfying (3.43) also satisfies (3.47), the optimal solution to $\mathsf{P_U'}$ achieves an upper bound of $\mathsf{P_U}$. From (3.47), if node n is allowed to use s_n subcarriers, it can now choose the best s_n subcarriers regardless of whether or not those subcarriers are used by other nodes. Then, the problem is to deter-

mine the optimal values for $\{s_n\}_{\forall n}$ satisfying $\sum_{n=1}^{N} s_n \leq S$, and it can be solved using dynamic programming with a polynomial complexity in N and S [43]. Finally, by combining the optimal solution to $\mathsf{P_D}$ and the upper bound of $\mathsf{P_U}$, we can find an upper bound of $\mathsf{P_R}$ in polynomial time, which is also an upper bound of P.

Clearly, UB is not achievable in practice due to the interference between the uplink and the downlink. Also, the tightness of UB depends on the correlation between the uplink and downlink channels. When the uplink and the downlink channels are symmetric, the original solution to the sum-rate maximization is not much different from the solution to each subproblem that maximizes only uplink (or downlink) rate, due to symmetric property. In this case, UB becomes a tight upper bound as shown in Fig. 2 later. However, in the asymmetric channel case, the solution to each subproblem is significantly different from that to the original problem, and consequently the performance gap between UB and FD-P becomes large.

3.7 Performance Evaluation

In this section, we evaluate our resource allocation solution through numerical simulations. We use typical parameter values of LTE system [36]. We assume 2.1 GHz frequency band and configure the bandwidth of a subcarrier as 180 kHz, which corresponds to the bandwidth of a resource block in LTE system. The noise power N_0 is set to -119

dBm. The increase of the noise power[3] σ due to the residual self-interference is set to 1 dB unless otherwise specified. The maximum transmission powers for the BS and each node n are set to 43 dBm and 24 dBm, respectively. For the path loss model, we use the Hata propagation model for urban environments where path loss P_{loss} (dB) is calculated as [36]

$$\begin{aligned} P_{loss}(d) = 69.55 + 26.16 \cdot \log f - 13.83 \cdot \log h_{BS} - C_H(f) \\ + (44.9 - 6.55 \cdot \log h_{BS}) \log d, \end{aligned} \tag{3.48}$$

where d (km) denotes the distance between the transmitter and the receiver, f (MHz) is the center frequency, and h_{BS} (m) denotes the height of the BS. $C_H(f)$ is the antenna height correlation factor defined as,

$$C_H(f) = 0.8 + (1.1 \cdot \log f - 0.7)\, h_N - 1.56 \cdot \log f, \tag{3.49}$$

where h_N (m) is the height of the terminal node. We assume that each node is placed at an equal distance d from the BS. Table 3.1 summarizes our simulation settings.

We assume a time-slotted system and adopt the model of *i.i.d.* Rayleigh block fading channel in [46]. A time slot corresponds to a scheduling time unit of the system, during which the channel gain of each node is time-invariant, and the channel gain for each subcarrier

[3] According to [6], the increase of the noise power due to the residual self-interference is at most 1 dB.

Table 3.1: Simulation Parameters

Parameter	Value
Center frequency	2.1 GHz
Subcarrier bandwidth	180 kHz
Noise power N_0	-119 dBm
Residual self-interference σ	1 dB
Base station's power P_{BS}	43 dBm
Node n's power P_n	24 dBm
h_{BS}	30 m
h_N	1.5 m

follows an independent Rayleigh distribution in each time slot. Also, ρ denotes the correlation between the uplink and the downlink channels. When $\rho = 1$, the uplink and the downlink channel gains are the same, i.e., symmetric channel. In contrast, when $\rho = 0$, the uplink and the downlink channel gains are chosen independently, i.e., asymmetric channel. Note that the reciprocity-in-order also holds in the symmetric channel model.

For performance evaluation, we compare the following schemes:

- Upper Bound (UB): Performance upper bound obtained from Section 3.6.

- Full-Duplex Optimal solution (FD-O): Optimal subcarrier assignment $\mathbf{X}^*$ obtained by exhaustive search. Since the complexity to find $\mathbf{X}^*$ is $O(N^K)$, we try FD-O only for small-size networks.

- Full-Duplex Proposed solution (FD-P): Proposed subcarrier assignment $\widetilde{\mathbf{X}}$ maximizing the sum-rate.

- Full-Duplex Downlink optimal solution (FD-D): Subcarrier assignment $\mathbf{X}^d$ maximizing the downlink rate, i.e., assign each subcarrier to a node with the largest downlink channel gain.

- Full-Duplex Uplink Near-optimal solution (FD-U): Subcarrier assignment $\mathbf{X}^u$ maximizing the uplink rate, i.e., assign each subcarrier according to [43].

- Half-Duplex (HD): $\mathbf{X}^u$ and $\mathbf{X}^d$ are used for the uplink and the downlink, respectively.

In all schemes, the water-filling algorithm is used for the power allocation. Given a subcarrier assignment pattern $\mathbf{X}$, $R^u(\mathbf{X})$ and $R^d(\mathbf{X})$ denote the uplink rate and the downlink rate, respectively, i.e., $R^u(\mathbf{X}) = \sum_{n,s} x^u_{n,s} \log(1 + p^u_{n,s} g^u_{n,s})$ and $R^d(\mathbf{X}) = \sum_{n,s} x^d_{n,s} \log(1 + p^d_{n,s} g^d_{n,s})$. The sum-rate of HD is calculated as $0.5 \times R^d(\mathbf{X}^d) + 0.5 \times R^u(\mathbf{X}^u)$. Also, we define *full-duplex gain* as the performance gain of FD-P over HD.

3.7.1 Simulation Results

We first consider the symmetric channel model where the uplink and downlink channels are the same. We compare the performance of each scheme according to S values (number of subcarriers) when $N = 50$ and $d = 200$ m. Fig. 3.2 shows the sum-rates of all schemes as S increases from 10 to 100, i.e., the bandwidth increases by 10 times. For each value of S, the performance gap between UB and FD-P is negligible, which means that FD-P is near-optimal while UB gives

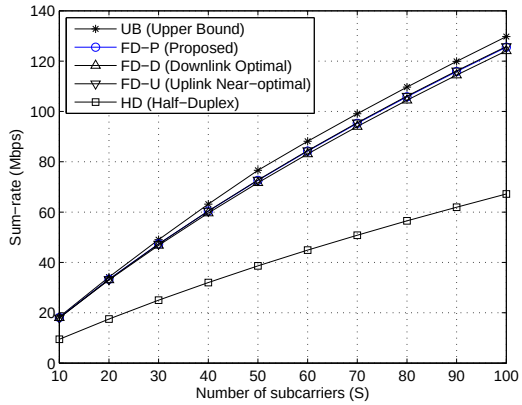

Figure 3.2: Performance comparison according to S values in symmetric channel model.

a near-tight upper bound. Also, the sum-rates of FD-P, FD-D, and FD-U are almost identical. This is because $\widetilde{\mathbf{X}}$, $\mathbf{X}^u$, and $\mathbf{X}^d$ are not much different from each other due to the channel symmetry. The full-duplex gain ranges from 87% ($S = 100$) to 91% ($S = 10$). Due to the residual self-interference, achieving the ideal doubling of spectral efficiency is not possible even in the symmetric channel case.

Fig. 3.3 depicts the sum-rate performance of each scheme as a function of N (number of nodes) when $S = 50$ and $d = 200$ m. With more nodes, the sum-rate of each scheme increases due to the multi-user diversity. Also, the average uplink power allocated in each subcarrier grows with N. As N increases, each uplink node is likely to use less subcarriers ($\frac{S}{N}$ subcarriers on average) and it can allocate more power to each of assigned subcarriers. Again, FD-P, FD-D, and FD-U show a similar performance. The full-duplex gain ranges from

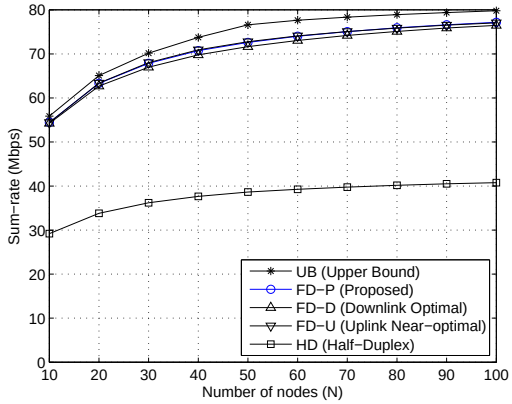

Figure 3.3: Performance comparison according to N values in symmetric channel model.

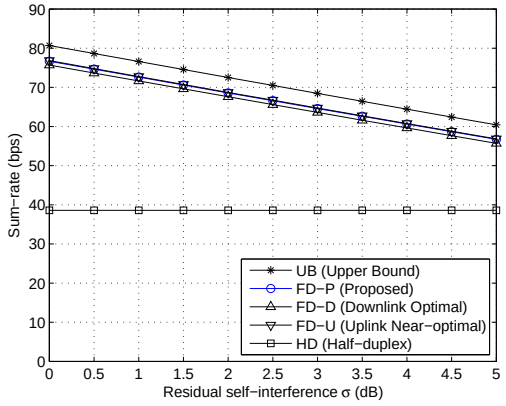

Figure 3.4: Performance comparison according to σ values in symmetric channel model.

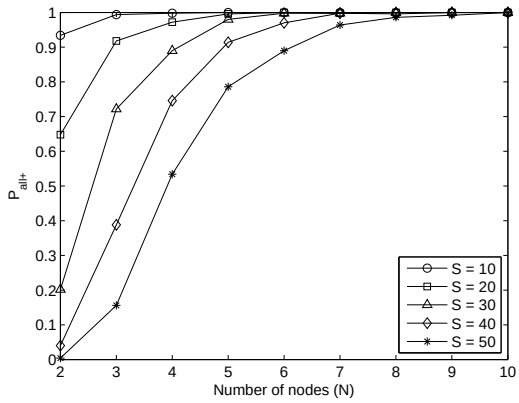

Figure 3.5: The probability of $\widetilde{\mathbf{P}}$ being an all-positive power allocation vector for $d = 400$ m.

86 % ($N = 10$) to 89 % ($N = 100$).

The impact of residual self-interference σ is plotted in Fig. 3.4 when $N = 50$, $S = 50$, and $d = 200$ m. The sum-rates of all schemes except HD decreases with σ due to the increasing noise power. The full-duplex gain reaches 99% in case of the perfect cancellation ($\sigma = 0$). Since $\widetilde{\mathbf{X}}$ and $\mathbf{X}^d$ ($\mathbf{X}^u$) are similar in the symmetric channel case, FD-P can almost double both the uplink and the downlink rates. This indicates that full-duplex can achieve near-double spectral efficiency if the channel reciprocity holds and the interference cancellation is perfect. However, as σ increases from 0 dB to 5 dB, the full-duplex gain decreases from 99% to 47%.

We calculate the probability P_{all+} of $\widetilde{\mathbf{P}}$ being an all-positive power allocation vector. Note that P_{all+} is a lower bound of the probability that our solution guarantees the local Pareto optimality. Fig. 3.5

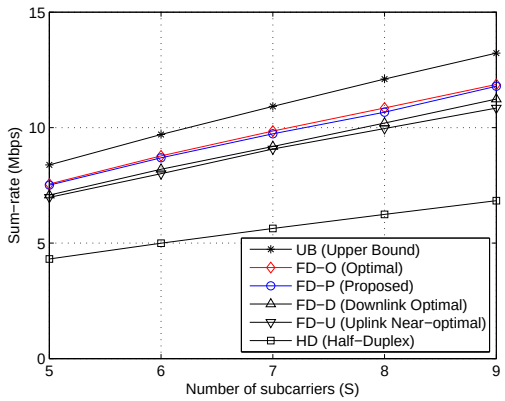

Figure 3.6: Performance comparison in small-size networks.

shows that for various S values, P_{all+} approaches 1 very quickly even with a small number of nodes, e.g., less than 10 nodes. For example, when $S = 50$, P_{all+} reaches 1 only after N becomes 10. When there are more nodes, each subcarrier is assigned to a node with a larger channel gain due to the multi-user diversity, and each subcarrier is assigned positive (uplink and/or downlink) power with a higher probability. Considering that the number of nodes in a cell is typically larger than 10, our solution is highly likely to guarantee the local Pareto optimality in practice.

Now, we consider the asymmetric channel model where the uplink and the downlink gains are chosen independently. The simulation results including FD-O are plotted in Fig. 3.6 when $N = 5$ and $d = 200$ m. FD-P achieves almost the same performance as FD-O, and thus FD-P is empirically near-optimal even in asymmetric channel environments. The performance gap between UB and FD-P is about

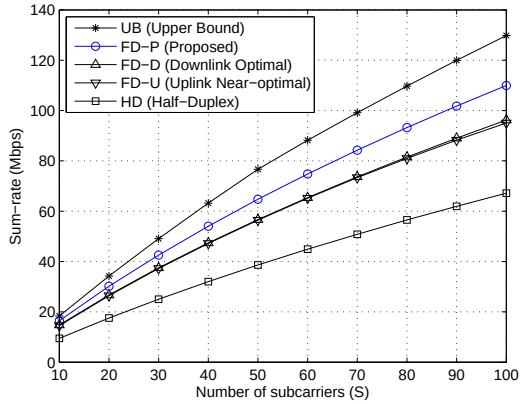

Figure 3.7: Performance comparison according to S values in asymmetric channel model.

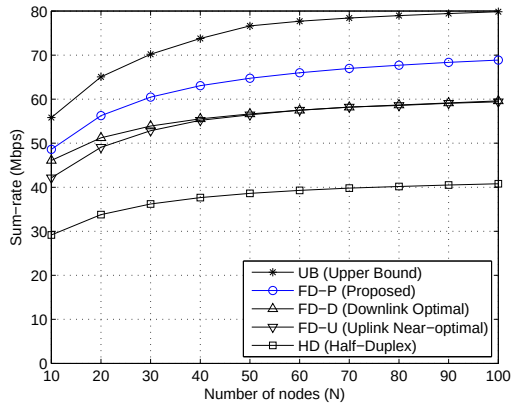

Figure 3.8: Performance comparison according to N values in asymmetric channel model.

11%, which is a huge increase compared to the symmetric channel case. Due to the channel asymmetry, $\widetilde{\mathbf{X}}$ and $\mathbf{X}^d$ ($\mathbf{X}^u$) significantly differ from each other, and consequently, the performance gap between UB and FD-P enlarges.

We compare the performance of each scheme in large-size networks. We omit FD-O due to its high computational complexity. Fig. 3.7 shows the sum-rate of each scheme as a function of S when $N = 50$ and $d = 200$ m. FD-P outperforms both FD-D and FD-U with a gain of 11% ($S = 10$) to 14% ($S = 100$). Due to the channel asymmetry, $\widetilde{\mathbf{X}}$ and $\mathbf{X}^u$ ($\mathbf{X}^d$) are different to each other. Consequently, FD-P achieves a better performance than FD-D (FD-U) that only maximizes the downlink (uplink) rate rather than the sum-rate. The full-duplex gain ranges from 64% ($S = 100$) to 74% ($S = 10$), which are lower than those (87% to 91%) in the symmetric channel case. This is because the gap between $R^d(\mathbf{X}^d)$ and $R^d(\widetilde{\mathbf{X}})$ (also $R^u(\mathbf{X}^u)$ and $R^u(\widetilde{\mathbf{X}})$) widens in the asymmetric channel case.

The performance of each scheme as a function of N is shown in Fig. 3.8 when $S = 50$ and $d = 200$ m. When $N = 10$, the performance gap between FD-P and FD-D is negligible (5%), and FD-U achieves the lowest sum-rate. Since P_{BS} (= 43 dBm) is about 80 times larger than P_n (= 24 dBm), the downlink rate dominates the sum-rate when there are few nodes. Thus, FD-P and FD-D show a similar performance in case of small N. As N grows, however, the sum of each node's uplink power, i.e., $N \cdot P_n$, also linearly increases, balancing the impact of

downlink and uplink rates on the sum-rate. As a result, the sum-rates of FD-D and FD-U become closer while FD-P outperforms both of them with a gain of 16% ($S = 100$). In addition, the full-duplex gain is about 68% for every value of N.

Fig. 3.9 shows the sum-rate of each scheme according to d values when $N = 50$ and $S = 50$. Interestingly, as the distance d increases, the full-duplex gain decreases from 79% ($d = 100$ m) to 34 % ($d = 500$ m). When d is small (i.e., high SINR), the gap between $R^d(\mathbf{X}^d)$ and $R^d(\widetilde{\mathbf{X}})$ is relatively small due to the shape of a logarithmic function, i.e., the derivative of $\log(x)$ is low at a small x. However, as d increases (i.e., low SINR), the gap between $R^d(\mathbf{X}^d)$ and $R^d(\widetilde{\mathbf{X}})$ widens due to the large derivative of $\log(x)$ at a small x. In other words, the degradation of downlink rate due to a suboptimal allocation $\widetilde{\mathbf{X}}$ is more remarkable at low SINR regions. Also, the gap between $R^u(\mathbf{X}^u)$ and $R^u(\widetilde{\mathbf{X}})$ increases with d for the same reason.

Fig. 3.10 shows the performance of each scheme according to σ values when $N = 50$, $S = 50$, and $d = 200$ m. The sum-rates of all schemes except HD decreases with σ due to the increasing noise power. Even with the perfect cancellation ($\sigma = 0$), the full-duplex gain is only 74%, which is far below the ideal gain of 100%. Furthermore, as σ reaches 5 dB, the full-duplex gain is reduced to 24% and FD-U (FD-D) has a marginal gain over HD. This results indicates that the full-duplex gain is limited when there exists a substantial amount of residual self-interference.

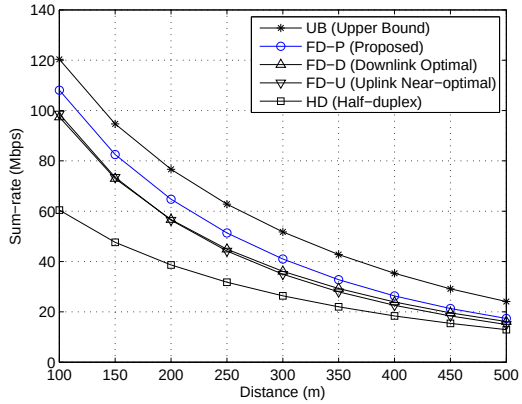

Figure 3.9: Performance comparison according to d values in asymmetric channel model.

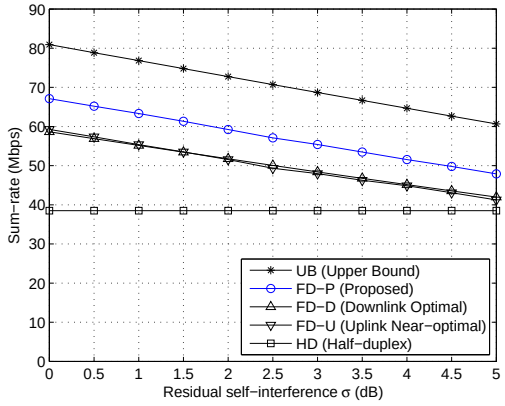

Figure 3.10: Performance comparison according to σ values in asymmetric channel model.

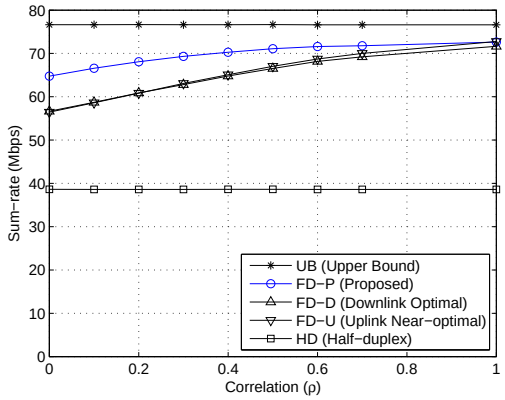

Figure 3.11: Impact of channel correlation ρ on performance.

Lastly, we investigate the impact of channel correlation ρ on the performance. Fig. 3.11 shows the performance of each scheme as a function of ρ when $N = 50$, $S = 50$, and $d = 200$ m. Since the uplink and the downlink transmissions are separated in UB and HD, their sum-rates are not affected by ρ. In contrast, the performance of FD-P improves by 12% (from 64.8 Mbps to 72.7 Mbps) as ρ increases from 0 to 1. This is because $\widetilde{\mathbf{X}}$ and $\mathbf{X}^u$ ($\mathbf{X}^d$) become more similar to each other with ρ. The full-duplex gain also increases with ρ, ranging from 68% ($\rho = 0$) to 88% ($\rho = 1$).

3.8 Summary

In-band wireless full-duplex is a promising technology to boost the network throughput. While a near-double capacity is anticipated in point-to-point wireless links, the performance gain remains unclear

in large-scale networks due to the complicated resource allocation in multi-carrier and multi-user environments In this chapter, we have developed a new resource allocation algorithm for full-duplex OFDMA networks using a necessary condition for the optimal solution. The proposed algorithm assigns subcarriers to nodes in an iterative manner with low complexity. We have proved that our algorithm achieves local Pareto optimality under certain conditions that hold frequently in practice. By separating the uplink and downlink transmissions, we have obtained an upper bound on performance that is near-tight in symmetric channel cases. Through extensive numerical simulations, we have demonstrated that our algorithm achieves near-optimal performance and outperforms other resource allocation schemes designed for half-duplex networks. Also, we have investigated the impact of various factors such as channel correlation, distance, and residual self-interference on the performance of full-duplex.

Chapter 4

Resource Allocation with Inter-node Interference in Full-duplex OFDMA Networks

4.1 Introduction

Orthogonal Frequency Division Multiple Access (OFDMA) has been a key technology in most 4G cellular systems [39]. Dividing the spectrum band into multiple orthogonal subcarriers and distributing them over different nodes, OFDMA benefits from both multiuser and frequency diversities. To exploit such benefits, radio resource allocation

algorithms handle subcarrier assignment and power allocation. In downlink case, an optimal allocation for the sum-rate maximization is a combination of the channel-based subcarrier assignment and the well-known water-filling power allocation [41]. In contrast, the uplink problem is in general difficult to solve due to the distributive nature of power constraints, i.e., each uplink node has its own power budget. Most previous results achieve suboptimal performance by solving relaxed problems [42, 43], or using a randomized iteration method [46].

Recently, *in-band wireless full-duplex* has attracted great attention as a promising technology for next-generation wireless systems. A full-duplex radio can transmit and receive simultaneously on the same frequency band by cancelling *self-interference* that results from its own transmission to the received signal, and thus potentially double the spectral efficiency. The main challenge in building a full-duplex system is in suppressing the self-interference to a sufficiently low level. Extensive researches have been conducted for self-interference cancellation techniques, which can be categorized into antenna cancellation, analog cancellation, and digital cancellation [18]. In antenna cancellation techniques, a pair of transmission antennas are placed such that the signal from one antenna destructively adds with that from the other [1, 4, 5]. Analog cancellation methods tap a copy of the transmitted signal from the transmit chain, process it with delay and attenuation, and subtract it on the receive path [1, 3]. Lastly, digital cancellation is used to clean out any residual self-interference caused

by non-ideal and non-linear components in RF chains [1, 3]. The state-of-the-art work has demonstrated that self-interference can be suppressed to the noise floor level by the combination of multiple cancellation techniques [6].

When the full-duplex technology is introduced in OFDMA networks, base stations (BSs) need to be full-duplex capable while mobile nodes (user terminals) operate in either full-duplex or half-duplex. If nodes are also full-duplex capable, the BS can communicate with them in a bidirectional manner by assigning each subcarrier to a single node for both uplink and downlink transmissions. However, it is unlikely that nodes are equipped with full-duplex radios in the foreseeable future due to the cost and complexity of interference cancellation techniques. Considering this limitation, a typical deployment scenario will be the full-duplex transmission between a full-duplex BS and legacy half-duplex nodes, where the BS assigns a subcarrier to two different nodes, one for uplink and the other for downlink. In this case, already complicated resource allocation problems become much more challenging due to i) the coexistence of uplink and downlink transmissions in the same subcarrier, and ii) resultant *inter-node interference* from uplink nodes to downlink nodes. To fully exploit the full-duplex gain, it is essential to allocate the radio resource considering the inter-node interference.

There are several works that address the resource allocation problem in full-duplex networks. In [46], the authors considered a single-

cell full-duplex network consisting of a full-duplex BS and nodes and proposed a randomized iteration method which achieves a near-optimal performance. However, the proposed solution cannot cover the case with half-duplex nodes, which is more challenging due to the inter-node interference. In [47], the authors considered the case where mobile nodes operate in half-duplex, and proposed a resource allocation algorithm using matching theory. The proposed subcarrier allocation algorithm potentially leads to a non-convex power allocation problem, which is generally hard to solve.

In this paper, we investigate the joint problem of subcarrier assignment and power allocation in a single-cell full-duplex OFDMA network, which consists of a full-duplex BS and multiple half-duplex nodes. Our goal is to maximize the sum-rate performance by optimizing the uplink and downlink resource allocations taking into account the inter-node interference. Specifically, we consider two different scenarios: i) the BS knows full channel state information (full CSI), and ii) the BS obtains limited channel state information (limited CSI) through channel feedbacks from nodes. We aim to solve the problem from theoretical perspective in the former case while focusing on more practical issues in the latter. The contributions of this chapter are three-fold:

- In the full CSI scenario, we show that the resource allocation problem is NP-hard due to the inter-node interference. To make the problem tractable, we propose to use a subcarrier assignment

condition that leads each subcarrier to be assigned to a pair of uplink and downlink nodes that have lower inter-node channel gain compared to the uplink channel gain. Based on the above condition, we develop sequential resource allocation algorithms which assigns subcarriers to uplink and downlink nodes sequentially with two different orders, i.e., uplink first and downlink first.

- In the limited CSI scenario, we first identify the prohibitive channel measurement/feedback overhead in full-duplex networks and propose a design principle for efficient channel feedback. Then we propose a low-overhead feedback protocol where downlink nodes can estimate the inter-node interference in a distributed manner. We also analyze the sum-rate performance of the proposed feedback protocol and obtain the optimal feedback probability. To the best of our knowledge, this is the first scheme for full-duplex networks that can operate with limited CSI.

- Through simulation, we evaluate our algorithms under various scenarios. In the full CSI scenario, we compare our resource allocation scheme with conventional schemes oblivious to the inter-node interference. We also identify how much gain the full-duplex bring compared to half-duplex and when the full-duplex gain is maximized. In the limited CSI scenario, we investigate

the performance of the limited CSI scheme compared to the full CSI scheme, and the full-duplex gain in practical limited CSI scenario.

The rest of this chapter is organized as follows. In Section 4.2, we present a detailed description of our system model and formulate the resource allocation problem. In Section 4.3, we consider the problem with full CSI where the BS knows all channel gains. We design a simple subcarrier assignment condition and develop a sequential resource allocation algorithm. In Section 4.4, we consider a scenario where the BS obtains limited channel information through channel feedback from nodes. We propose a low-overhead channel feedback protocol for full-duplex networks where downlink nodes can measure interference in a distributed manner. The performance evaluation of our solutions is provided in Section 4.5. Finally, we conclude this paper in Section 4.6.

4.2 System Model and Problem Formulation

We consider a single-cell OFDMA network which consists of one full-duplex base station (BS) and multiple half-duplex mobile nodes, as shown in Fig. 4.1. Each node is predetermined as either an uplink node or a downlink node. Let $\mathcal{N}$ denote the set of uplink nodes, and $\mathcal{M}$ denote the set of downlink nodes. Without loss of generality, we assume that the number of uplink nodes is equal to the number of

downlink nodes, i.e., $|\mathcal{N}|= |\mathcal{M}|= N$. The spectrum band is partitioned into S orthogonal subcarriers, denoted by $\mathcal{S} = \{1, 2, \ldots, S\}$. A subcarrier[1] is the basic physical unit of channel assignment and power allocation in the system. All the subcarriers are perfectly orthogonal to each other without inter-carrier interference. We assume that the perfect self-interference[2] at the BS exploiting various interference cancellation techniques [10, 16, 48]. However, due to simultaneous uplink and downlink transmissions in the same subcarrier, there exists inter-node interference from uplink nodes to downlink nodes [10].

Let us represent the uplink and downlink subcarrier assignment patterns by two binary vectors $\mathbf{X^u} := \left\{x^u_{n,s}\right\}_{n\in\mathcal{N},s\in\mathcal{S}}$ and $\mathbf{X^d} := \left\{x^d_{m,s}\right\}_{m\in\mathcal{M},s\in\mathcal{S}}$, respectively, where $x^u_{n,s}$'s and $x^d_{m,s}$'s are defined as

$$x^u_{n,s} = \begin{cases} 1, \text{ if subcarrier } s \text{ is assigned to node } n \in \mathcal{N}, \\ 0, \text{ otherwise,} \end{cases}$$

$$x^d_{m,s} = \begin{cases} 1, \text{ if subcarrier } s \text{ is assigned to node } m \in \mathcal{M}, \\ 0, \text{ otherwise.} \end{cases}$$

Also, let us define $\mathbf{X} := (\mathbf{X^u}, \mathbf{X^d})$. We assume that a subcarrier is exclusively assigned to at most one uplink node and one downlink node. Given $\mathbf{X}$, the uplink and downlink nodes using subcarrier s are

[1]For simplicity, we use the term "subcarrier" to refer to the basic scheduling unit. In practical wireless systems, the basic scheduling unit can be a single subcarrier or a cluster of subcarriers.

[2]In practice, the perfect cancellation is infeasible even with the state-of-the-art implementation. However, we assume the perfect cancellation to isolate the physical layer issues and focus on the resource allocation issues as in [16, 48].

denoted by n_s and m_s, respectively.

For each subcarrier s, let $g^u_{n,s}$ ($g^d_{m,s}$) denote the uplink (downlink) channel gain between uplink node n (downlink node m) and the BS, and let $g^i_{n,m,s}$ denote the inter-node channel gain from uplink node n to downlink node m. Each channel gain includes the path loss and Rayleigh fading, and it is normalized by the noise power N_0. Let $p^u_{n,s}$ denote the uplink power allocated by uplink node n, and $p^d_{m,s}$ denote the downlink power allocated by the BS for downlink node m. The uplink and downlink power allocations are represented by two vectors $\mathbf{P^u} := \left\{p^u_{n,s}\right\}_{n\in\mathcal{N},s\in\mathcal{S}}$ and $\mathbf{P^d} := \left\{p^d_{m,s}\right\}_{m\in\mathcal{M},s\in\mathcal{S}}$, respectively, and let $\mathbf{P} := (\mathbf{P^u}, \mathbf{P^d})$. The power budgets at the BS and uplink node u are limited to P_{BS} and P_n, respectively.

Assuming that interference is treated as noise, the full-duplex rate R_s (the sum of uplink rate R^u_s and downlink rate R^d_s) for each subcarrier s is given by

$$\begin{aligned} R_s(\mathbf{X},\mathbf{P}) = &\sum_{n=1}^{N} x^u_{n,s} \log\left(1 + g^u_{n,s} p^u_{n,s}\right) \\ &+ \sum_{m=1}^{N} x^d_{m,s} \log\left(1 + \frac{g^d_{m,s} p^d_{m,s}}{1 + \sum_{n=1}^{N} x^u_{n,s} g^i_{n,m,s} p^u_{n,s}}\right), \end{aligned} \tag{4.1}$$

where the first and second terms are the uplink and downlink rates, respectively, and $\sum_n x^u_{n,s} g^i_{n,m,s} p^u_{n,s}$ represents the inter-node interference. Also, let $R(\mathbf{X},\mathbf{P})$ denote the sum-rate over all the subcarriers, i.e., $R(\mathbf{X},\mathbf{P}) = \sum_{s=1}^{S} R_s(\mathbf{X},\mathbf{P})$.

Our goal is to find an optimal resource allocation that maximizes the sum-rate under given power budget constraints. We formulate the problem as

$$
\begin{aligned}
(\mathsf{P}) \quad \underset{\mathbf{X},\mathbf{P}}{\text{maximize}} \quad & R(\mathbf{X},\mathbf{P}) && \text{(4.2a)}\\
\text{subject to} \quad & \sum_{s=1}^{S} p_{n,s}^{u} \leq P_n, \forall n \in \mathcal{N}, && \text{(4.2b)}\\
& \sum_{s=1}^{S}\sum_{m=1}^{N} p_{m,s}^{d}, \leq P_{BS}, && \text{(4.2c)}\\
& \sum_{n=1}^{N} x_{n,s}^{u} \leq 1, \forall s \in \mathcal{S}, && \text{(4.2d)}\\
& \sum_{m=1}^{N} x_{m,s}^{d} \leq 1, \forall s \in \mathcal{S}, && \text{(4.2e)}\\
& x_{n,s}^{u} \in \{0,1\}, \forall n \in \mathcal{N}, \forall s \in \mathcal{S}, && \text{(4.2f)}\\
& x_{m,s}^{d} \in \{0,1\}, \forall m \in \mathcal{M}, \forall s \in \mathcal{S}. && \text{(4.2g)}
\end{aligned}
$$

Notice that subcarrier s is used in full-duplex mode if $\sum_n x_{n,s}^{u} = \sum_m x_{m,s}^{d} = 1$, or in half-duplex mode otherwise. In the following, we solve the problem under full CSI and limited CSI, respectively.

4.3 Resource Allocation with Full CSI

In this section, we solve the problem assuming that the BS knows all channel gains. We first show that the problem is a NP-hard problem and propose a subcarrier assignment condition which leads to a

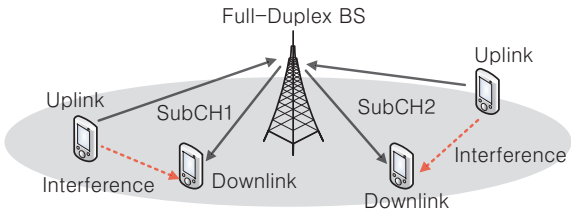

Figure 4.1: A single-cell full-duplex OFDMA network which consists of one full-duplex base station and multiple half-duplex mobile nodes. Due to the simultaneous uplink and downlink transmissions, there exists inter-node interference from uplink nodes to downlink nodes.

convex power allocation problem. We then design a sequential resource allocation algorithm by decomposing the problem into uplink and downlink subproblems.

4.3.1 Subcarrier Assignment Condition

Due to the exclusive nature of subcarrier assignment, problem P is an integer optimization problem, which is generally difficult to solve. In fact, the following theorem proves that problem P is NP-hard.

Theorem 4. The resource allocation problem P is NP-hard.

Proof. When there are only one uplink node and only one downlink node, the resource allocation problem is equivalent to the power allocation problem in Chapter 2, which is proven to be NP-hard. Thus, the resource allocation problem is NP-hard. □

Since it is difficult to obtain an optimal allocation, we instead assign subcarriers according to the following intuitive condition. Intuitively, it is reasonable to assign subcarrier s to a pair of (uplink

node u, downlink node d) satisfying that i) the uplink $g^u_{n,s}$ and downlink $g^d_{m,s}$ channel gains are large, and ii) the inter-node channel gain $g^i_{n,m,s}$ is small. With a large $g^u_{n,s}$, if $g^i_{n,m,s} > g^u_{n,s}$, the inter-node interference is strong enough to reduce the downlink rate significantly. To avoid this situation, we propose to assign each subcarrier s to a pair of (uplink node u, downlink node d) such that the inter-node channel gain $g^i_{n,m,s}$ should be less than the uplink channel gain $g^u_{n,s}$, i.e.,

$$g^i_{n,m,s} \leq g^u_{n,s}, \forall s. \tag{4.3}$$

The above condition prevents the excessive inter-node interference to protect downlink transmissions.

When a certain subcarrier assignment is given, we can reduce problem P to the following power allocation problem:

$$\begin{aligned} (\mathsf{P}_{\mathsf{P}}) \quad & \underset{\mathbf{P}}{\text{maximize}} \quad \sum_{s=1}^{S} R_s(p^u_{n,s}, p^d_{m,s}) \\ & \text{subject to} \quad \text{(4.2c) and (4.2b)}. \end{aligned} \tag{4.4}$$

In half-duplex case, the optimal power allocation is the per-node water-filling allocation [42, 43]. In contrast, this does not hold in full-duplex case due to the inter-node interference. Moreover, problem P_{p} is not a convex problem since R^s_F is not a concave function in general. This implies that it is hard to obtain the optimal power allocation $\mathbf{P}^*$ even if the optimal subcarrier assignment $\mathbf{X}^*$ has been

found.

Although problem $\mathsf{P_p}$ is difficult to solve in general, fortunately it becomes a convex problem if the given subcarrier assignment satisfies the condition (4.3).

Proposition 8. Let $\mathbf{X}$ be a given subcarrier assignment vector. If $\mathbf{X}$ satisfies the condition (4.3), the power allocation problem $\mathsf{P_p}$ is a convex optimization problem.

Proof. Since the power constraints (4.2b) and (4.2c) are linear and the objective function is the sum of R_s's, problem $\mathsf{P_p}$ is a convex optimization problem if each R_s is a concave function. Let $x^u_{n,s} = 1$ and $x^d_{m,s} = 1$. Then we can write $R_s(p^u_{n,s}, p^d_{m,s})$ as

$$R_s(p^u_{n,s}, p^d_{m,s}) = \log\left(\frac{1+g^u_{n,s}p^u_{n,s}}{1+g^i_{n,m,s}p^u_{n,s}}\right) + \log(1 + g^i_{n,m,s}p^u_{n,s} + g^d_{m,s}p^d_{m,s}).$$

The first term is a concave function of p^s_u, since it has a non-positive second-order derivative [30]

$$\frac{\partial^2}{\partial (p^s_u)^2}\log\left(\frac{1+g^s_u p^s_u}{1+g^s_{u,d}p^s_u}\right) = \frac{(g^s_{u,d}-g^s_u)(2g^s_u g^s_{u,d}p^s_u + g^s_u + g^s_{u,d})}{(g^s_{u,d}p^s_u+1)^2(g^s_u p^s_u+1)^2} \leq 0,$$

where the inequality comes from the assumption of $g^s_{u,d} \leq g^s_u$. The second term is a logarithm of a linear function, which is (jointly) concave. Thus, $R^s_F(p^s_u, p^s_d)$ is a concave function of (p^s_u, p^s_d). □

From Proposition 8 and the standard dual optimization method, we can easily solve problem $\mathsf{P_P}$ in low-complexity for any given sub-

carrier assignment satisfying the condition (4.3). In the following, we propose three resource allocation algorithms under the condition (4.3).

4.3.2 Proposed Resource Allocation Algorithms

In this section, we develop a sequential resource allocation algorithm under the condition (4.3); i) assign subcarriers to downlink nodes first and uplink nodes, ii) assign subcarriers to uplink nodes first and downlink nodes. Before proposing our algorithm, we first consider downlink and uplink resource allocation algorithms separately.

Downlink Resource Allocation

Given an uplink allocation $(\mathbf{X^u}, \mathbf{P^u})$, we solve the downlink allocation problem to maximize the sum-rate. Recall that n_s denotes the uplink node using subcarrier s. We define $\mathcal{M}^s_{n_s} = \{m \in \mathcal{M} | g^i_{n_s,m,s} \leq g^u_{n_s,s}\}$, i.e., the set of downlink nodes which are allowed to use subcarrier s under the condition (4.3). Also, we define the downlink channel gain to interference and noise ratio (CINR) $\tilde{g}^d_{m,s}$ in subcarrier s as

$$\tilde{g}^d_{m,s} = \frac{g^d_{m,s}}{1 + g^i_{n_s,m,s} p^u_{n_s,s}}, \forall m, s,$$

where $\tilde{g}^d_{m,s} = g^d_{m,s}$ when subcarrier s is not assigned to any uplink nodes. The downlink rate R^d_s in subcarrier s is given by

$$R^d_s(\mathbf{X^d}, \mathbf{P^d} | n_s, p^u_{n_s,s}) = \sum_{m=1}^{N} x^d_{m,s} \log\left(1 + \tilde{g}^d_{m,s} p^d_{m,s}\right).$$

Since the uplink rate is independent of the downlink power, the optimal downlink allocation[3] is the one which maximizes the sum of downlink rates $\sum_s R^d_{m,s}$. We formulate the problem as

$$(\mathsf{P_{DL}}) \quad \underset{\mathbf{X^d}, \mathbf{P^d}}{\text{maximize}} \ \sum_{s=1}^{S} \sum_{m=1}^{N} x^d_{m,s} \log\left(1 + \tilde{g}^d_{m,s} p^d_{m,s}\right) \qquad (4.5)$$
$$\text{subject to (4.2c), (4.2e), and (4.2g).}$$

Clearly, problem $\mathsf{P_{DL}}$ and the resource allocation problem in downlink OFDMA have an identical structure except that $\tilde{g}^d_{m,s}$ is regarded as channel gain and the condition (4.3) should be satisfied. Thus, we obtain an optimal solution by assigning each subcarrier s to downlink node $d \in \mathcal{M}^s_{n_s}$ with the largest $\tilde{g}^d_{m,s}$ while allocating the power according to the water-filling algorithm, i.e.,

$$m^* = \underset{m \in \mathcal{M}^s_{n_s}}{\arg\max} \left(\tilde{g}^d_{m,s}\right) \text{ and } x^d_{m^*,s} = 1, \qquad (4.6a)$$

$$p^d_{m,s} = \begin{cases} \left[\alpha - 1/\tilde{g}^d_{m,s}\right]^+, & \text{if } x^d_{m,s} = 1, \\ 0, & \text{if } x^d_{m,s} = 0, \end{cases} \qquad (4.6b)$$

[3]This is an optimal downlink allocation for the given uplink allocation, but not a globally optimal downlink allocation.

where $[\cdot]^+ := \max(\cdot, 0)$ and α is the water-level satisfying $\sum_m \sum_s p^d_{m,s} = P_{BS}$.

Uplink Resource Allocation

Given a downlink resource allocation $(\mathbf{X^d}, \mathbf{P^d})$, we solve the uplink allocation problem. Before proceeding to the allocation algorithm, let us first show how an uplink node n can optimally allocate its power given an uplink subcarrier assignment $\mathbf{X^u}$ satisfying the condition (4.3). Let $\mathcal{S}_n$ denote the set of subcarriers assigned to uplink node n. Given $(\mathbf{X^d}, \mathbf{P^d})$ and $\mathbf{X^u}$, in each subcarrier $s \in \mathcal{S}_n$, the full-duplex rate $R_{n,s}(p^u_{n,s})$ is a function of $p^u_{n,s}$, defined as

$$\begin{aligned} R_{n,s}(p^u_{n,s}) := R_s\left(p^d_{n,s}, p^d_{m_s,s}\right) &= \log\left(1 + g^u_{n,s}p^u_{n,s}\right) \\ &\quad + \log\left(1 + \frac{g^d_{m_s,s}p^d_{m_s,s}}{1 + g^i_{n,m_s,s}p^u_{n,s}}\right). \end{aligned} \tag{4.7}$$

Since $\mathbf{X^u}$ satisfies (4.3), $R_{n,s}(p^u_{n,s})$ is a concave function of $p^u_{n,s}$ by Proposition 8. Each uplink node n allocates its power p^s_u over subcarriers $s \in \mathcal{S}_n$ to maximize $\sum_{s\in\mathcal{S}_u} R_{n,s}(p^u_{n,s})$. Then we formulate the problem as

$$\begin{aligned} (\mathsf{P_{UL}}) \quad \underset{\mathsf{p^s_u}}{\text{maximize}} \quad & \sum_{s\in\mathcal{S}_n} R_{n,s}(p^u_{n,s}) \\ \text{subject to} \quad & \sum_{s\in\mathcal{S}_n} (p^u_{n,s}) \le P_n. \end{aligned} \tag{4.8}$$

Since this is a convex optimization problem, we can easily solve it through the dual optimization. Specifically, we can obtain the solution by using the bisection method with the complexity of $O(S)$.

We now explain the proposed uplink resource allocation algorithm. The algorithm operates in an iterative manner and runs for S times, where S is the number of subcarriers. In each iteration, we assign a single subcarrier to an uplink with the largest full-duplex rate. We use superscript k in square bracket to indicate the result up to iteration k.

Let $\mathcal{S}_n^{[k]}$ denote the set of subcarriers assigned to uplink node n up to iteration k, and $\mathcal{A}^{[k]}$ denote the set of unassigned subcarriers up to iteration k. Also, let us define $\mathcal{A}_n^{[k]} = \{s \in \mathcal{A}^{[k]} \ | g_{u,m_s,s}^i \leq g_{n,s}^u\}$, i.e., the set of subcarriers which can be allocated to uplink node n. All the subcarriers are unassigned in the beginning, i.e., $\mathcal{A}^{[0]} = \mathcal{S}$ and $\mathcal{S}_n^{[0]} = \emptyset, \forall u$.

In iteration k ($1 \leq k \leq S$), given $\mathcal{S}_n^{[k-1]}$ and $\mathcal{A}^{[k-1]}$, we compute the (potential) full-duplex rate and select a pair of (uplink node, subcarrier) with the largest full-duplex rate. To further elaborate, we compute the full-duplex rate R_u^s for each uplink node u as follows:

1. Allocate the uplink power $p_{n,s}^u$ to subcarriers $s \in \mathcal{S}_n^{[k-1]} \cup \mathcal{A}_n^{[k-1]}$ by solving (4.8). That is, $p_{n,s}^u$ is allocated as if subcarriers $s \in \mathcal{A}_n^{[k-1]}$ are assigned to uplink node u.

2. Compute the (potential) full-duplex rate $R_{n,s}(p_{n,s}^u)$ for each sub-

carrier $s \in \mathcal{A}_n^{[k-1]}$ by (4.7).

Among the unassigned subcarriers, we assign subcarrier $s \in \mathcal{A}^{[k-1]}$ to uplink node n with the largest full-duplex rate as follows:

$$(n^*, s^*) = \underset{n \in \mathcal{N}, s \in \mathcal{A}^{[k-1]}}{\arg\max} R_{n,s} \text{ and } x^u_{n^*,s^*} = 1. \tag{4.9}$$

Then we update the result as follows:

$$\mathcal{S}_{n^*}^{[k]} \leftarrow \mathcal{S}_{n^*}^{[k-1]} \cup \{s^*\} \text{ and } \mathcal{A}^{[k]} \leftarrow \mathcal{A}^{[k-1]} \backslash \{s^*\}.$$

We repeat the above procedures S times and obtain the uplink subcarrier assignment $\mathbf{X}^u$. Then we allocate the uplink power $\mathbf{P}^u$ by solving (4.8) with $\mathbf{X}^u$.

In each iteration, we perform the power allocation for each uplink node, which has the complexity of $O(S)$. Considering N nodes and S iterations, the total complexity is $O(NS^2)$.

Sequential Resource Allocation Algorithms

When we apply the above downlink and uplink allocation algorithms, we consider two types of resource allocation according to the order in application, i.e., downlink first (D-First) or uplink first (U-First).

In the D-First scheme, subcarriers are first assigned to downlink nodes, assuming $\mathbf{P}^u = 0$. That is, we solve problem P_{DL} with $\tilde{g}^d_{m,s} = g^d_{m,s}$. Next, we obtain the uplink allocation $(\mathbf{X}^u, \mathbf{P}^u)$ by solv-

ing the uplink problem given $(\mathbf{X}^d, \mathbf{P}^d)$. Finally, we take the subcarrier assignment $\mathbf{X} = (\mathbf{X}^u, \mathbf{X}^d)$ as the outcome and reallocate the (uplink and downlink) power by solving $\mathsf{P_P}$, i.e., the power allocation obtained in each individual solution is discarded.

In the U-First scheme, subcarriers are first assigned to uplink nodes, assuming $\mathbf{P}^d = 0$. Then given $(\mathbf{X}_U, \mathbf{P}_U)$, we obtain the downlink allocation $(\mathbf{X}_D, \mathbf{P}_D)$ by solving problem $\mathsf{P_{DL}}$. Finally, we reallocate power by solving $\mathsf{P_P}$.

4.3.3 Asymtotic Analysis of Full-duplex Gain

We define *full-duplex gain* as the performance ratio of full-duplex to half-duplex. Since the analysis of full-duplex gain in general cases is difficult, we adopt a simple asymtotic method to understand how the full-duplex gain varies with channel gain. Consider a single-carrier network with one uplink node and one downlink node. Let g^u and g^d denote the uplink and downlink channel gains, respectively, and g^i denote the inter-node channel gain. Also, p^u and p^d denote the uplink and downlink powers, respectively.

In the considered simple example, the sum-rate R_{FD} of full-duplex is given by

$$R_{FD} = \log(1 + g^u p^u) + \log\left(1 + \frac{g^d p^d}{1 + g^i p^u}\right).$$

Also, the sum-rate R_{HD} of half-duplex (in a TDMA manner) is ob-

tained as

$$R_{HD} = 0.5\log(1 + g^u p^u) + 0.5\log(1 + g^d p^d).$$

Then the full-duplex gain G_{FD} is expresses as

$$G_{FD} = \frac{\log(1 + g^u p^u) + \log\left(1 + \frac{g^d p^d}{1+g^i p^u}\right)}{0.5\log(1 + g^u p^u) + 0.5\log(1 + g^d p^d)}.$$

Now, let us consider a case where all channel gains are sufficiently large, i.e., $g^u, g^d, g^i \to \infty$. In this case, the full-duplex gain is approximated as

$$G_{FD} \approx \frac{\log(1 + \infty \times p^u) + \log\left(1 + \frac{\infty \times p^d}{1+\infty \times p^u}\right)}{0.5\log(1 + \infty \times p^u) + 0.5\log(1 + \infty \times p^d)} \approx 1, \qquad (4.10)$$

where p^u and p^d are assumed to be the same. Eq. (4.10) indicates that if all channel gains are sufficiently large, there is no full-duplex gain. In practice, this occurs when a large number of nodes are located in a small-size cell.

Next, consider a case where all channel gains are sufficiently small, i.e., $g^u, g^d, g^i \ll 1$. Using the approximation of $1+g^i p^u \approx 1$, we obtain the full-duplex gain as

$$G_{FD} \approx \frac{\log(1 + g^u p^u) + \log(1 + g^d p^d)}{0.5\log(1 + g^u p^u) + 0.5\log(1 + g^d p^d)} = 2, \qquad (4.11)$$

Since the interference level $g^i p^u$ is sufficiently smaller than the noise

power (which has a value of 1 due to the normalization), the sum-rate of full-duplex is approximated as if there were no interference, and the full-duplex gain approaches 2, i.e., achieving near-double throughput. In practice, this corresponds to cases where few nodes are in a large-size cell.

4.4 Resource Allocation with Limited CSI

In this section, we consider a scenario where the BS obtains limited channel information through channel feedbacks from nodes. We first discuss the overhead for channel measurement and feedback in full-duplex networks and identify the requirements for low-overhead solution. Then we propose a novel low-overhead channel measurement and feedback scheme and analyze its sum-rate performance.

4.4.1 Challenge of Channel Feedback

In the previous section, the resource allocation problem is solved under the full CSI assumption. While it is meaningful to obtain a theoretical solution, full channel knowledge at the BS is infeasible in wideband OFDMA due to the large amount of channel feedback for numerous subcarriers. In fact, the overhead for channel measurement/feedback becomes more problematic in full-duplex networks due to the following reasons:

- Channel measurement overhead:

A typical approach for channel measurement is using a training sequence, where a known signal is transmitted and the channel gain is estimated by comparing the transmitted and received signals. In conventional half-duplex systems, the BS broadcasts a training sequence that allows all nodes to measure their downlink channel gains while each node can also estimate its uplink channel gain using *channel reciprocity*, i.e., forward (downlink) and reverse (uplink) channels are reciprocal. In full-duplex networks, along with the BS, every uplink node also needs to transmit a training sequence in turn to allow downlink nodes to estimate inter-node channel gains. Since a dedicated transmission opportunity should be given to each uplink node, the required resource increases linearly with the number of uplink nodes, which will be a huge overhead.

- Channel feedback overhead:

  For channel feedback, the channel gain for each subcarrier is quantized to a real number and the corresponding value is reported to the BS. The feedback overhead for downlink channel is SB bits per downlink node, where B is the required number of bits for quantization, and similarly the overhead is SB bits per uplink node for uplink channel. In addition, the feedback overhead for inter-node channel is NSB bits per downlink node. Then the total feedback overhead over N uplink (downlink)

nodes sums up to $N(SB)+N(SB)+N(NSB) = N^2SB+2NSB$. Compared to half-duplex networks, the feedback overhead in full-duplex networks increases by (approximately) $\frac{N}{2}$ times due to inter-node channel gains.

Considering the prohibitive overhead for channel measurement and feedback, it is of great importance to design a low-overhead resource allocation scheme for full-duplex networks.

A well-known approach to reduce feedback overhead is using *opportunistic feedback*, where a node reports its channel gain if it is larger than a given threshold [50]. Specifically, all nodes contend in the shared feedback medium, which consists of multiple feedback slots associated with pre-defined threshold values which are in decreasing order. In a feedback slot, each node transmits a feedback message to the BS if its channel gain is larger than the given threshold. Then the BS chooses a node which transmitted in the earliest slot without collision and schedules it to use a certain subcarrier.

There have been many resource allocation schemes based on the opportunistic feedback, targeting either downlink [50, 51, 52] or uplink [53]. While the conventional schemes reduce the feedback overhead in half-duplex networks, they consider interference-free environments and thus cannot be applied to full-duplex networks, where downlink nodes experience inter-node interference. Due to the large overhead, it is impossible for a downlink node to measure the inter-node channel gains between itself and all uplink nodes. To circumvent this difficulty,

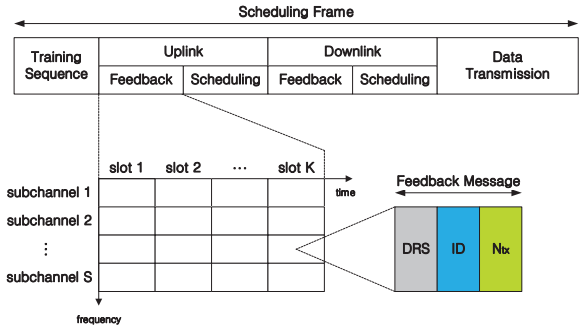

Figure 4.2: Superframe structure.

we adopt the idea behind the U-First scheme that subcarriers are first assigned to uplink nodes and then to downlink nodes. In this case, each downlink node only needs to estimate the interference from the scheduled uplink node in each subcarrier without having to know all inter-node channel gains. This raises a natural question: how can a downlink node estimate the interference level and report it to the BS in a low-overhead manner? In the following, we answer this question and develop a low-overhead channel measurement and feedback scheme for full-duplex networks.

4.4.2 Proposed Feedback Protocol

Fig. 4.2 illustrates the structure of the proposed scheduling frame, which consists of training sequence, feedback and scheduling period, and data transmission period. A scheduling frame is the basic time unit of resource allocation, during which channel gains are invariant. The feedback and scheduling period is decomposed into uplink and

downlink parts. The key idea for interference measurement is to let downlink nodes to overhear uplink feedback messages during the uplink feedback period. The detailed operation is as follows.

In the beginning of every scheduling frame, the BS broadcasts a training sequence to allow each node to measure its downlink channel gain. The channel measurement using training sequence is assumed to be perfect. In addition, each uplink node n calculates an estimate $\hat{g}^u_{n,s}$ of its uplink channel gain using the channel reciprocity, i.e., $\hat{g}^u_{n,s} = g^d_{n,s}$. Note that the channel reciprocity holds in principle on the same frequency band [55].

After receiving the training sequence, uplink nodes send feedback messages in the uplink feedback period. In the time domain, there are K feedback slots associated with K thresholds $\delta_1, \cdots, \delta_K$, which are in decreasing order, i.e., $\delta_1 > \cdots > \delta_K$. Given a fixed length of scheduling frame, the BS can tune K to adjust the ratio of channel feedback period and data transmission period. The threshold values are the same for all subcarriers, and the BS notifies the values to each node during the initial association process. The feedback processes for all subcarriers are identical and performed in parallel. The feedback for each subcarrier s operates as follows. In slot k ($1 \leq k \leq K$), an uplink node n transmits a feedback message to the BS over subcarrier s if its estimated uplink channel gain $\hat{g}^u_{n,s}$ satisfies the condition $\delta_{k-1} > \hat{g}^u_{n,s} \geq \delta_k$, where $\delta_0 = \infty$. Since δ_k's are in decreasing order, uplink nodes with larger channel gains can transmit in earlier slots. If node

n transmits alone in slot k, the BS can decode the feedback message successfully and know that it is from node n. If two or more nodes transmit at the same time, then a collision occurs and the BS cannot decode any colliding feedback messages.

A feedback message consists of three parts: demodulation reference signal (DRS), transmitter identifier (ID), and the number of simultaneously transmitted messages N_{tx}. The DRS is used to enable the uplink channel measurement and coherent signal demodulation at the BS. When an uplink node transmits N_{tx} feedback messages simultaneously (in the same slot over different subcarriers), the transmission power is equally distributed over the feedback messages. Also, there is a limit P^f for the power allocated in each feedback message to limit inter-node interference. Thus, when an uplink node n transmits N_{tx} feedback messages at the same time, it transmits each message with a power of $p^f_{n,s} = \min(\frac{P_n}{N_{tx}}, P^f)$ and records the power $p^f_{n,s}$ for each subcarrier s. Note that the BS can measure the uplink channel gain $g^u_{n,s}$ since it knows the transmitted signal from the DRS and N_{tx}.

In the uplink scheduling period, the BS announces the uplink scheduling information, which is a S-dimensional vector $\mathbf{X^u} = \{x^u_1, \cdots, x^u_S\}$. Among the nodes whose feedback messages were successfully received, the BS assigns each subcarrier s to the node with the largest channel gain. Specifically, for each subcarrier s, the BS selects the earliest slot k^* where i) only one node n transmitted its feedback message and ii) its actual uplink channel gain $g^u_{n,s}$ satisfies the condition $g^u_{n,s} \geq \delta_{k^*}$.

Note that the second condition is required in case the channel reciprocity does not hold[4], i.e., $\hat{g}^u_{n,s} = g^d_{n,s} \geq \delta_{k^*} > g^u_{n,s}$. Then the BS assigns subcarrier s to node n by setting $x^u_s = k^*$, which indicates that subcarrier s is assigned to the node which transmitted its feedback message in slot k^*. The reason of embedding a slot number rather than a node ID is to allow downlink nodes to estimate the interference level using the slot number, which will be explained later. If there is no slot with a successfully received feedback message, the BS leaves subcarrier s unassigned by setting $x^u_s = 0$. After receiving the scheduling vector $\mathbf{X^u}$, each uplink node can know whether or not each subcarrier s is assigned to itself by comparing x^u_s to the slot number it used for feedback.

During the uplink feedback period, each downlink node m measures the received signal strength $I_{m,s,k}$ in each of (subcarrier s, slot k). If uplink node n transmits alone in (subcarrier s, slot k), $I_{m,s,k}$ will be given as $I_{m,s,k} = g^i_{n,m,s} p^f_{n,s}$. Note that downlink nodes can estimate the received signal strength of a message from the DRS part. Next, downlink nodes overhear the uplink scheduling vector $\mathbf{X^u}$ to know which slot is selected in each subcarrier. If slot k^* is selected in subcarrier s ($x^u_s = k^*$), each downlink node m can estimate the interference level $I_{m,s}$ by $I_{m,s} = I_{m,s,k^*}$. In contrast, if subcarrier s is unassigned ($x^u_s = 0$), there will be no interference, i.e., $I_{m,s} = 0$.

[4]While the physical wireless channel is reciprocal in principle, the non-symmetric characteristics of the radio-frequency (RF) electronic circuitry would break the reciprocity property [55].

Since the uplink scheduling result is given in the form of slot number rather than node ID, downlink nodes can determine the interference level even if it failed to decode feedback messages.

The downlink feedback and scheduling period is similar to the uplink case except that two different types of thresholds are used depending on the uplink scheduling result. If subcarrier s is unassigned in the uplink, i.e., $x_s^u = 0$, the threshold values $\delta_1, \cdots, \delta_K$ are used and each downlink node m selects a slot according to its downlink channel gain $g_{m,s}^d$. In contrast, if subcarrier s is assigned to some uplink node, then another threshold values $\gamma_1, \cdots, \gamma_K$ are newly introduced. Also, each downlink node m selects a slot based on its channel to interference and noise ratio (CINR) $\tilde{g}_{m,s}^d = g_{m,s}^d/(1+I_{m,s})$. That is, each downlink node m transmits a feedback message in slot k if $\tilde{g}_{m,s}^d$ satisfies the condition $\gamma_{k-1} > \tilde{g}_{m,s}^d \geq \gamma_k$. We set $\delta_k > \gamma_k$ to reflect the SINR reduction due to the inter-node interference. After receiving downlink feedback messages, the BS assigns each subcarrier to the downlink node with the largest channel gain (or CINR), and broadcasts the downlink scheduling vector $\mathbf{X^d} = \{x_1^d, \cdots, x_S^d\}$.

In the data transmission period, the BS and uplink nodes allocate power according to the scheduling result. For each subcarrier s, let n_s and m_s denote the scheduled uplink and downlink nodes, respectively. Each uplink node n first allocates its power over the assigned

subcarriers by the water-filling algorithm, i.e.,

$$p_{n,s}^{u} = \begin{cases} \left[\alpha - \frac{1}{\delta_{x_s^u}}\right]^+, & \text{if } n = n_s, \\ 0, & \text{otherwise,} \end{cases}$$

where α is the water-level satisfying $\sum_s p_{n,s}^u = P_n$. Note that node n allocates $p_{n,s}^u$ according to $\delta_{x_s^u}$ rather than $g_{n,s}^d$ because it only knows that $g_{n,s}^u$ is larger than $\delta_{x_s^u}$, but does not know the actual value. Then node n compares $p_{n,s}^u$ with the feedback power $p_{n,s}^f$ and if $p_{n,s}^u \geq p_{n,s}^f$, $p_{n,s}^u$ is set to $p_{n,s}^f$. This is to ensure that the actual interference level in the data period is no greater than the interference level measured in the uplink period. For the downlink power allocation, the BS also uses the water-filling algorithm as

$$p_{m,s}^{d} = \begin{cases} \left[\beta - \frac{1}{\delta_{x_s^d}}\right]^+, & \text{if } m = m_s \text{ and } x_s^u = 0, \\ \left[\beta - \frac{1}{\gamma_{x_s^d}}\right]^+, & \text{if } m = m_s \text{ and } x_s^u > 0, \\ 0, & \text{otherwise,} \end{cases}$$

where β is the water-level satisfying $\sum_m \sum_s p_{m,s}^d = P_{BS}$. Again, the downlink power for subcarrier s is allocated according to $\delta_{x_s^d}$ ($\gamma_{x_s^d}$) rather than $g_{m_s,s}^d$ ($\tilde{g}_{m_s,s}^d$).

4.4.3 Calculation of Thresholds

The threshold values determine the feedback probability in each slot, which in turn impacts the overall performance. Since the optimal

threshold values depend on the distribution of channel gain, the number of nodes, and the considered objective function [49], optimization of thresholds is a difficult design issue and is out of the scope of this paper. Instead, we simply set the threshold values such that each node transmits its feedback message in each slot with probability p [49, 51, 54], and find the corresponding threshold values.

For analytical tractability, we assume that all uplink, downlink, and inter-node channel gains $g^u_{n,s}$, $g^d_{m,s}$, and $g^i_{n,m,s}, \forall n, m, s$ are independent and identically distributed (*i.i.d.*) exponential random variables[5]. Also, assume that the channel reciprocity holds, i.e., $\hat{g}^u_{n,s} = g^u_{n,s}$. Let $\bar{g}$ denote the average channel gain, i.e., $\bar{g} = E[g^u_{n,s}] = E[g^d_{m,s}] = E[g^i_{n,m,s}], \forall n, m, s$. The cumulative distribution function (CDF) and probability density function (PDF) of each channgel gain are given by $F_g(x) = 1 - \exp\left(-\frac{x}{\bar{g}}\right)$ and $f_g(x) = \frac{1}{\bar{g}} \exp\left(-\frac{x}{\bar{g}}\right)$, respectively.

We first calculate the values of $\delta_1, \cdots, \delta_K$. The probability that an uplink node n transmits its feedback message in slot 1 is given by

$$\Pr\left(g^u_{n,s} \geq \delta_1\right) = 1 - F_g(\delta_1) = \exp\left(-\frac{\delta_1}{\bar{g}}\right) = p.$$

By some manipulations, we obtain $\delta_1 = \overline{g}\ln(\frac{1}{p})$. Given δ_1, the feed-

[5]The *i.i.d.* assumption is widely used in the literature [49, 51].

back probability in slot 2 is given by

$$\Pr\left(\delta_1 > g^u_{n,s} \geq \delta_2\right) = F_g(\delta_1) - F_g(\delta_2) = \exp\left(-\frac{\delta_2}{\bar{g}}\right) - p = p.$$

Again, we obtain $\delta_2 = \overline{g}\ln\left(\frac{1}{2p}\right)$ and in a similar manner, $\delta_k = \overline{g}\ln\left(\frac{1}{kp}\right)$. Note that a smaller p leads to a larger δ_k.

To calculate the values of $\gamma_1, \cdots, \gamma_K$, we need to derive the distribution of CINR $\tilde{g}^d_{m,s}$ of downlink node m in subcarrier s. Recall that n_s is the uplink node using subcarrier s and $p^f_{n_s,s}$ is its transmission power for feedback message. Then $\tilde{g}^d_{m,s}$ is given by

$$\tilde{g}^d_{m,s} = \frac{g^d_{m,s}}{1 + g^i_{n,m,s}p^f_{n_s,s}},$$

where $g^i_{n,m,s}p^f_{n_s,s}$ represents the interference level $I_{m,s}$ measured during the uplink feedback period. Since $p^f_{n_s,s}$ is determined by the number of simultaneously transmitted messages, it is not easy to calculate the exact value. Instead, we set $p^f_{n_s,s} = P^f$, which is a conservative assumption that leads to the maximum interference level $g^i_{n,m,s}P^f$. In this case, the CDF of $\tilde{g}^d_{m,s}$ is given by

$$F_{\tilde{g}}(x) = 1 - \frac{e^{-x/\bar{g}}}{1 + xP^f}.$$

From $F_{\tilde{g}}(x)$, the probability that each downlink node m transmits its

feedback message in slot 1 is given by

$$\Pr\left(g_{m,s}^{d} \geq \gamma_1\right) = 1 - F_g(\gamma_1) = \frac{\exp\left(-\frac{\gamma_1}{\bar{g}}\right)}{1 + \gamma_1 P^f} = p.$$

Due to the complex form of $F_{\tilde{g}}(x)$, we cannot obtain an analytical solution for γ_1, and thus find γ_1 (also other γ_k's) using numerical methods.

4.4.4 Performance Analysis and Optimal Feedback Probability

In this subsection, we derive the sum-rate analytically and obtain the optimal feedback probability p^*. We first derive the scheduling probability in each subcarrier. Without loss of generality, we focus on the uplink feedback in a random subcarrier s. The probability $P_{k,1}$ that only one node transmits in slot k is given by

$$P_{k,1} = \Pr\left(1 \text{ feedback in slot } k\right) = Np(1-p)^{N-1}. \tag{4.12}$$

Then the probability P_k that slot k is selected for scheduling can be obtained as

$$P_k = \Pr\left(x_s^u = k\right) = P_{k,1} \prod_{i=1}^{k-1} (1 - P_{i,1}). \tag{4.13}$$

Lastly, the scheduling probability P_{sch} in subcarrier s (i.e., subcarrier s is assigned to some uplink node) is given by

$$P_{sch} = \Pr\left(x_s^u \geq 0\right) = \sum_{k=1}^{K} P_k. \tag{4.14}$$

Note that $P_{k,1}$, P_k, and P_{sch} can be applied to other subcarriers and to the downlink.

We now derive the uplink rate R_s^u in a random subcarrier s. To obtain R_s^u, we need to find the uplink power in subcarrier s. Suppose that subcarrier s is assigned to uplink node n_s. Since node n_s allocates its power by the water-filling algorithm, the uplink power $p_{n_s,s}^u$ in subcarrier s depends on the channel gains of other subcarriers which are also assigned to node n_s, and thus it is not easy to obtain $p_{n_s,s}^u$. To circumvent this difficulty, we resort to a well-known property of the water-filling algorithm that it converges to a flat-power allocation at high SNR regimes [56]. If p is small and the corresponding threshold values are sufficiently large (i.e., high SNR), node n allocates an almost-equal power to the subcarriers assigned to itself. In addition, since all nodes are equally likely to use a subcarrier due to the *i.i.d.* channel conditions, node n_s uses SP_{sch}/N subcarriers on average. Thus, we approximate the uplink power $p_{n_s,s}^u$ in subcarrier s by

$$p_{n_s,s}^u = \min\left(P^f, \frac{NP_n}{SP_{sch}}\right). \tag{4.15}$$

Then we obtain R_s^u as

$$R_s^u = \sum_{k=1}^{K} P_k \log\left(1 + \delta_k p_{n_s,s}^u\right). \tag{4.16}$$

Since the expected uplink rate is the same in each subcarrier, the sum R^u of uplink rates over all subcarriers is given by

$$R^u = \sum_{s=1}^{S} R_s^u = SR_s^u. \tag{4.17}$$

We next derive the downlink rate R_s^d in a random subcarrier s. Again, we assume that the BS allocates an equal power p_s^d to each subcarrier s, which is given by

$$p_s^d = \frac{P_{BS}}{SP_{sch}}, \forall s. \tag{4.18}$$

The uplink scheduling result determines which type of threshold is used in the downlink feedback, i.e., δ_k or γ_k. When subcarrier s is unassigned in the uplink, we obtain R_s^d as

$$R_s^d = \sum_{k=1}^{K} P_k \log\left(1 + \delta_k p_s^d\right). \tag{4.19}$$

On the other hand, if subcarrier s is assigned to some uplink node, R_s^d is given by

$$R_s^d = \sum_{k=1}^{K} P_k \log\left(1 + \gamma_k p_s^d\right). \tag{4.20}$$

From Eqs. (4.19) and (4.20), we have

$$R_s^d = \sum_{k=1}^{K} P_k \left\{ (1 - P_{sch}) \log \left(1 + \delta_k p_s^d \right) + P_{sch} \log \left(1 + \gamma_k p_s^d \right) \right\}. \tag{4.21}$$

As in the uplink case, the sum R^d of downlink rates over all subcarriers is

$$R^d = \sum_{s=1}^{S} R_s^d = S R_s^d. \tag{4.22}$$

Lastly, combining Eqs. (4.17) and (4.22), we obtain the sum-rate R as

$$R = R^u + R^d. \tag{4.23}$$

To validate the analysis (4.23), we compare it with the simulation results. The comparison between analysis and simulation is shown in Fig. 4.3 where $N = 60$, $K = 8$, $S = 20$, and $\overline{g} = 733$. There is a close match between the analysis and the simulation, validating the accuracy of the analysis.

Since the sum-rate $R(p)$ is a function of p, we can numerically obtain the optimal feedback probability p^* using (4.23). Fig. 4.4 shows the value of p^* when the number of subcarriers is $S = 50$ and the mean channel gain is $\overline{g} = 733$. We can see that p^* decreases with the number of nodes N. This is because p^* should be reduced to prevent a high collision probability with more nodes. In addition, p^* has a smaller value when there are more feedback slots.

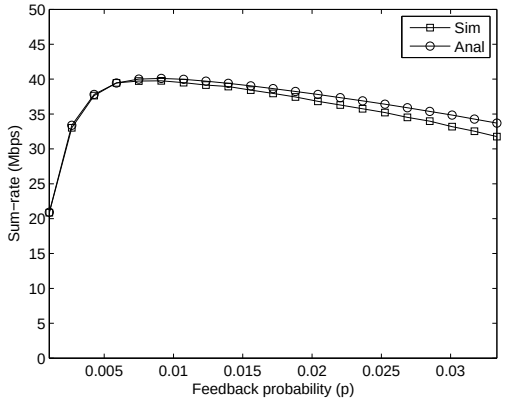

Figure 4.3: Comparison between analysis and simulation.

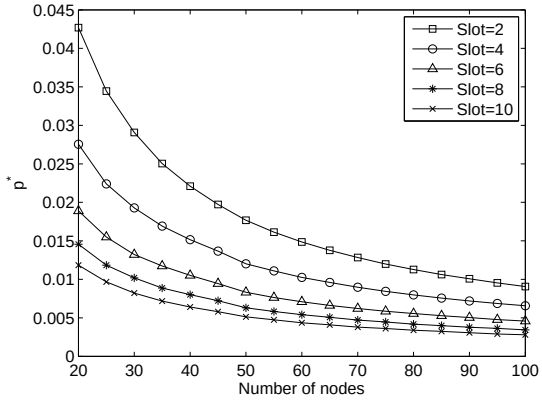

Figure 4.4: Optimal feedback probability p^* obtained through analysis.

Table 4.1: Simulation Parameters

Parameter	Value
Center frequency	2.1 GHz
Subcarrier bandwidth	180 kHz
Noise power	-119 dBm
Base station's power P_{BS}	43 dBm
Node n's power P_n	24 dBm
Antenna gain	0.0
Height of BS h_{BS}	30 m
Height of node h_N	1.5 m

4.5 Performance Evaluation

4.5.1 Simulation Setting

Simulation parameters are configured according to the typical values of LTE system [36]. We assume 10 MHz spectrum band and 50 subcarriers[6] with 180 kHz and set the noise power to -119 dBm. The Hata urban propagation model is used for the path loss. The power budgets are set as $P_{BS} = 43$ (dBm) and $P_n = 24$ (dBm) for all uplink nodes. Other simulation parameters are summarized in Table 4.1.

In the simulation for full CSI, we conduct 100 simulation runs and obtain the average result. Each channel gain includes a location-dependent path loss and a Rayleigh fading term. We consider two different topologies:

- Cell topology: Nodes are randomly distributed within a cell radius r.

[6]Since the basic scheduling unit in LTE systems is a resource block (180 kHz), we set the bandwidth of a subcarrier as 180 kHz

- Ring topology: Nodes are at an equal distance d from the BS. As a result, all uplink and downlink channel gains have the same distribution. In addition, we assume that inter-node channel gains also have the same distribution.

For performance evaluation, we compare the following schemes:

- Downlink first allocation algorithm (D-First): Subcarriers are first assigned to downlink nodes.
- Uplink first allocation algorithm (U-First): Subcarriers are first assigned to uplink nodes.
- Baseline (BL): As a point of reference, we consider a simple combination of (half-duplex) uplink and downlink allocation schemes without considering the inter-node interference. The optimal solution [41] is used for the downlink while a near-optimal allocation algorithm [43] is used for the uplink.
- Half-duplex (HD): Downlink and uplink transmissions switch over time slots using the algorithms [41] and [43], respectively.

In the simulation for limited CSI, we also conduct 100 simulation runs and obtain the average result. We only consider the ring topology. For performance evaluation, we compare the following schemes:

- Full-duplex limited CSI: Proposed limited feedback scheme.
- Full-duplex full CSI: U-First scheme with full CSI.

- Half-duplex limited CSI: Half-duplex transmissions with limited CSI.

For the schemes with limited CSI, we use the optimal feedback probability p^* obtained through the analysis.

4.5.2 Simulation Results: Full CSI

We first provide the simulation results obtained in the ring topology. Fig. 4.5(a) shows the sum-rate of each scheme for various d values when the number of uplink (downlink) nodes is 50, i.e., $N = 50$. FD-P and FD-U show a similar performance and outperform the baseline scheme. As shown in Figs. 4.5(b) and 4.5(c), U-First gives priority to the uplink traffic and achieves a high uplink rate while D-First operates in the opposite way. Although the baseline scheme achieves the highest uplink rate, its downlink rate becomes severely low due to the excessive inter-node interference. The performance gain over the baseline scheme shrinks with the distance, and the proposed schemes and the baseline scheme achieve a similar sum-rate at $d = 500$ m.

Fig. 4.6 depicts the full-duplex gain as function of distance d when $N = 50$. The full-duplex gain increases with the distance, and it ranges from 164% ($d = 100$ m) to 185% ($d = 500$ m). As explained in (4.11), this is because the ratio of interference level to the noise power shrinks with the distance.

We next show the simulation results obtained in the cell topology. Fig. 4.7 shows the sum-rate of each scheme for various r values when

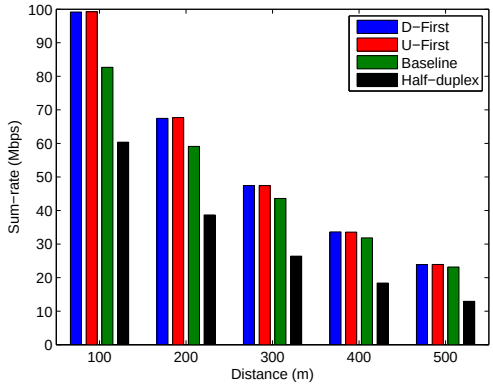

(a) Sum-rate $\sum_s R_s$

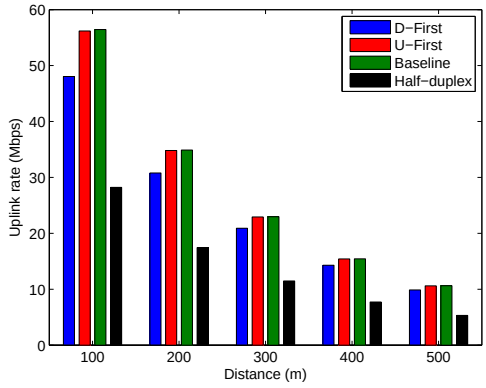

(b) Uplink rate $\sum_s R_s^u$

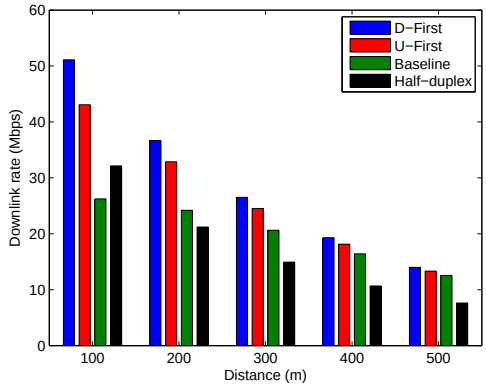

(c) Downlink rate $\sum_s R_s^d$

Figure 4.5: Performance comparison in ring topology.

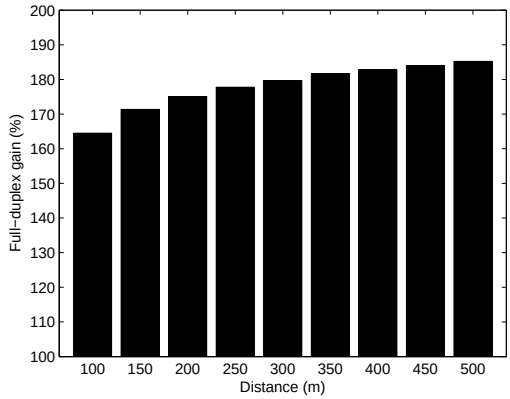

Figure 4.6: Full-duplex gain as a function of distance d.

the number of uplink (downlink) nodes is 50, i.e., $N = 50$. The results are similar to those obtained in the ring topology. One difference is that D-First achieves a larger sum-rate than U-First.

Fig. 4.8 depicts the impact of the number of nodes N on the performance. The cell radius r is set to 500 m and the number of uplink (downlink) nodes is changed from 20 to 100. When there are 10 uplink (downlink) nodes, our schemes and the baseline scheme show a similar performance. This is because the inter-node interference is weak in a sparse node distribution. As the node density increases, our scheme outperforms the baseline scheme with a gain of 13%.

Fig. 4.9 shows the gain of D-First over HD as a function of N. The full-duplex gain decreases from 180% ($N = 10$) to 170% ($N = 100$). As explained in (4.11), this indicates that the full-duplex gain is maximized in weak interference environments, i.e., sparse node distribution.

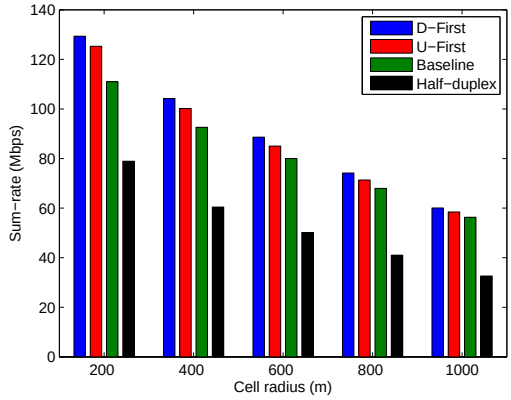

Figure 4.7: Performance comparison in the cell topology.

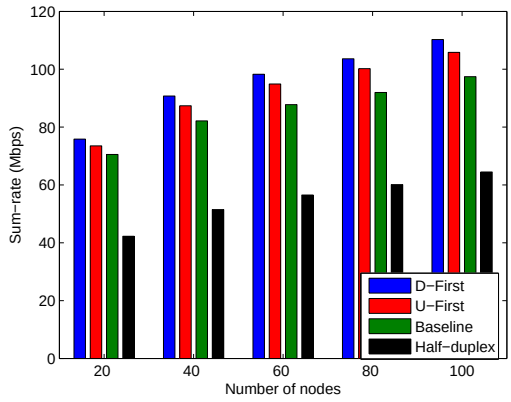

Figure 4.8: Impact of the number of nodes on the performance. The performance gain of our schemes over the baseline scheme increases with more nodes.

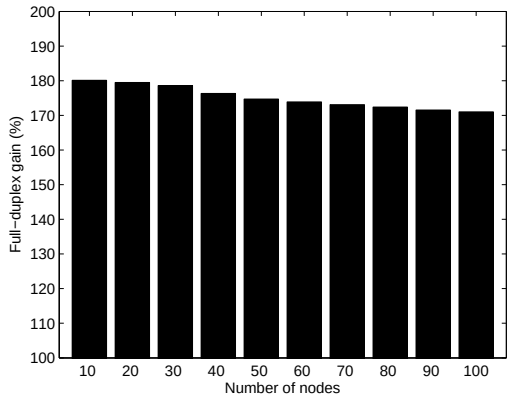

Figure 4.9: Full-duplex gain as a function of N.

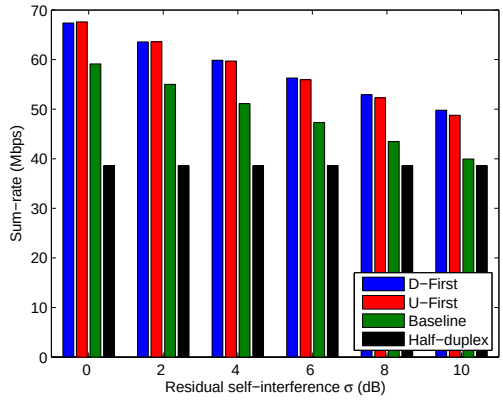

Figure 4.10: Impact of residual self-interference σ on performance.

Lastly, we investigate the impact of residual self-interference on the performance. We assume that under imperfect interference cancellation, the noise power increases by σ (dB) due to the residual self-interference. Fig. 4.10 shows the sum-rate of each scheme for various σ values in the ring topology when $d = 200$ m. The sum-rates of all schemes expect Half-duplex decreases with σ due to the increasing noise power. Also, the full-duplex gain decreases from 175% ($\sigma = 0$) to 129% ($\sigma = 10$).

4.5.3 Simulation Results: Limited CSI

We first compare the performance of full CSI and limited CSI schemes. Fig. 4.11 shows the sum-rate of limited CSI scheme for various K values (number of slots) when $N = 50$ and $d = 300$ m. As K increases, the sum-rate of limited CSI grows from 160 bps ($K = 2$) to 237 bps ($K = 20$). When $K = 20$, the limited CSI scheme achieves about 90% of the sum-rate of full CSI scheme. The performance improvement is more obvious when K increases from a small value, and as K grows beyond 10, the sum-rate increase rate is reduced.

We next compare the performance of full-duplex and half-duplex schemes under limited CSI to see the full-duplex gain in practical scenarios. Fig. 4.11 shows the sum-rate of each scheme when $N = 50$ and $d = 300$ m. As expected, the sum-rates of both schemes increase with K. Fig. 4.12 depicts the full-duplex gain for various K values. The gain is almost the same as 172% regardless of K and N. This

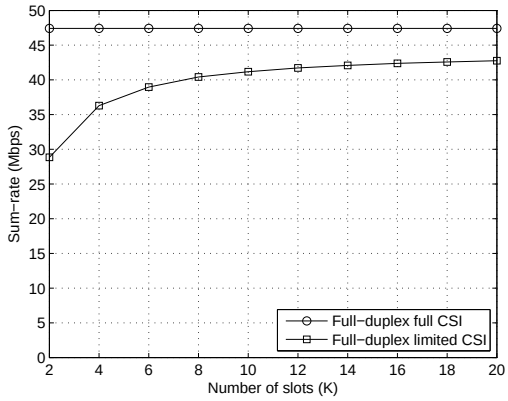

Figure 4.11: Performance comparison of full CSI and limited CSI schemes for various K values.

implies that the full-duplex with the proposed feedback protocol can bring a constant performance gain over the half-duplex in various scenarios.

4.6 Summary

To fully exploit the promising gain of full-duplex technology, it is of great importance to design a resource allocation algorithm tailored for a full-duplex network. In this chapter, we have considered the radio resource allocation problem in a single-cell full-duplex OFDMA network. We consider two different scenarios with full and limited CSIs and propose a solution for each case. In the problem with full CSI, we have proved that the problem is NP-hard, and proposed a subcarrier allocation condition, where each subcarier is assigned only when its inter-node channel gain is smaller than its uplink channel gain. Using

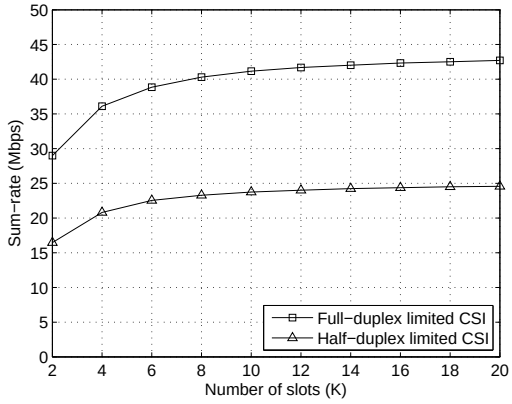

Figure 4.12: Performance comparison of full-duplex and half-duplex under limited CSI.

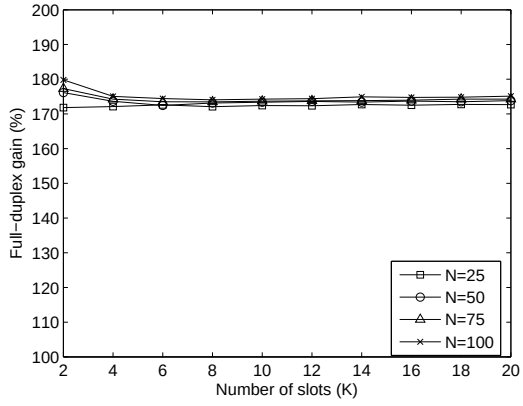

Figure 4.13: Full-duplex gain under limited CSI. The gain is almost the same regardless of K and N.

this condition, we have designed a sequential resource allocation algorithms. In the problem with limited CSI, We proposed a low-overhead feedback protocol where downlink nodes can measure the interference in a distributed manner. Through simulations, we have confirmed that our algorithms perform better than other algorithms oblivious to the interference, and identified the gain of full-duplex over hall-duplex in practical scenarios. We leave extension of our algorithms to multi-cell environments as future work, where the inter-cell interference should be considered along with the inter-node interference.

Chapter 5

Conclusion

5.1 Research Contributions

In this dissertation, we address the resource allocation problems in full-duplex OFDM and OFDMA networks.

First, we have addressed the OFDM subcarrier power allocation problem in the three-node full-duplex OFDM networks with the inter-node interference. We have formulated the sum-rate maximization problem with and without joint decoding. We have proved that when the joint decoding is used, the problem is a convex optimization problem, which can be efficiently solved through our low-complexity Lagrangian dual method. When the inter-node interference is always treated as noise, finding an optimal power allocation is proven to be NP-hard. Thus, we have proposed a heuristic power allocation algorithm where only subcarriers with lower interference channel gains

(compared to uplink channel gains) are shared by the uplink and downlink. Through extensive simulations, we have evaluated the performance of our solution in various scenarios, and demonstrated that they outperform other existing schemes.

Secondly, we have developed a new radio resource allocation algorithm for full-duplex OFDMA networks where the BS and mobile nodes are full-duplex capable. The proposed algorithm assigns subcarriers to nodes in an iterative manner with low complexity. We prove that our algorithm achieves local Pareto optimality under certain conditions that hold frequently in practice. By separating the uplink and downlink transmissions, we have obtained an upper bound on performance that is near-tight in symmetric channel cases. Through extensive numerical simulations, we demonstrate that our algorithm achieves near-optimal performance and outperforms other resource allocation schemes designed for half-duplex networks.

Thirdly, we have considered the radio resource allocation problem in full-duplex OFDMA networks which consists of one full-duplex BS and multiple half-duplex mobile nodes. We consider two different scenarios with full and limited CSIs and propose a solution for each case. In the problem with full CSI, we have proved that the problem is NP-hard, and proposed a subcarrier allocation condition, where each subcarier is assigned only when its inter-node channel gain is smaller than its uplink channel gain. Using this condition, we have designed a sequential resource allocation algorithms. In the problem with limited

CSI, We proposed a low-overhead feedback protocol where downlink nodes can measure the interference in a distributed manner. Through simulations, we have confirmed that our algorithms perform better than other algorithms oblivious to the interference, and identified the gain of full-duplex over hall-duplex in practical scenarios.

To summarize, the full-duplex capability has opened new possibilities to boost the network capacity. Although there still remain some physical layer issues to resolve, it is anticipated that the full-duplex networks will be appear soon in the near future. Besides the three resource allocation problems in this dissertation, there remain many interesting problems, which require further investigation. This dissertation can be viewed as a guideline for modelling and solving new problems in full-duplex networks.

5.2 Future Research Directions

Based on the results of this thesis, there are several new research directions which require further investigation. We highlight some of them as follows.

While we have focused our attention on a single-cell scenario, a natural extension is to consider multi-cell environments where multiple base stations are deployed in proximity. In this case, inter-cell interference from neighboring cells arises, and resource allocation considering both the inter-node and inter-cell interferences is an interest-

ing open problem.

Another interesting research direction is to incorporate the proposed channel feedback protocol in practical wireless systems. Most of currently deployed wireless systems obtain channel information through a polling-based feedback. In this case, we can still apply the proposed interference measurement process, but need to select a pair of uplink and downlink nodes for channel feedback. An efficient polling algorithm for channel feedback considering the inter-node interference is worth exploring and will be an essential component in full-duplex networks.

Bibliography

[1] J. I. Choi, M. Jain, K. Srinivasan, P. Levis, and S. Katti, "Achieving Single Channel Full Duplex Wireless Communication," in Proc. of ACM MobiCom, 2010.

[2] M. Duarte, C. Dick, and A. Sabharwal, "Experiment-Driven Characterization of Full-Duplex Wireless Systems," IEEE Transactions on Wireless Communications, vol. 11, no. 12, 2012.

[3] M. Jain, J. I. Choi, T. M. Kim, D. Bharadia, S. Seth, K. Srinivasan, P. Levis, S. Katti, and P. Sinha, "Practical, Real-time, Full Duplex Wireless," in Proc. of ACM MobiCom 2011.

[4] E. Everett, M. Duarte, C. Dick, and A. Sabharwal, "Empowering Full-Duplex Wireless Communication by Exploiting Directional Diversity," in Proc. of IEEE ASILOMAR, 2011.

[5] A. Sahai, G. Patel, and A. Sabharwal, "Pushing the limits of full-duplex: design and real-time implementation," Rice Univer-

sity Technical Report TREE1104, June 2011. Available: http://arxiv.org/abs/1107.0607

[6] D. Bharadia, Emily McMilin, and Sachin Katti, "Full-duplex Radio," in Proc. of ACM SIGCOMM, 2013.

[7] N. Singh, D. Gunawardena, A. Proutiere, B. Radunovic, H. V. Balan, and P. Key, "Efficient and Fair MAC for Wireless Networks with Self-interference Cancellation," in Proc. of IEEE WiOpt, 2011.

[8] W. Cheng, X. Zhang, and H. Zhang "Optimal Dynamic Power Control for Full-Duplex Bidirectional-Channel Based Wirelss Networks," in Proc. of IEEE INFOCOM, 2013.

[9] W. Cheng, X. Zhang, and H. Zhang "Full/Half Duplex Based Resource Allocations for Statistical Quality of Service Provisioning in Wireless Relay Networks," in Proc. of IEEE INFOCOM, 2012.

[10] J. Bai and A. Sabharwal, "Distributed Full-Duplex via Wireless Side-Channels: Bounds and Protocols," IEEE Transactions on Wireless Communications, vol. 12, no. 8, 2013.

[11] K. Tamaki, H. Ari, Y. Sugiyama, M. Bandaiy, S. Saruwatari, and T. Watanabe, "Full Duplex Media Access Control for Wireless Multi-Hop Networks," in Proc. of IEEE VTC, 2013.

[12] J. Y. Kim, O. Mashayekhi, H. Qu, M. Kazandjieva, and P. Levis, Janus: A Novel MAC Protocol for Full Duplex Radio, Stanford University, Technical Report, 2013.

[13] S. Goyal, P. Liu, O. Gurbuz, E. Erkip, S. Panwar, "A Distributed MAC Protocol for Full Duplex Radio," in Proc. of IEEE ACSSC, 2014.

[14] X. Fang, D. Yang, and G. Xue, "Distributed Algorithms for Multipath Routing in Full-Duplex Wireless Networks," in Proc. of IEEE MASS, 2011.

[15] D. Ramirez and B. Aazhang, "Optimal Routing and Power Allocation for Wireless Networks with Imperfect Full-Duplex Nodes," IEEE Transactions on Wireless Communications, vol. 12, no. 9, 2013.

[16] Y. Yang, B. Chen, K. Srinivasan and N.B. Shroff, "Characterizing the Achievable Throughput in Wireless Networks with Two Active RF chains," in Proc. of IEEE INFOCOM, 2014.

[17] A. Goldsmith, *Wireless Communications*, Cambridge University Press, 2005.

[18] A. Sabharwal, P. Schniter, D. Guo, D. W. Bliss, S. Rangarajan, and R. Wichman, "In-Band Full-Duplex Wireless: Challenges and Opportunities," IEEE Journal on Selected Area in Communications, vol. 32, no. 9, 2014.

[19] B. P. Day, A. R. Margetts, D. W. Bliss, and P. Schniter "Full-Duplex Bidirectional MIMO: Achievable Rates Under Limited Dynamic Range," IEEE Transactions on Signal Processing, vol. 60, no. 7, 2012.

[20] W. Li, J. Lilleberg, and K. Rikkinen, "On Rate Region Analysis Of Half- and Full-Duplex OFDM Communication Links," IEEE Journal on Selected Areas in Communications, vol. 32, no. 9, 2014.

[21] Y. Y. Kang and J. H. Cho, "Capacity of MIMO Wireless Channel with Fulld-Duplex Amplify-and-Forward Relay," in Proc. of IEEE PIMRC, 2009.

[22] S. Simoens, O. Munoz-Medina, J. Vidal, and A. del Coso, "On the Gaussian MIMO Relay Channel with Full Channel State Information," IEEE Transactions on Signal Processing, vol. 57, no. 9, 2009.

[23] T. Baranwal, D. Michalopoulos, and R. Schober, "Outage Analysis of Multihop Full Duplex Relaying," IEEE Communications Letters, vol. 17, no. 1, 2013.

[24] B. P. Day, A. R. Margetts, D. W. Bliss, and P. Schniter "Full-Duplex MIMO Relaying: Achievable Rates Under Limited Dynamic Range," IEEE Journal on Selected Areas in Communications, vol. 30, no. 8, 2012.

[25] O. Somekh, O. Simeone, H. Poor, and S. Shamai, "Cellular Systems with Full-Duplex Amplify-and-Forward Relaying and Cooperative Base-Stations," in Proc. of IEEE ISIT, 2008.

[26] V. Cadambe and S. Jafar, "Can Feedback, Cooperation, Relays and Full Duplex Operation Increase the Degrees of Freedom of Wireless Networks?," in Proc. of IEEE ISIT, 2008.

[27] V. R. Cadambe and S. A. Jafar, "Degrees of Freedom of Wireless Networks With Relays, Feedback, Cooperation, and Full Duplex Operation," IEEE Transactions on Information Theory, vol. 55, no. 5, 2009.

[28] C. S. Vaze and M. K. Varanasi, "The Degrees of Freedom of MIMO Networks with Full-duplex Receiver Cooperation but No CSIT," IEEE Transactions on Information Theory, vol. 60, No. 9, 2014.

[29] D. Tse and P. Viswanath, *Fundamentals of Wireless Communication*, Cambridge University Press, 2005.

[30] S. Boyd and L. Vandenberghe, *Convex Optimization*, Cambridge University Press, 2004.

[31] S. Hayashi and Z.-Q. Luo, "Spectrum Management for Interference-Limited Multiuser Communication Systems," IEEE Transactions on Information Theory, vol. 55, no. 3, 2009.

[32] A. B. Carleial, "A case where interference does not reduce capacity (correspondence)," IEEE Transactions on Information Theory, vol. 21, 1975.

[33] D. P. Bertsekas, *Nonlinear Programming*, 2nd ed. Belmont, MA:Athena Scientific, 1999.

[34] S. Boyd and A. Mutapcic, "Notes for EE364b: Subgradient Methods," Stanford University, 2008. [Online]. Available: `http://see.stanford.edu/materials/lsocoee364b/02-subgrad_method_notes.pdf`

[35] IEEE P802.11ac/D2.0, "Draft STANDARD for Information Technology – Telecommunications and information exchange between systems – Local and metropolitan area networks – Specific requirements – Part 11: Wireless LAN Medium Access Control (MAC) and Physical Layer (PHY) specifications – Amendment 4: Enhancements for Very High Throughput for Operation in Bands below 6 GHz."

[36] LTE Encyclopedia. `https://sites.google.com/site/lteencyclopedia/lte-radio-link-budgeting-and-rf-planning`

[37] J. Papandriopoulos and J. Evans, "SCALE: A Low-Complexity Distributed Protocol for Spectrum Balancing in Multiuser DLS

Networks," IEEE Transactions on Information Theory, vol. 55, no. 8, 2009.

[38] "3GPP Long Term Evolution," Available: http://www.3gpp.org/technologies/keywords-acronyms/98-lte

[39] "3GPP LTE-Advanced," Available: http://www.3gpp.org/technologies/keywords-acronyms/97-lte-advanced

[40] "Mobile WiMax," Available: http://www.wimaxforum.org/index.htm

[41] J. Jang and K. B. Lee, "Transmit Power Adaptation for Multiuser OFDM Sysmtes," IEEE Journal of Selected Areas in Communications, vol. 21, no. 2, 2003.

[42] K. Kim, Y. Han, and S.-L. Kim, "Joint Subcarrier and Power Allocation in Uplink OFDMA Systems," IEEE Communications Letters, vol. 9, no. 6, 2005.

[43] C. Y. Ng and C. W. Sung, "Low Complexity Subcarrier and Power Allocation for Utility Maximization in Uplink OFDMA Systems," IEEE Transactions on Wireless Communications, vol. 7, no. 5, 2008.

[44] J. Huang, V. G. Subramanian, R. Agrawal, and R. Berry, "Joint Scheduling and Resource Allocation in Uplink OFDM Systems for Broadband Wireless Access Networks," IEEE Journal on Selected Areas in Communications, vol. 27, no. 2, 2009.

[45] M. A. Epelman, "Constrained Optimization – Optimality Conditions," University of Michigan, 2012. [Online]. Available: http://www-personal.umich.edu/~mepelman/teaching/NLP/Handouts/NLPnotes12_6.pdf

[46] Y. Yang, C. Nam and N.B. Shroff, "A Near-Optimal Randomized Algorithm for Uplink Resource Allocation in OFDMA Systems," in Proc. of IEEE WiOpt, 2014.

[47] B. Di, S. Bayat, L. Song, and Y. Li, "Radio Resource Allocation for Full-Duplex OFDMA Networks Using Matching Theory," in Proc. of IEEE INFOCOM (Student Poster Session), 2014.

[48] X. Xie and X. Zhang, "Doe Full-Duplex Double the Capacity of Wireless Networks?," in Proc. of IEEE INFOCOM, 2014.

[49] J. Leinonen, J. Hamalainen, and M. Juntti, "Performance Analysis of Downlink OFDMA Resource Allocation with Limited Feedback," IEEE Transactions on Wireless Communications, vol. 8, no. 6, 2009.

[50] S. Patil and G. de Veciana, "Feedback and opportunistic scheduling in wireless networks," IEEE Transactions on Wireless Communications, vol. 6, no. 12, 2007.

[51] R. Agarwal, V. R. Majjigi, Z. Han, R. Vannithamby, and J. M. Cioffi, "Low Complexity Resource Allocation with Opportunistic

Feedback over Downlink OFDMA Networks," IEEE Journal on Selected Areas in Communications, vol. 26, no. 8, 2008.

[52] T. Tang and R.W. Heath Jr., "Opportunistic Feedback for Downlink Multiuser Diversity," IEEE Communication Letters, vol. 9, no. 10, 2005.

[53] E. Yaacoub and Z. Dawy, "Distributed Probabilistic Scheduling in OFDMA Uplink using Subcarrier Sensing," in Proc. of IEEE WCNC 2009.

[54] R. Agarwal, C. S. Hwang, and J. M. Cioffi, "Opportunistic feedback protocol for achieving sum-capacity of the MIMO broadcast channel," in Proc. of IEEE VTC Fall, 2007.

[55] G. S. Smith, "A Direct Derivation of a Single-antenna Reciprocity Relation for the Time Domain," IEEE Transactions on Antennas and Propagation, vol. 52, no. 6, 2004.

[56] H. Moon, "Waterfilling Power Allocation at High SNR Regimes," IEEE Transactions on Communications, vol. 59, no. 3, 2011.